FACULTY OF TECHNOLOGY

Development of a methodology and validation of the Geopyörä breakage test

Tábatha Chávez Matus

Master Thesis in Mineral Processing

Oulu Mining School

Oulu

Supervisors:

Dr. Marcos de Paiva Bueno, Prof. Simon Michaux

University of Oulu

ABSTRACT

Development of a methodology and validation of the Geopyörä breakage test

Tabatha Chavez Matus

University of Oulu, Master's Program in Mining Engineering and Mineral Processing

Master’s thesis 2020, 88 pp. and three appendixes

Supervisor at the university: Dr Marcos de Paiva Bueno

Mining and metals industry extract, process and refine raw materials that are used in every aspect of modern society. It is also a priority sector to achieve a low carbon economy; commodities such as copper, cobalt, nickel and lithium, among others, are essential to developing clean energy technologies and electromobility plans. At the same time, the mining sector is energy-intensive and can have long-lasting impacts on the environment, depending on the exploitation method.

Mining industry represents 7% of the worldwide energy consumption and contributes 10% energy-related greenhouse emission gases. In the latest reports, the actions took for the mining industry to achieve the Paris agreement goals were qualified as insufficient, a problematic scenario, considering that the targets are most likely increase during the next agreement.

Comminution is the most power-demanding stage, using around 50% of the total consumption. In this context, optimisation in comminution processes is one of the biggest challenges in the industry. Geometallurgy is a discipline that aims to address the current challenges of the sector from an integrated mindset.

Geometallurgical models from the perspective of comminution currently face a problem, the lack of a fast and reliable test to allow mapping the distribution of rock properties in ore deposits. The lack of information on comminution parameters contributes to inefficient comminution processes and consequently, higher energy consumption and emitted amounts of GHG (Greenhouse Gasses).

This thesis work presents a methodology to perform breakage tests using a new device called Geopyörä. The research uses the parameters measured by the testing device to derive and validate comminution parameters such as JKDWT Axb, SMC Test® DWi and BWi.

A methodology to achieve the objective of this test was created, allowing to have a procedure for a fast test, requiring approximately 10 minutes per sample, which ultimately results in a low-cost operation. This test uses less than a kilogram of a halve of a meter of drill core to obtain parameters of rock competence and hardness.

The calculation and validation of parameters were carried out in comparison with tests widely used in the industry: JK Drop Weight Test, SMC Test® and Bond ball mill grindability test. The Geopyörä test could deliver reliable results for competence parameters, Axb and DWi (Drop Weight Index), within a margin of error of 7%. Additionally, a correlation between measured and BBMWi was also developed and validated. The results showed that the Geopyörä was also capable of measuring the Bond grindability parameter within an acceptable margin of error of 10%.

Keywords: *Geometallurgy, comminution, ore breakage characterization, variability.*

FOREWORD

This thesis is written as completion to the master's program in Mining Engineering and Mineral Processing at the University of Oulu. This work was supported by the Business Finland public agency for research funding. The prototype machine was constructed and tested as a collaboration between the Intelligent Machines and Systems research unit and the Oulu Mining School at the University of Oulu. I thank the collaborating mines for providing the samples for the experimental work.

I am sincerely grateful to my supervisor Dr Marcos de Paiva Bueno, for his inspiring guidance and encouragement throughout this thesis and for introducing me to this fascinating world of comminution. I would like to thank my co-supervisor Professor Simon Michaux, for his guidance and suggestions on this thesis and to Janne Torvela for his valuable help during the prototype testing. I am also grateful to the mentorship and support of Professor Juan Yianatos that has been essential for my professional development.

I am eternally grateful to my friends for their unconditional support. To Alejandra, Jorge, Hector, Paulina, Max, Cote, Ceci and Hernan, from Chile and to my new family in Finland; Vilde, Manuel, Francisca and Topi. I would like to thank my parents, Daphne and Felipe for their love and support, for raising me with love to be strong, free and happy. To my siblings Macarena, Sebastian and Esteban, for being the most essential thing in my life and always being there for me. And finally, I thank Cesar, the eternal love of my life, for being my partner on this journey, for his unconditional love and for always encouraging me to be a strong woman regardless of the obstacles.

I hope to contribute with this thesis on the arduous task of achieving equality in an industry with 15% female participation. Thanks to all the women who have inspired me.

Oulu, 29.06.2020

Tabatha Chavez Matus

ABBREVIATIONS

AG: Autogenous grinding

Axb: JK Drop Weight Test ore hardness index

BBMWi: Bond Ball Mill Work Index

C_i: Crushing parameter

COV: Coefficient of variation

DWi: Drop Weight Index

DWT: Drop Weight Test

E: Young´s modulus of Elasticity

Ecs: Specific Comminution Energy

E_{is}: Specific input energy

F_{80}: 80% of the feed passing

f_{SAG}: Proprietary function

g: Acceleration of gravity

GHG: Greenhouse Gasses

Grp: Rod Mill Grindability

HDI: HIT Test Hardness Index

HIT: Comminution Test

HPGR: High Pressure Grinding Rolls

ICS: Impact of the crushing parameter

m: Mass of the particle

$\overline{m}$: Mean mass of the set of particles

m_d: mass of the drop weight

MPa: Mega Pascals

M-W_i: Mergan Work Index

P: Power draw

P_{80}: 80% of the product passing

PCCL: pebble crusher circulating load

PLI: Point Load Test

RQD: Rock Quality Designation

SAG: Semi-Autogenous Grinding

SG: Specific Gravity

SMC: Steve Morrell Comminution

SPI: SAG power index

T: Throughput

t_{10}: Value as cumulative weight percentage passing one tenth of the size of the original particle

t_n: Value as cumulative weight percentage passing.one n of the original particle size

UCS: Uniaxial Compressive Strength

W: Work Input

WI: Work Index

Wi_{GP}: Work Index Geopyörä

W_{iR}: Rod Mill Work Index

υ: Poisson´s Ratio (υ).

TABLE OF CONTENTS

LIST OF FIGURES

LIST OF TABLES

1 INTRODUCTION

Around 7% of the worldwide energy consumption is destinated to the mining and metals industry (Manouchehri et al., 2016) where comminution, as the most power-consuming stage in the mining process, represent 50% of the overall processing plant energy, with a consumption range between 35% and 80%, depending on the deposit characteristics and the metal recovery process (Radziszewski, 2013). Concurrently, it has been estimated that 3,6 x 10^{12} kg of CO_2e are associated with primary mineral and metal production, representing 10% of the total energy-related greenhouse gases (Azadi et al., 2020).

The average ore grade has been decreasing over the years, and it is expected that it will continue with this trend. A clear example can be observed in the copper industry, where the average ore grade has declined by 25% in ten years. During the same period, production and energy consumption increased by over 30% and 46% respectively (Calvo et al., 2016).

The mining industry is facing a challenging moment to fulfil future demands in a scenario of low-grade mineralisation projects. Efficiency improvements in all the mining stages are essential to achieve this goal; a clear example is that without the development of low-cost comminution technology almost none of the porphyry deposits would have been feasible in the past century (Napier-Munn et al., 1996).

A better understanding of an ore variability has been pointed as crucial to improve the efficiency in running operations and to diminish the uncertainty in feasibility studies. In this context, geometallurgy is a discipline that complements design and operation approaches by providing constrain inputs that give information about the geological variability and how this affects the metallurgical performance.

Geometallurgy adds parameters to the typical block model used in geostatistics by incorporating data to create an integrated view of the economic optimisation in mining operations (Tolosana-Delgado & van den Boogaart, 2018). Geometallurgical models include ore hardness, energy consumption, mineral liberation, recovery, metallurgical

performance, among others as parameters, by using these parameters, strong relationships between easily obtainable measure tests and metallurgical performance predictions are crucial to improve the overall mine performance (Lund & Lamberg, 2014).

Even though the ore-body variability issue is well acknowledged, the design of most of the processing plant is realised by using discrete properties values of the deposit as input for the project development (Bueno et al., 2015). A common mistake is to consider the average as appropriate design input, and another is to determine a reliable correlation between two properties (e.g., lithology and ore competence) without an adequate number of tests conducted (David, 2019).

A clear example of the inaccuracy of assuming an average without proper testing and statistical significance is present by Morell (2011). For 650 deposits, the coefficient of variation of the ore competence parameter, Drop Weight Index (DWi), was analysed, as is shown in Figure 1. Half of the ore deposits had a coefficient of variation (COV) higher than 26%, meaning that, for example, for an ore-body with a DWi of 7 kWh/m^3 and a standard deviation of 1,82 kWh/m^3 (COV=26%), the competences values range from 3,6 to 10,4 kWh/m^3, a significant range considering that the values of the DWi vary from 1 to 14 kWh/m^3.

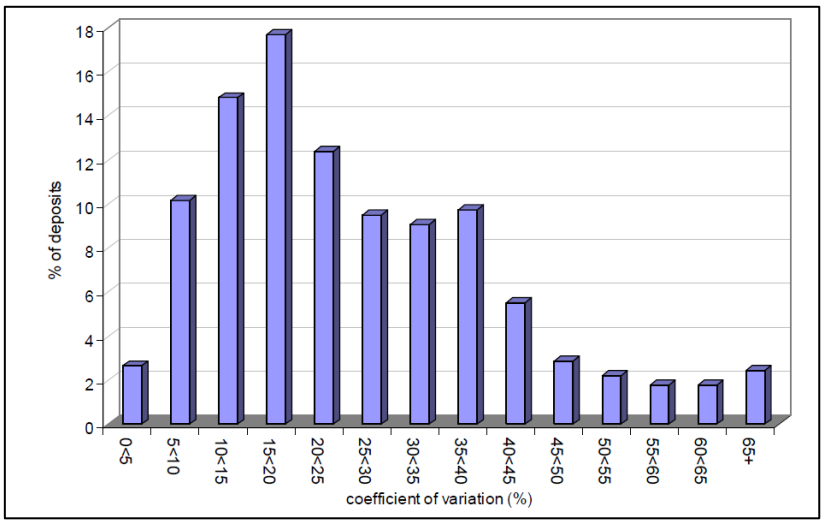

Figure 1 Histogram of the Coefficients of Variation of DWi Values (Morrell, 2011).

Considering that competence is one of the primary input parameters for the design of SAG and AG mills (Putland et al., 2019), a three times difference between the lower and the higher value present a clear opportunity of improvement. Grinding is the most energy-consume stage and for half of the deposits analyse in this study, coefficients of variation than are higher than 26%.

New development and implementations of techniques of design and testing that allows understanding the ore variability, especially in terms of comminution properties are needed. Mwanga et al., (2015) describe an optimal comminution test as one that should be simple, repeatable, easy to execute, with a maximum time of execution of 1 hour and that uses less than 0.5 kg of samples. Is also describe that an optimal test should give measured values of crushability and grindability, the parameters of this test should give direct parameters for modelling and simulation of comminution circuits (Mwanga, Rosenkranz, et al., 2015).

Traditional comminution tests required samples amount of between 15 to 95 kg of bulk sample and 20 meters of drill core, these are extensive in sampling and testing time and consequently are expensive. A geometallurgical mapping uses between 1500 to 2000 meters of drill core to have a representative perspective of the ore body (Michaux & O'connor, 2019). Some properties measure in the geometallurgical program (e.g., chemical assay, lithology) are recorded meter by meter. At the same time, the amount of comminution test is considerably less due to the time, sample and economic difficulties of using traditional comminution test. Morell (2011) acknowledge that a significant amount of data points is the best approach; however, the recommendation is to keep the sample selection and laboratory test work costs at a minimum.

A new breakage test device, called Geopyörä, has recently been developed this problematic (PCT/FI2020/050100). The prototype was developed at the University of Oulu and consists of two instrumented wheels, powered by integrated electric motors placed in the frame with an adjustable gap (Torvela, 2020) that measure the energy consume in a breakage event.

This thesis work aims to create a methodology of sampling and testing, to achieve an accurate breakage characterisation for small samples, in a short amount of time. The results of the initial testing would be compared to traditional comminution test (i.e., JKDWT, SMC Test®, BBMWi) to analyse if the is it possible to obtain strong hardness and competence parameters.

1.1 Objective and Hypotheses

The scope of this thesis is to develop and validate a methodology to use a new prototype to test comminution properties for geometallurgical purposes that aim to be a fast and cost-effective solution to analyse more samples.

This work is divided into the following secondary objectives:

- Create a literature review of the current comminution tests and the fundamental theory behind them in a geometallurgical.
- Develop a methodology to test bulk samples.
- The creation of sample preparation to develop a methodology to use one half of a meter of drill core as a reliable sample for testing.
- Validate the parameters of the results by comparing it with traditional tests of hardness and competence; DWi, Axb and BBMWi.

The hypotheses to be answered in this study are:

- The Geopyörä test can be performed with small amounts of bulk and drill core samples to derive reliable comminution parameters for geometallurgy and optimisation purposes.

1.2 Thesis Structure

The thesis includes five chapters including this introduction as *Chapter 1*

Chapter 2: Reviews the basic principles of rock breakage and presents the main comminution tests, revealing their inherent problems. The last part of the bibliographic review covers the principles of geometallurgy and the lack of comminution tests suitable for geometallurgical programs.

Chapter 3: Presents a description of the new testing device, the way it operates and accounts for applied energy. The work methodology for drill core and bulk samples is presented in this chapter. The last part of this chapter presents the results of the tests with which the validation would be carried out.

Chapter 4: Presents the results of the experimental results and the validation of the new Geopyörä test. Different scenarios are proposed to establish the ideal test methodology and achieve optimum results. Parameters are correlated to obtain comminution properties from the data measured by the apparatus.

Chapter 5: Summarise the outcomes of this thesis. Conclusions and recommendation are presented in this chapter.

2 LITERATURE REVIEW

The literature review covers four main topics: rock breakage, comminution models, comminution tests and geometallurgy. In comminution the rock breakage phenomena depend upon how the material behaves under an applied load and is dependent of the form how this load is applied, meaning the unit process (e.g., crusher and mills) (Wills & Finch, 2016).

Optimisation is a critical process for maximising the profitability of all metallurgical facilities within the constraints of the operation. Comminution models are especially attractive due to the room for improvement in a cost-intensive process from both a capital and operating perspective.

Comminution models require ore breakage properties; the determination of this is achieved by controlled breakage tests. Comminution tests can be divided into batch grinding tests and single-particle breakage tests.

Geometallurgy is a multidisciplinary approach to mitigate production risks and improving economic and environmental performance in the mining industry. Ore variability is fundamental to avoid a fixed recovery target for the whole process without considering the different ore types. Grade and geology domains are the most measured properties when the ore deposits are analysed; however, this information is not enough to map the ore type process behaviour into the deposit.

A good understanding of the comminution properties across the whole ore deposit is crucial to optimise the mill performance. However, traditional tests are expensive and time-consuming. This chapter ends reviewing the challenges of geometallurgy from a comminution perspective.

2.1 Rock breakage

Rock breakage exhibits two behaviour, macro-measure and microfracture mechanisms. Macro measures address the compression and tension of the ultimate stress that represents the properties that describe the loading response and microfractures describe the crack initiation and propagation (Napier-Munn et al., 1996).

Macro measures relate compressional response properties of rocks by three widely know parameters; Uniaxial Compressive Strength (UCS), Young´s modulus of Elasticity (E) and Poisson´s Ratio (υ).

The Uniaxial Compressive Strenght is defined as the maximum force recorded in the point of ductile-brittle transition in a specific area, the range values of UCS is from less than 50 Mpa for weak competent to 450 MPa to highly competent materials (Napier-Munn et al., 1996).

The second property related to macro measures is Young´s modulus, which depends on the degree of linearity of the response, meaning that is the slope of the elastic region of the stress versus strain. The values range from <10 GPa for marble and weak rocks to >70 GPa for rocks capable of sustaining high stresses with restricted longitudinal strains.

Poisson´s ratio is determined as the ratio of the lateral strain to the longitudinal strain, to obtain this parameter, strain gauges must be applied on laterally and longitudinally to the surface of the sample. Values between 0,05 to 0,15 are associated with weak rock types, over 0,25 indicate rocks able to deform under load while maintaining integrity which is competent, linear elastic rocks.

Most of the breakage events start from an area of stress concentration that propagates inward the particle. This breakage can occur along cleavage planes or inter-granular (Gupta & Yan, 2016).

2.2 Comminution models

Comminution models must find a way of representing the application of energy by a breakage machine (such as a crusher or ball mill) to an ore. Models describe two elements of the problem:

- The breakage properties of the rock – essentially the breakage which occurs as a result of the application of a given amount of specific energy
- The comminution machine; refereeing to the amount and nature of the energy applied, and the transport of the rock through the machines.

Comminution models can be dived into three categories; empirical, phenomenological and fundamental models (Wills & Finch, 2016).

2.2.1 Empirical models

Empirical models consider a comminution device as a transform between a feed and product size distribution. The objective of these models is to represent the phenomenon of breakage, rather than underlying physical principles.

Under this category, power-based models, are broadly used in comminution optimization plan and geometallurgy (Morrell, 2014). Power-based models aim to predict the product size distribution from an ore feed size distribution, breakage characterisation and experience with similar devices.

Comminution processes are analysed by the particle breakage and the broken particle product distribution. A relationship between particle size distribution and energy input of a comminution device is the key for power-based models. The first energy model was developed by Walker et al. (1937), as is shown in Equation 1.

$$dE = -k \cdot x^n dx \qquad (1)$$

This equation describes the increment in energy (dE) related to a decrease in the particle size x, n and K are constants. The values of n can be 2, 1 and 1,5 depending on the theory of Von Rittinger, Kick or Bond, as is shown in Figure 2.

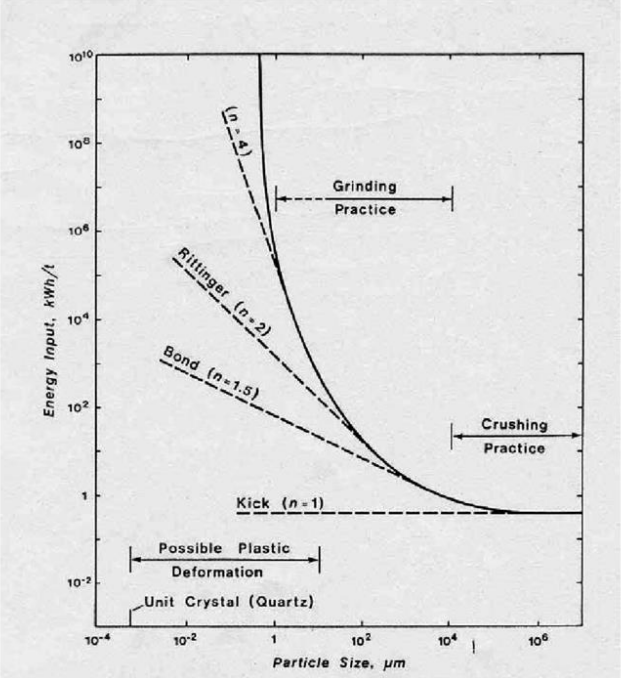

Figure 2 Energy vs particle size for Von Rittenger, Kick, and Bond equations (Hukki, 1961)

In 1952 Fred Bond published the approach that is one of the significant comminution design parameters used by industry, to design, evaluate and optimise crushing and grinding circuits. Bond tests are based on Bond´s third theory of comminution, that describes that the work input is proportional to the crack length produced in the particle breakage with the work represented by the product and the feed (Bond, 1952). This relationship is expressed in Equation 2 and Equation 3.

$$W = 10 \cdot WI \left(\frac{1}{\sqrt{P_{80}}} - \frac{1}{\sqrt{F_{80}}} \right) \quad (2)$$

Where:

W = work input (kWh/t)

WI = work index (kWh/t)

P_{80} = size at which 80% of the product passes (µm)

F_{80} = size at which 80% of the feed passes (µm)

$$P = T \cdot W \tag{3}$$

Where:

T = Throughput of new feed (t/h)

P = Power draw (kW)

Work index represents the resistance of a specific material to crushing and grinding. This comminution parameter is the kilowatt-hour per tonne require reducing the size of the material from a theoretically infinite feed size of 80% passing of 100 microns (Bond, 1961).

The relationship between the energy applied, as specific comminution energy (Ecs), and the cumulative fraction passing by the geometric mean product size 1/10th to the geometric mean specimen size (t_{10}) is described in the curve presented in Figure 3.

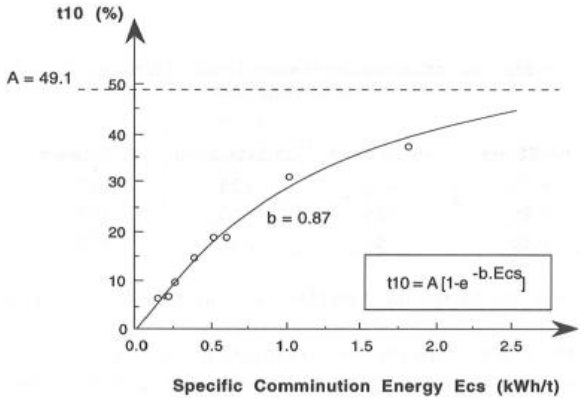

Figure 3 Specific communion energy (Ecs) vs t10 (%) curve (Napier-Munn et al., 1996)

From this curve, Equation 4 is derived. The A and b are fitted parameters, where A is the asymptote and b is the slope of the curve.

$$t_{10} = A(1 - e^{-b \cdot Ecs}) \tag{4}$$

To understand the phenomena related to the single-particle breakage, ore breakage functions are used to describe the product size distribution related to the specific comminution energy as is shown in Equation 5.

$$t_n = 1 - (1 - t_{10})^{\left[\left(\frac{9}{n-1}\right)^{\alpha}\right]} \tag{5}$$

Figure 4, also refers as the one-parameter family curve, represents in each vertical line represents a complete size distribution, represented in a t_{10} value as cumulative weight percentage passing.

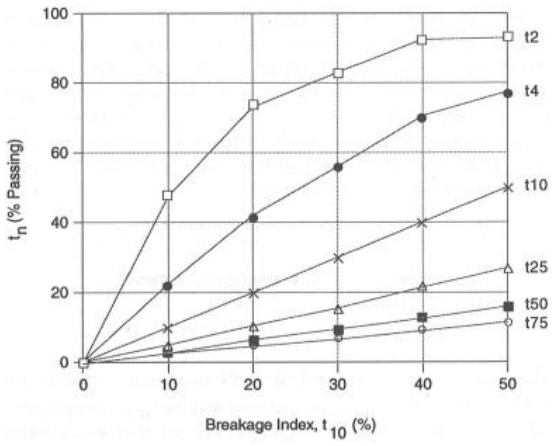

Figure 4 One parameter family curve (Napier-Munn et al., 1996).

The data represented in the graph can be measured for an ore type is also used to predict the size distribution, which results in any known t_{10} value (Napier-Munn et al., 1996). An extensive database validates that the same family of curves describe the breakage distribution of a wide range of ores for different apply comminution energy. Power-based models require estimated parameters of the ore, such as hardness and competence to understand the resistance to breakage.

2.2.2 Population balance models

Phenomenological models are widely used in circuit simulators (Gupta & Yan, 2016). Population balances have some underlying principles but also uses parameter fitted by calibration for different comminution equipment (Wills & Finch, 2016).

This model is a first-order rate model that assumes that the production of the material in a time interval depends on the mass of that size fraction for a rate constant for each fraction creating a matrix term that describes the probability of each size class breaks and another matrix to represent the product sizes of each breakage.

Complete size distribution is required to simulate the behaviour classifiers and screens on a comminution circuit. Software's such as JKSimMet and USIMpac uses population-based models for this reason.

Population models allow simulating grinding circuits without the assumption of a standard shape. This is a significant difference compare to energy-based models; however, they are time and cost consuming due to the required model setting parameters.

2.2.3 Fundamental models

Fundamental models present a sophisticated computational approach which considers every element in the process, meaning that the interactions of ore particles and elements within the machine, based on Newtonian mechanics.

Fundamental models represent a better approach for comminution modelling (Powell & Morrison, 2007). This technique required advance computational tools to combine physical models to describe the motion of balls, feed material behaviour and the breakage of particles under the influenced by moving liners and grates. Fundamental models include discrete element methods (DEM) and computational fluid dynamics (CFD).

2.3 Comminution tests

Hardness itself is a difficult property to define, and its relationship with any given breakage machine will not necessarily be straightforward. For example, an autogenous mill treating a soft ore may have a low capacity because of the lack of hard ore media to promote grinding; a cone crusher of a given set can crush a wide range of ores to a similar product size but would draw different power in doing so (Putland et al., 2019).

Standard rock mechanics tests of strength, such as fracture toughness and uniaxial compressive strength, are not usually seen as appropriate in comminution studies (Morrell, 2019). They provide information on the stress required to cause failure under specific modes of loading, in the form of a single hardness or a strength parameter. In comminution, it is also essential to identify the product size distribution resulting from applying a breakage mechanism to given feed size, and the energy required to generate that product size.

The energy-size reduction relationship is the focus of the laboratory tests developed to assist in comminution equipment specification, circuit design and optimisation. These include Bond grindability tests, batch grinding, and single-particle breakage tests. However, the evidence is that an accumulation that some rock mechanics fracture tests can also be usefully interpreted in comminution terms, as discussed below.

Being able to decouple the influence of the breakage function (material-specific properties) from the breakage rates that address to the machine-specific properties is fundamental for modelling industrial grinding operations. In this context batch grinding tests are not ideal for separating these two properties.

The determination of ore-specific breakage distribution functions was achieved by means of controlled breakage tests, which use individual particles to identify three types of breakage phenomena´s: impact, slow compression and shear (Narayanan & Whiten, 1988). The main tests developed to measure the breakage (appearance) function of individual particles are presented in Table 1.

Table 1 Modified summary of the most used comminution tests. Modified from Morrell, 2019

Test type	*Test*	*Use*	*References*	*Sample Quantity, kg*	*Material Size*	*Minimum Core Size*
Batch tests	Bond Impact crushing test	Conventional crushers SAG mills	Bond 1946, 1961 Barratt and Allan 1986	40-50	2-3 in.	PQ
	Bond rod mill work Index	Rod mills/ball mills SAG mills	Bond and Maxon 1943; Rowland 1982 Barrat and Allan 1986	10-15	100% - 12,7 mm	NQ
	Bond ball mill work index	Ball Mills SAG mills	Bond and Maxon 1943; Rowland 1982 Barrat and Allan 1986	15	100 – 3,35 mm	NQ
	Bond abrasion Index	Wear prediction for crushers and tumbling mills	Bond 1963; Giblet and Seidel 2011	2	12-19 mm	NQ
	SPI Test	SAG mills	Starkey et al. 1994	10	80 -12,7 mm	NQ
Single-particle tests	SMC Test®	Conventional crusher, AG/SAG mills, HPGR	Morell 2004, 2009	20	19-31 mm	NQ
	JK Drop weight test	SAG mills, conventional crushers	Napier-Munn et al. 1996	75	13,2 – 63 mm	PQ
	HIT Test	SAG mills, conventional crushers	Kojovic 2016	0,5	13,2-31,5 mm	NQ
	JKRBT	SAG mills, conventional crushers	Shi et al., 2009	75	-53+13,2 mm	PQ
	Point Load Test	Conventional crushers	Bearman et al., 1997	1	N/A	N/A

2.3.1 Batch grinding tests

A Batch grinding test is a simple method to determine the breakage function. The main principle of a batch grinding to test is to use an initial amount of sample in a known particle size fraction, grind it for a period of time and determine its size distribution. This procedure is done multiple times taking in consideration that a short grinding time can provide insufficient mass for accurate sieving and on the opposite case, an excessive amount of time can cause excessive re-breakage creating a non-reliable test to describe the comminution phenomena.

2.3.1.1 Bond rod mill work Index

The Bond Rod Mill Grindability test used a feed product of material under 12,7 mm, in a 1250 cc graduated test tube. The feed is weighted, screen and ground dry with a 100% circulating load (Bond, 1961). The apparatus is a rod mill of 0,305 m diameter by 0,610 long (Bond, 1961). The grinding charge comprises six 31, 8 mm diameter and two 44.5 mm diameter steel rods, and the total weight is 33,38 kilograms, as is shown in Figure 5.

Figure 5 Bond´s Rod Mill test (JKTech, 2017c)

Equation 6 describes how the rod mill work index (W_{iR}) is calculated:

$$W_{iR} = \frac{68}{P_1^{0,23} \cdot (Grp)^{0,625} \cdot 10\left(\frac{1}{\sqrt{P}} - \frac{1}{\sqrt{F}}\right)} \quad (6)$$

Where P_1 is the opening in microns of the sieve size test, Grp is the rod mill grindability presented as the last three net grams per revolution.

2.3.1.2 Bond ball mill work Index

This test uses a batch mill of 0,305 m of diameter and 0,305 long with rounded corners and smooth liners (Bond, 1961). The charge of the mill corresponds to a specified quantity of balls of given sizes and weights. To prepare the feed sample, the feed should be crushed to 100% passing 3,35 mm. For the sample preparation and depending on the size of the starting material, stage crushing may be necessary, in that case, the first stage of coarse crushing using a crusher setting of about 25 mm must be done. After this stage, a second crushing is performed with a setting of 3-4 mm. The initial charge is the weight of 700 cc measured in a test tube.

Because of the time, each grind cycle is adjusted. The proportion between the oversize and the undersize mass is 2,5. The test approximates the performance of a continuous closed-circuit mill with circulating load is 250% (Napier-Munn et al., 1996). Equation 7 describes how the work index (kWh/t) is calculated:

$$W_{iB} = \frac{49{,}1}{P_1^{0,23} \cdot (Grp)^{0,82} \cdot 10\left(\frac{1}{\sqrt{P}} - \frac{1}{\sqrt{F}}\right)} \qquad (7)$$

P_1 refers to the closing Size; this is selected according to the required application, being the most used 150 and 75 mm. After the work index is calculated, Equation (1) and Equation (2) are used to calculate for a given throughput (t/h) the specific power can be converted to a power draw (kW). Due to a mill size-power correlation, mill dimensions for an industrial unit can be chosen for a required power.

A widely used form to measure rock hardness is the Bond work index; this is related to the UCS, as is shown in Table 2.

Table 2 UCS and Bond Wi correlation (Napier-Munn et al., 1996).

Property	*Soft*	*Medium*	*Hard*	*Very Hard*
UCS (MPa)	50 – 100	100 – 150	150 – 250	>250
Bond Wi (kWh/t)	7 - 9	9 - 14	14 - 20	>20

A correction factor for the Bond work index is applied for both ball and rod mills in six different conditions to design comminution industrial. Dry grinding, oversized feed, diameter efficiency, fine grinding, open circuit and reduction ball milling that is low or high (Rowland, 1982). In conclusion, the Bond-Rowland model is an accurate and widely test to calculate specific energy requirements in different grinding conditions.

2.3.1.3 JK Bond Ball Mill

The JK Bond Ball mill was developed as a version that uses less material than the original Bond Ball Mill test. The original test required 10 kg of sample, while this version needs half of it, 5 kilograms (JKTech, 2017a). The main difference between both methodologies is that the JKTech version has specific protocols regarding the apparatus design and charge (Matei et al., 2015b) this prevents variations, allowing to be able to work with less sample.

This test was validated by comparing its results against a database of 1380 original BBMWi results of 148 varieties of rocks. The results of this validation show results with an error of 4.1% comparing the short version with the original Bond Ball Mill test.

2.3.1.4 Mergan Test

In 1970 Niitti describes that the grindability can be calculated directly as energy consumption of the 74 μm material produced or as energy consumption per 1000 cm^2/cm^3 of the surface area product (Niitti, 1970) "Mergan work index" ($M\text{-}W_i$) is calculated according to Equation 8:

$$M - W_i = E_0 \left(\frac{\sqrt{F_{80}}}{\sqrt{F_{80}} - \sqrt{P_{80}}} \right) \sqrt{\frac{P_{80}}{100}} \quad (8)$$

The energy consumption is represented with the parameter E_0 in kWh/t. These tests correlate with the Bond work index and have the advantage that instead of being a lock cycle test, like the Bond Ball test, is a batch test. With this information, a new approach of the test was developed, aiming to use the Mergan test as a grindability test that also can be used as the flotation feed preparation (Heiskari et al., 2019).

The objective of replacing the Bond Ball Test with the Mergan test is based in a geometallurgy scope of finding a test that with the same sample (5 kg) can fulfil different purposes by using the less amount of time and money possible. The Mergan mill used in this research is shown in Figure 6.

Figure 6: Mergan Mill (Heiskari, 2017).

The Bond Ball Test has fixed screen-opening values, while the Mergan test has different P_{80}. The new approach normalised the E_0 value to try to obtain a P_{80} value as close as possible to the Bond Ball Test (106 µM sieve opening) in order to make a comparison of the two methods. A model was applied to calculate the modified M-W_i with good correlation compared to the Bond Ball Work Index.

Nappier-Munn et al. (1996) describe that the assumption behind batch grinding approach works well for ball milling and fine grinding; however, the problem is that is not possible the decoupling of breakage function and breakage rates, meaning that for more complex grinding systems the assumption of a first-order breakage and constant rates is not accurate.

2.3.1.5 SPI Test

SAG power index (SPI) was created in 1994 (Starkey et al., 1994)and is currently owned by SGS S.A. The test is performed in a bench comminution mill of 10 cm diameter by 30 cm long, as shown in Figure 7, the mill is loaded with 15% by volume of 1-in. balls (SGS, 2005).

Figure 7 SPI mill (Morrell, 2019)

The required mass sample is 2 kg, the feed should have a P_{80} of 12,5 mm. The test consists of measures the time required to grind the feed sample to a product with a P_{80} of 1,7 mm. Additional to this test, a crushing test is performed; this second test required 10 kg of material to obtain a crushing parameter C_i. Equation 9 describes how the test predicted the specific energy (Dobby et al., 2001) where K and n are fitted parameters and f_{SAG} is a proprietary function that describes the effects of feed size and pebble crusher circulating load (PCCL).

$$SAG\ \left(\frac{kWh}{t}\right) = K(SPI \cdot T_{80}^{-0,5})^{n} \cdot f_{SAG} \quad (9)$$

The second test parameter C_i is used to predict feed size distribution by the assumption that the feed followed a Rosin-Rammler function.

Over 25.000 SPI tests have been performed due to the ability to represent all the breakage mechanisms that influence the SAG mill performance; Impact breakage, single-particle nipping, abrasion breakage and autogenous compression (Dobby et al., 2004).

2.3.2 Single-particle breakage tests

2.3.2.1 Bond impact crushing test

The first twin pendulum equipment was developed by Bond (1946) known as the Bond crushability test. The size distribution of the crushed particle and the new surface was performed by Gaudin and Hukki (1946).

Bond developed an equipment that includes two opposite hammers of 13.6 kg each that work through the action of counter-rotating wheels, as is shown in Figure 8. The particles used for this test are pass 75 mm and retained on a 50 mm (Bond, 1946) . Each particle is positioned in between the hammers, and they are realised simultaneously.

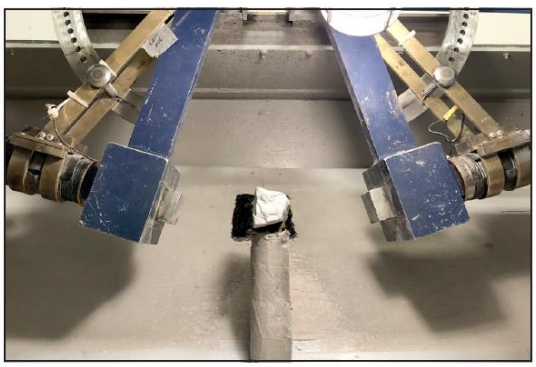

Figure 8 Bond's crushing work index (Morrell, 2019)

The height of the fall is increased until the rocks break; the work index is obtained from the average of ten breaks and calculated according to Equation 10:

$$W_{iC} = 53{,}49\frac{ICS}{SG} \tag{10}$$

Where ICS describe the impact of the crushing measured in Joules per mm of the rock thickness and SG is the specific gravity of the sample.

Automated versions of the pendulum test have been developed in order to record more information about the pendulum mechanism (Sahoo et al., 2004) (Weedon & Wilson, 2000).

Thanks to the studies performed using the pendulum test, (Fahernwald et al., 1937) (Gaudin & Hukki, 1946) relationships between size distribution and surface determined a limit to the material produce by a theoretical infinite increase of specific energy. An increase in the impact velocity increases fine production due to breakage. Another theory that it was proven is that if we compared irregular specimens against spherical particles, the irregular shapes would have the highest crushing efficiency in a broad energy spectrum (Yashima et al., 1981).

2.3.2.2 JK Drop weight test

For Drop Weight test, a weight with a known mass is dropped from a known height onto a particle, and the size distribution of the broken product is measured. The applied energy is the potential energy, calculated as described in Equation 11

$$E = m \cdot h \cdot g \tag{11}$$

Where m is the mass of the weight in kilograms, h is the drop height in meters and g is the acceleration of gravity in m/s^2. To use this principle in a suitable standard way, a known weight is dropped from a specific height to crush a particle using nominal fixed energy (Morrell & Morrison, 1989).

The JK Drop Weight test was developed in 1992 (Napier-Munn et al., 1996) . The equipment comprises an impact with a steel weight position in the top, as is shown in Figure 9. The steel weight varies to perform the test at different energy levels.

Figure 9: JK Drop weight test

The test required 75 kg of sample and consisted in 3 repetitions at different energy levels, between 0,25 kWh/t to 2,5 kWh/t in five size fractions –63+53 mm, –45+37.5 mm, –31.5+26.5 mm, –22.4+19 mm, –16+13.2 mm. The test can be used with the drill core material, and the most common Size is PQ (85 mm) in order to have enough particles for the largest size.

The height from which the drop weight is realised is determined Equation 12, where h_i is the initial height in centimetres from where the weight drops, M_d is the mass of the drop weight in kilograms, $\bar{m}$ is the mean particle mass of the set sample and E_{is} is the specific input energy (kWh/t),

$$h_i = \frac{\bar{m} \cdot E_{is}}{0{,}0272 Md} \tag{12}$$

The parameter E_{ic} is similar to the specific comminution energy (E_{cs}) for values under 3 kWh/t (Napier-Munn et al., 1996). This assumption applies to breakage events without rebounds. To ensure a proper E_{cs} value, usually, 10 mm is added to the calculated drop

weight test. The average offset of the height can be measure to each particle, as is shown in Equation 13.

$$E_{is} = \frac{0{,}0272 \cdot Md \cdot \left(h_i - h_f\right)}{\overline{m}} \tag{13}$$

Fifteen points are generated from the JK Drop Weight Test, each of one with specific energy and its respective size distribution. The size distribution is quantified with the parameter t_{10}.

2.3.2.3 JK Rotary Breakage Test

The JK Rotary Breakage Test (JKRBT) uses fixed energy as the JKDWT. The feed material is placed in the tester to be accelerated to a controlled velocity. The specific energy is obtained by using the kinetic energy formula, as is shown in Equation 14.

$$E_{cs} = \frac{1}{2} \cdot m \cdot v^2 \tag{14}$$

Figure 10 shows the JKRBT device. The sample amount required is 75 kg of crushed rock in the -53 x 13,2 mm size range or 90 kg of drill core. Four size fractions are used for the test, -45+37,5 mm -31,5+26,5 mm and -16+13,2 mm. Three sets of 20 or 30 particles are prepared to broken in 3 energy levels, having in total twelve points.

Figure 10 JK Rotary Breakage Tester® (JKTech, 2017b)

To obtain the Axb parameters uses the JK size-dependent model (Shi & Kojovic, 2007), as is shown in Equation 15. Where f_{mat} is the material breakage property, x is the initial particle size, k is the successive number of impacts with the simple impact energy, and E_{min} is the minimum energy to have a breakage event. The Axb parameter can be obtained by using Equation 16.

$$t_{10} = M(1 - exp[-f_{mat} \cdot x \cdot k(E_{cs} - E_{min})] \quad (15)$$

$$Axb = 3600 \cdot M \cdot f_{mat} \cdot x \quad (16)$$

SMC Test®

Morell developed SMC Test® as with the same principles of the Drop Weight Test to be used with drill cores samples cut into several identical pieces by a diamond saw (Morrell, 2014). Associated equations for the application of the SMC Test® were developed to cover AG/SAG and HPGR circuits in addition to the application covers by the JK Drop-Weight Test (Morrell, 2010) (Morrell, 2009).

The SMC Test® can be performed with drill core, and bulk samples, 15 to 20 kilograms of sample are required for each test. The test is performed in one of the following three fractions: 31,5 + 26,5 mm, –22,4 + 19 mm, or –16 + 13.2 mm.

For the drill core procedure, the size fraction would be chosen according to the sample diameter available. The particles from drill cores are produced by cutting the drill core into wedges by using a diamond saw, as is shown in Figure 11.

Figure 11 SMC Test® drill core diamond saw cutting (Morrell, 2004).

If the drill core mass is abundant (over 20 kg), the particles can be produced by crushing the core and selecting particles from the required size after sieving. The crushing procedure, in this case, is performed in stages, where the gap setting decreases in each stage to preserve a small reduction ratio (F_{80}/P_{80}). This technique is used to ensure an optimal number of particles in the desired size, minimising the amount of fines (Morrell, 2019).

50.000 SMC Tests have been conducted in over 2000 ore bodies across 82 countries, constituting one of the most important data set in terms of comminution properties (Morrell, 2015).

2.3.2.4 HIT test

HIT (Hard Index Tester) is one of the newest tests in the industry that seeks to position itself as a reliable, low-cost test that can use a small sample. The HIT test requires a minimum of ten fragments in size fractions similar to JKDWT, e.g. -22,4 + 19 mm. HIT test set a mass tolerance around the bulk sample mean to ensure that the set mass is within five per cent of the population mean (Kojovic, 2016). The particle selection procedure follows a similar protocol than the SMC Test®.

This test derives the Axb parameter with only one pair of energy and t_{10}, which is its main characteristic and difference from the JKDWT and SMC Test®. The Axb calculation, as shown in Equation 17, is based on the principle of the zero energy (Napier-Munn et al., 1996), assuming that the relationship between specific energy and t_{10} can linear for low energies.

$$HID = \frac{t_{10}}{Ecs} \tag{17}$$

To validate this hypothesis, HDI (Raw Hardness Index) calculations were made, using raw t_{10} values of the at 100 JK Drop Weight Test that registers specific energy of 0,25 kWh/t. The database used considered 32 ore deposits with a particle size of 31,5 x 26,5 mm. Kojovic (2016) reports that the slope at a low energy (0,25 kWh/t) would be marginally lower than the actual Axb.

Choosing 0,25 kWh/t as fixed energy seems convenient, especially to compare it with the JKDWT, which uses the same Ecs level as its lowest. For harder ores, i.e. with lower Axb, 0,25 kWh/t is an appropriate value to consider linearity in the zero-energy curve. However, softer ores with larger Axb values, this energy value do not assure the linearity of the methodology assumption.

This case can be exemplified with two industrial cases where the Axb parameters were analysed (Altman et al., 2014) (Allaire et al., 2013) HDI was calculated by using the zero-energy slope at 0,25 kWh/t. An error between two similar Axb (92,2 and 98,6) values was compared to the HDI showing error values of 10% and 18%, as is shown in Table 3.

Table 3 Axb exercise

	A	*b*	*Axb*	*HDI*	*Error %*
Ore 1	91,7	1,07	98,1	88,3	10
Ore 2	47,4	2,08	98,5	80,7	18,2

Matei et al. (2015) highlighted the importance of understanding the Axb parameter as a parameter without physical meaning. For less competent ores, the Axb difference is less significant. However, the difference between the error of both cases, suggest that for softer ores, where theoretical maximum Ecs is reached at a lower t_{10}, the fluctuation of the slope and the asymptote of the curve behave in a complex form. Figure 12(a) shows the curve for both scenarios to exemplify the different behaviour for a similar Axb value. Figure 12(b) shows a close up of each curve from 0 to 0,25 kWh/t, showing that the linear tendency is observed in lower Ecs values than 0,25 kWh/t. These phenomena not also increase the error as long Axb decrease, but also shows that a corrector factor base in linearity might not address the different scenarios adequately for similar Axb values.

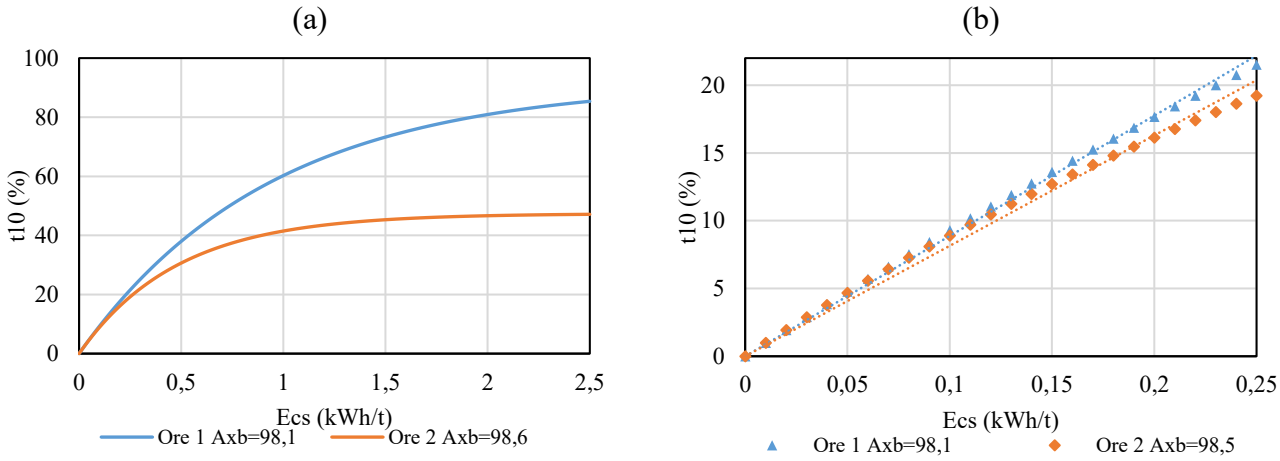

Figure 12 Ecs vs t10 curve for Ore 1 and 2 (a) full curve (b) close up at 0,25 kwh/t

Figure 13 shows a representation of the HIT device, that works with similar principles of a Drop Weight Test. A cup is located at the bottom of the device, where each particle is placed to be broken, and a crusher hammer is located in the top of the apparatus. The height and weight of the crusher assembly were modified in order to obtain a specific energy of 0,25 kWh/t (Bergeron et al., 2017)

Figure 13: HIT device (Kojovic et al., 2019)

The bond work index BWi can also be derived from HIT test results, allowing both competency and harness parameters to be determined with a single test. The estimation of the BWi uses information obtained from the product size distribution, such as the mass passing the 150 μm and 3,35 mm sieve, P_{80} and the initial sample mass (M20), Equation 18 describes the model proposed to obtain the BWi parameter.

$$BWi = K + a.SLOPE + b.R2 + c.P150 + d.P335 + e.P80 + f.M20 \quad (18)$$

In this equation, the parameter "Slope" and R are the slope and the coefficient of determination of the linear trend fitted to the product size distribution.

2.3.2.5 Point Load Test

The Point Load Test (PLT) provides information about the rock strength index of a rock specimen, such as the point load strength, impact strength index and the uniaxial compressive strength. The PLT uses drill core specimens in three configurations: diametrical, axial and irregular lumps.

The Point Load tester, as is shown in Figure 14, consisting of a loading frame with a jack piston, a hydraulic ram and a pressure gauge that indicates the maximum load (ASTM, 2008) of the test. Empirical correlations are being made to link the crushing reduction

ratio of Crushability Index with the compressive strength or Impact Strength Index (Toraman et al., 2010).

Figure 14 Point Load Tester

The PLT is a standard test in geometallurgy because it enables UCS data outcome at a low cost, this test is mainly used to determine geotechnical properties of the ore body. However strong correlation has been obtained between the Point Load Strength and the Drop Weight Index (Morrell, 2006), as is shown in Figure 15.

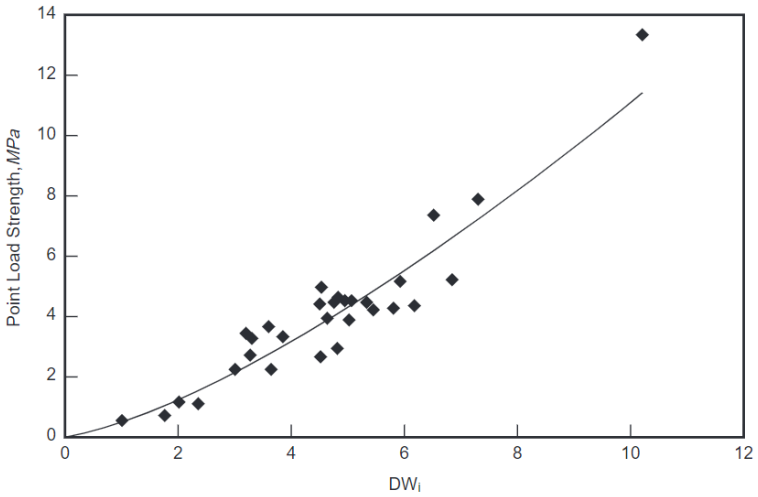

Figure 15: Point Load Strength vs DWi correlation (Morrell, 2006)

2.4 Geometallurgy

Geometallurgy is an interdisciplinary approach that uses 3D models of an ore deposit, which enable the optimisation for effective management while minimising technical and operational risk to ultimately provide more resilient operations (Dominy et al., 2018).

The need for an increase in optimisation comes from the current situation of more complex ores, lower ore grades, variability in the ore quality, the increase of production volumes, the more ambitious gasses emission goals, the metal price fluctuation and stricter environmental regulations. These are some of the challenges that the mining industry faces nowadays. (Lishchuk & Pettersson, 2020).

Prediction of throughput and recovery performance for each ore domain by using geometallurgical models are created by linking the block model, mine plan and the metallurgical information. Table 4 describes five stages to create a successful geometallurgical program, contemplating the validation of the model. This model can be used for forecasting, planning and longer-term optimisation purposes (Kham et al., 2014)

Table 4 Planning framework for geometallurgical program (McKay et al., 2016).

Stage	*Activity*	*Actions*	*Outputs*
1	Drilling	Measure-while-drilling core/chip logging	Rock types/alteration geotechnical geophysical
2	Test work	Analysis Mineralogy - Physical test work Recovery test work	Assay/geochemistry Metal/Mineral deportment Comminution/Hardness Flotation, leaching, gravity
3	Modelling	Domain analysis Geological modelling Geostatistical modelling	Update strategic block model Ore control block model Integrated mine mapping Block allocation
4	Mining	Mine design/planning Reconciliation	Blast design Blending strategy Stockpile management Validate model
5	Processing	Plant feed optimisation Reconciliation	Optimised plant Validated model

For a geometallurgical program, the scope of the project depends on multiple factors, such as resource size, number of geological domains, ore and metallurgical response variability, flowsheet complexity, among others. The question about the number of samples required to have a proper understanding of the ore variability has been raised on several occasions. Morell (2011) differentiates between a pre-feasibility study where the required number of samples is much lower than a geometallurgical model that aims to forecast a daily comminution throughput, in which case, the number of samples can increase in at least one order of magnitude.

Understanding of the ore variability is an essential role in understanding the effect of properties that affect a deposit in terms of processing. From the statistical point of view, variability must be understood by using values as the range between the most significant and smallest number, such as the variance, coefficient of variation and the standard deviation. Accordingly, the variance and standard deviation occupy the same exalted position among measures of variability as does the mean among measures of central tendency.

The knowledge of ore variability in the context of comminution optimization is fundamental to maximise equipment capacity and optimise throughput requirements. The variability analysis must be thorough, in this case, the criteria to adopt the 80_{th} percentile of the ore properties as a design value is not the best approach to account feed variability (Bueno *et al.,* 2015).

In terms of comminution, the rock structure is a measure of the natural fractures and discontinuities in the rock. It This is determined by the in-situ joints and fractures and can be estimated with rock quality designation (RQD), which is a fracture frequency and joint mapping performed by geologists when logging the drill core samples. Rock strength is a measure of the hardness of the rock matrix and can be measured with laboratory tests such as PLI, JK Drop Weight parameters (A, b, ta) and SMC Test® Drop Weight Index.

Several authors such as Powell and Morrison (2007), Mwanga *et al*. (2015) and Lois-Morales *et al*. (2020) have highlighted the importance of developing comminution tests capable of decoupling the breakage properties from the machine environment to have

comminution models that can carry particle information downstream in the process simulations.

The main standard ore characterisation tests and measurements used geometallurgy and comminution optimisation are described in Table 5.

Table 5 Characterisation tests for comminution optimisation (Valery et al., 2019)

Fragmentation Modelling	*Comminution Modelling*
Rock quality designation	Bond crushability work index
Fracture frequency	JK Drop Weight test
Joint and plane mapping Sirovision system	SMC Test®
Unconfined compressive strength	Bond rod mill work index
Point load Index	Bond ball mill work index
Young´s modulus	Bond impact work tests
	SAG Power Index

A sufficient number of tests must be done to measure both competency, with parameters like Axb, DWi or SPI, and hardness which is typically measured with the BWi. For a better understanding of the effect of ore variability in a comminution circuit, Bueno *et al.* (2015) explained the difference and importance of these two properties. While ore competency is directly related to SAG mill throughput, hardness has a strong influence on ball mill specific energy and grind size. These differences are essential at the moment of design SAB or SABC grinding circuits.

Al Ruiz *et al*. (2009) highlighted that for a robust model to describe a comminution circuit performance, the identification and selection of enough and relevant samples are

essential. Morell (2011) emphasised that it is essential to keep the cost at the minimum; which is one of the bases of the investigation and development of comminution for geometallurgy. Therefore, the aim is to test a higher number of samples while maintaining costs at a similar magnitude when compared to traditional standard tests. David (2019) mention the importance to separate two stages for the estimation of the number of samples required to have a suitable understanding of the ore-body variability. The first is to estimate the degree of variability of the deposit by testing a sufficient number of samples and the second is to test an adequate amount of samples to validate the confidence needed for design and simulation purposes.

3 METHODOLOGY DEVELOPMENT

The Geopyörä is a new breakage test device (PCT/FI2020/050100) which is capable of rapidly process a large number of smaller samples (< 2 kg) and reliably generate comminution parameters at a low cost. These features are in line with the description of an optimal geometallurgical test (Mwanga, 2016) which is a current need in the mining industry.

The test methodology was developed by testing both bulk and drill core samples from six mine sites. To preserve the confidentiality of the companies that collaborated with the project, the mines have been identified using letters, from A to E. Table 6 shows a description of the deposit type.

Table 6 Mine sample description

	Deposit type	*Sample type*
Mine A	Gold ore	Bulk and Drill core
Mine B	Polymetallic ore	Bulk and Drill core
Mine C	Nickel – Zinc ore	Bulk
Mine D	Polymetallic ore	Bulk and Drill core
Mine E	Phosphate ore	Bulk
Mine F	Silver – Zinc ore	Drill core

This chapter firstly describes the operation and functionality of the Geopyörä apparatus as well as the principles behind it. Secondly, the methodology used to obtain particles from both drill core and bulk samples for testing. Lastly, the sample preparation for conventional standard tests and their results which were later used to validate the test methodology presented in this thesis.

3.1 Geopyorä

To develop a fast, low-cost, and reliable breakage characterisation test for geo-metallurgical modelling, a new prototype device was commissioned as a part of a project. The device records the amount of energy, force and impulse of each breakage event

Geopyörä (Bueno et al., 2020) is a variation of an instrumented roll crusher with an adjustable gap to measure breakage forces and energy applied to rock particles during the breakage process. The prototype was developed at the University of Oulu and consists of two instrumented wheels of 600 millimetres diameter each, with an adjustable gap (Torvela et al., 2020) as shown in Figure 16. The steel wheels are powered by integrated electric motors placed in the frame; the available energy is ranged between 100 to 250 Joules. The device provides data on the impact force and measures the loss of rotational moment to determine the energy required for each particle breakage event

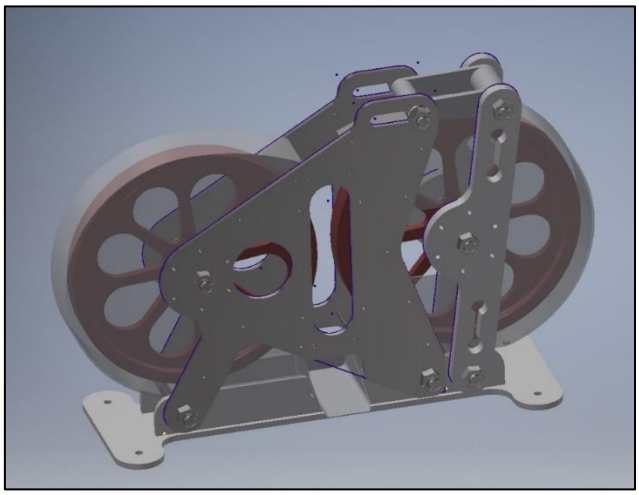

Figure 16 Representation of the Geopyorä device (Torvela, 2020)

The device processes a single particle at a time; the amount of energy spent on breaking each particle could be measured directly from the change in the speeds of the wheels over the crushing event. Besides, if the mass of each particle is recorded, the specific comminution energy of every individual event can be calculated. Design criteria, as is

shown in Table 7, were set in order to fulfil the objectives to have proper functioning in order to compare this new test with the traditional ones.

Table 7 Designs criteria for the Geopyörä prototype (Torvela, 2020).

Criteria	*Value*	*Notes*
Particle size range	16 – 50 mm	Main interest: 20 – 30 mm
Maximum gap ratio	4:1	
Gap adjustment range	4 – 50 mm	
Energy output	100 – 250 J	
Feed rate	5–10 seconds per particle	
Peak loading	70 kN	30 mm spherical particle; 100 MPa strength
Highest average power demand	50 W	250 Joules every 5 seconds
Peak estimated power output	12,5 kW	250 Joules over 20 milliseconds
Maximum roll surface speed	3 m/s	95 RPM for a roll of 600 mm in diameter
Roll diameter	530–796 mm	20–30 mm particle size; μ=0,24; See text.

After the building and assembly of the pieces and the electrical system, a software to record sensor signals were created by Torvela 2020. A disc with a gear tooth pattern on each wheel is converted into an electrical signal recorded by the software in order to measure the speed. The signal has three stages that record 100 ms before the breakage event, 400 ms during the rock breakage and 100 ms after the measurement ends.

In these 400 milliseconds of the main event, the software measure 2000 data points. For the breakage event, the software calculates the wheel speeds at particle entry and exit and

converts the data to a difference in stored kinetic energy- The energy is measure using Equation 19 for each wheel.

$$E = \frac{1}{2} \cdot J \cdot w^2 \tag{19}$$

Where J is the inertia of the wheel and w is the angular velocity. This test differentiates from the SMC Test®, JKDWT and HIT because instead of choosing an amount of energy to apply, the equipment records the energy applied for each breakage event.

The procedure of recording the energy contemplates an energy discount because of the friction of the wheels running freely.

The prototype is calibrated before every test session, in a friendly user fast way (around 5 minutes). The friction of the wheels to discount is calculated for every breakage event, by measuring the energy difference between the first and third stage, this value correlates with the velocity of each wheel. The energy recorded for each event is described in Equation 20.

$$E = \sum Energy\ wheels - \sum Friction \tag{20}$$

The angular speed used to perform the test was 80 rpm. This value was set by analysing particles of a wide range of competency. Crushing a particle with a higher rpm value means to apply a higher strain rate, causing more energy to be absorbed into more branching fractures, secondary cracking, and micro-cracking. Tests with lower rpm were tested, presented issues with the larger particle sizes of the most competent rocks.

The gap opening range is extensive, allowing to try different gap ratios between the primary particle geometrical mean and the gap. Gap ratios between the geometrical mean of the tested particles and the gap were; 25% 50% and 75%.

The particle sizes that can be tested for analyse are the following: –31,5+26,5 mm, –22,4+19 mm, –19+16 mm, –16+13,2 mm, –13,2+11,2 mm and –13,2+11,2 mm. Particles under 13,2 mm present accuracy problems with the energy measurements while the –31,5+26,5 mm particles of the hardest ore, in the 25% gap ratio, did not achieve a continues breakage event due to the lack of energy of the wheels.

3.2 Drill core preparation

The first part of the experimental work was to develop a methodology that allows enough particles to be obtained for testing by crushing one meter of half drill core. The reason behind this goal is that the commonly used procedure for handling bounded drill core samples is to use one half for geochemical analysis and preserve the other half in the archive for future purposes. In some cases, the first other half is used as a sample for metallurgical testing (Haldar, 2018).

This procedure, broadly used in mineral exploration and mine geology, of splitting the core along its length into two identical pieces, allows getting a similar mineral distribution on each side. For the drill core preparation, 15 meters of drill core from every mine in one-meter sections were used. The drill core diameter of the samples was sized as NQ and BQTK.

Table 8 Drill Cores size

Mine	*Core size*	*Core (inside) diameter, mm*
A	BQTK	40,7
D	BQTK	40,7
E	NQ	47,6

A pre-crushing and sieving stage to get enough particles of the desired particle sizes range were performed. In the pre-crushing stage, a jaw crusher was used to process the drill cores. Eight different gaps apertures were used, ranging from 23 mm to 8 mm.

Figure 17 shows the simple percentage of product mass retained in different size classes, from 26,5 to 8 mm. It can be observed that two extreme values, 23 mm and 8 mm, of the gap opening, presents the primary percentage values in the -26,5+22,4 mm and -9,5+8 mm respectively. This result is expected; however, it does not give enough information to determine the quantities of suitable particles for the test.

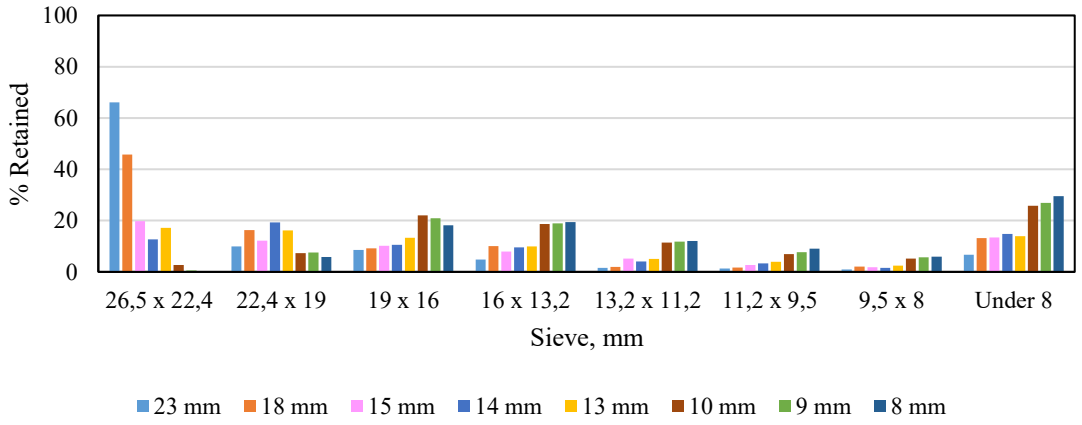

Figure 17 Percentage retained in specific particle size for the drill core preparation.

Figure 18 shows the distribution of the number of particles in different size classes for eight crusher gap settings. It can be observed that even though the 23 mm gap opening showed an apparently good percentage retained, the particles were not enough to assembly two sets of twenty particles for the test.

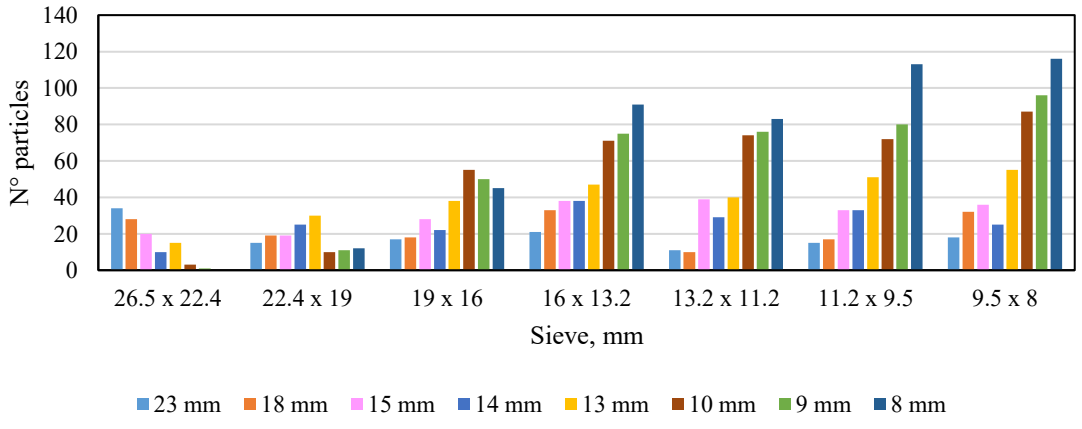

Figure 18 Distribution of the number of particles for the different gap scenarios

The shape of the particles was taken into consideration during this analysis, and flat particles were discarded. Figure 19 presents an example of the crushed product retained in the 19 mm sieve for the drill core of the mine E.

Figure 19 Crushed drill core particles retained in the 19 mm sieve

The optimum gap setting for the crushing stage was determined with a decision matrix, as is shown in Table 9. Two conditions were set to determine if a particular gap setting is optimal for given particle size. Ideally, the number of particles should be higher than 30 and lower than 70 particles.

Table 9 Gap scenarios matrix

	Crusher gap opening (mm)							
Size (mm)	23	18	15	14	13	10	9	8
26.5 x 22.4	1	0	0	0	0	0	0	0
22.4 x 19	0	0	0	0	1	0	0	0
19 x 16	0	0	0	0	1	1	1	1
16 x 13.2	0	1	1	1	1	0	0	0
13.2 x 11.2	0	0	1	0	1	0	0	0
11.2 x 9.5	0	0	1	1	1	0	0	0
9.5 x 8	0	1	1	0	1	0	0	0
Sum	**1**	**2**	**4**	**2**	**6**	**1**	**1**	**1**

The optimal pre-crushing gap aperture was found to be 13 millimetres because it generated the desired number of particles in six different size classes.

3.3 Bulk sample preparation

Three hundred kilograms of a bulk samples from each mine site were processed to perform tests using the Geopyörä apparatus and to prepare samples for other standard comminution tests. Each sample was crushed, sieved and separated in narrow size fractions from 63 mm to 8 mm. For each sample, the specific gravity was measured, as is shown in Table 10.

Table 10 Specific gravity for bulk samples

Mine sample	Specific gravity (kg/m^3)
A	2,95
B	3,20
C	2,98
D	2,90
E	2,80

Ore samples from the five mines were prepared and sent to the Wardell Armstrong laboratory in the UK, where standard JK Drop Weight and SMC Tests were performed.

At the same time, samples were prepared for the Geopyörä device, using the same particle selection criteria as for the JKDWT, in order to have duplicates as identical as possible. Table 11 shows the number of particles in each set, categorised per size and energy requirements.

For the Geopyörä test, after a preliminary evaluation of the prototype performance, the particle size selected to validate the test was -22,4+19 mm.

Table 11 Sample preparation sets

Size (mm)	JK Drop Weight Test		SMC Test®		Geopyörä
	Particles	Energy	Particles	Energy	Particles
-63+53	10	0,4			
	10	0,25	X	X	X
	10	0,1			
-45+37,5	15	1			
	15	0,25	X	X	X
	15	0,1			
-31,5+26,5	30	2,5	1,76	20	
	30	1	0,49	20	X
	30	0,25	X	X	
-22,4+19	30	2,5	1,76	20	30
	30	1	0,49	20	30
	30	0,25	X	X	30
-16+13,2	30	2,5			
	30	1	X	X	X
	30	0,25			

After the JKDWT and SMC Tests, the crushed samples were returned to the OMS facilities, where the final product sieving was conducted to obtain the t_{10} value of the 85 particle sets (75 from the JK Drop Weight Test and 10 from the SMC Test®).

Table 12 JKDWT parameters

	A	*b*	*Axb*	*SG*
A	57,9	0,55	31,8	2,95
B	71,2	0,49	34,9	3,20
C	78,3	0,40	31,3	2,98
D	67,6	0,89	60,2	2,90
E	67,8	1,31	88,8	2,80

Table 12 summarizes the JK Drop Weight Test results, where Axb parameter represents the competence of the ore. As is shown in Figure 20, Mine A and C are considered hard ores, Mine B intermediate, while D and E are soft ores.

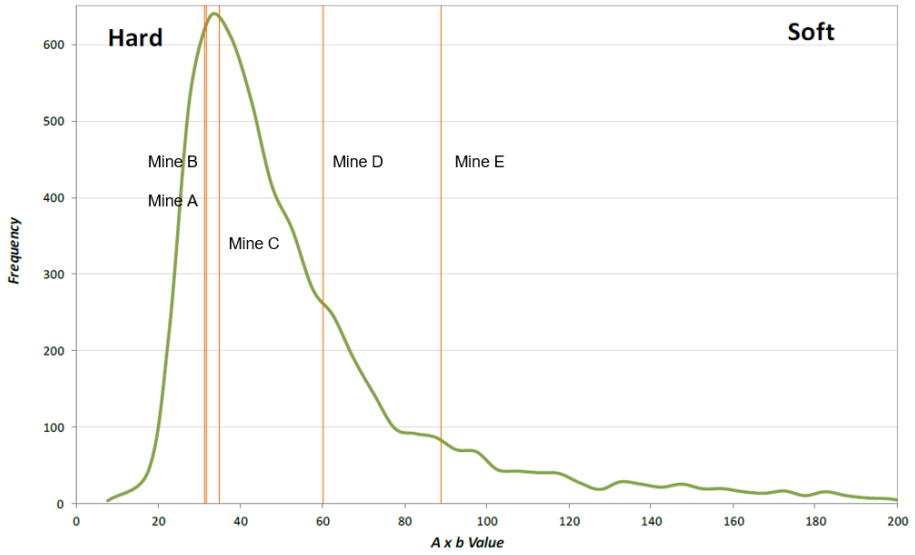

Figure 20 Frequency Distribution of Axb in the JKTech Database

The results from the SMC Test® present two key parameters, the Axb and the Drop Weight Index (DWi). Table 13 shows the Axb values with the respective fitting parameters, A and b. Drop Weight Index values are also shown; this parameter is a value that represents the resistance of a sample to impact breakage. The DWi is measured in kWh/m^3 and has a direct and inverse non-linear correlation with the Axb parameter.

Table 13 SMC Axb and DWi parameters

	A	*b*	*Axb*	*DWi (kWh/m^3)*	*DWi (%)*
A	72,7	0,41	29,8	9,8	86
B	81,9	0,44	36,0	8,8	77
C	100	0,30	30,0	9,7	85
D	72,7	0,85	61,8	4,4	22
E	66,2	1,44	95,3	2,7	9

The samples were further crushed until all the material was passing 3,35 millimetres to meet the feed size criteria of the standard Bond ball mill test (Bond, 1961), which were performed on each sample using a closing screen aperture of 150 µm. The results of the Bond Ball Mill Test are summarised in Table 14, where it can be observed that the highest

value (Hardest ore) is the ore A, followed by the ore C, showing consistency with the Axb and DWi parameters.

Table 14 Bond Ball Mill Test results

Ore Source	*Feed mass (g)*	*F80 (µm)*	*P80 (µm)*	*Bond Work Index (kWh/t)*
A	1211,2	2534	84	25,6
B	1400,5	2205	109	19,5
C	1301,9	2276	102	22,8
D	1366,3	2226	113	11,4
E	1300,0	2225	113	9,1

Detailed information of the Bond Ball Mill Work Test can be found in Appendix A, and the complete results for JKDWT and SMC Tests can be found in Appendix C.

4 RESULTS AND VALIDATION

Seventy-four tests were performed to the different ore samples in the following particles sizes classes: -31,5 + 26,5 mm, -22,4 + 19 mm, -19 + 16 mm, -16 + 13,2 mm, -13,2 + 11,2 mm and -11,2 + 9,5 mm. The tests were conducted at a range of specific energy levels, from 9,5 to 31,5. Considering that the Geopyörä test does not use pre-determined energy values, as in JKDW and SMC Tests, the energy is adjusted by changing gap apertures. The smaller the gap, the higher the breakage energy. Particle to gap ratios of 75%, 50% and 25% were used during the experiments.

Particles in the two smaller sizes (-13,2 + 11,2 mm and -11,2 + 9,5 mm) had a low detection rate at all the tested gap ratios (75%, 50% and 25%). The data was not reliable, and this can be explained due to the fact that the breakage energy was close to the detection and accuracy limits of the machine.

For the particles of -31,5 + 26,5 mm, technical issues were observed for the hardest ores (A, B and C), in the gap ratio of 25% (highest energy level). During some breakage events, the wheels stopped because they had not sufficient energy to break the particle.

The achieved specific energy ranges for the various tested samples are shown in Table 15. The maximum and minimum values obtained for six different particle sizes are presented. The maximum value, 1,35 kWh/t, almost half of the highest energy value that JKDWT use.

Table 15 Energy range per particle size

Particle size (mm)	High Energy (kWh/t)	Low Energy (kWh/t)
22.4 x 19	0.81	0.11
19 x 16	1.25	0.28
16 x 13.2	0.8	0.34

For this thesis, particles of -22,4 + 19 mm were chosen to validate the performance of this prototype thoroughly.

The reason why this particle size was determined is due to the excellent consistency in the parameters of the Geopyörä tests and to have similar conditions (size and amount) to the JK Drop Weight Test. The particle sets created for this validation were selected at the same time, with the same criteria and from the same particle population of the sets prepare to the Wardell Armstrong laboratory tests. Since these breakage tests use a manual particle selection method, there is a potential bias effect (Napier-Munn et al., 2020), and this procedure was adopted to minimise any bias in the particle selection.

4.1 Geopyörä measurements

The Geopyörä device records three parameters for every breakage event; energy (J), impulse (Ns) and peak force (F). The results of these three parameters and their respective parameter of variation are presented in this section.

The coefficient of variation was the main statistic parameter used in the data analysis because it represents the extent of variability within a sample. The coefficient of variation is a proportion between the mean and the standard deviation. Understanding the variability of the data for similar populations under different operation conditions can reflect operational or measurement errors or biases.

Impulse and energy are directly correlated properties; Figure 21 shows the energy mean values (J) against the impulse (Ns) recorded for the breakage events. A linear fit can be observed, meaning a cohesive measurement between the prototype measures.

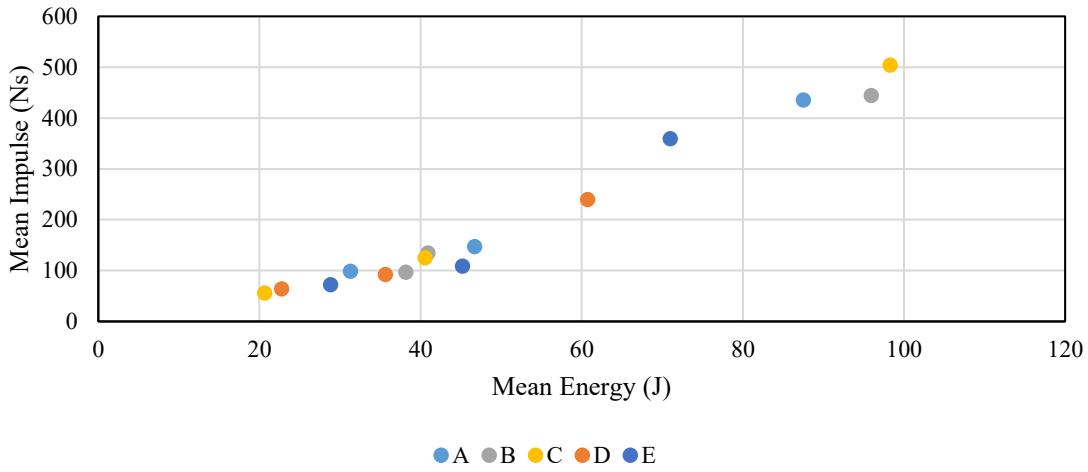

Figure 21 Impulse (Ns) vs Energy (J) for the 22,4x19 particles

Table 16 shows the results of the mean energy (J) of the three sets per ore type tested for the validation. In the column gap, close, medium and open represents gap ratios of (75%, 50% and 25%)

Table 16 Results of the energy measurements for the five mines

	Energy level	Mean (J)	Std dev (J)	Coeff. Of var. (%)
A	High	87,5	40,7	46,5
	Mid	46,7	19,1	40,9
	Low	31,3	19,2	61,5
B	High	96,0	37,5	39,1
	Mid	57,6	40,9	71,0
	Low	30,9	14,1	45,6
C	High	98,3	40,7	41,4
	Mid	40,6	27,1	66,9
	Low	20,7	9,3	44,8
D	High	55,9	20,2	36,1
	Mid	35,6	14,8	41,5
	Low	22,8	12,9	56,5
E	High	71,0	24,7	34,9
	Mid	45,2	19,3	42,8
	Low	28,9	8,7	30,2

Figure 22 shows the specific comminution energy (Ecs) compared to the register impulse values consistency in the data can be observed.

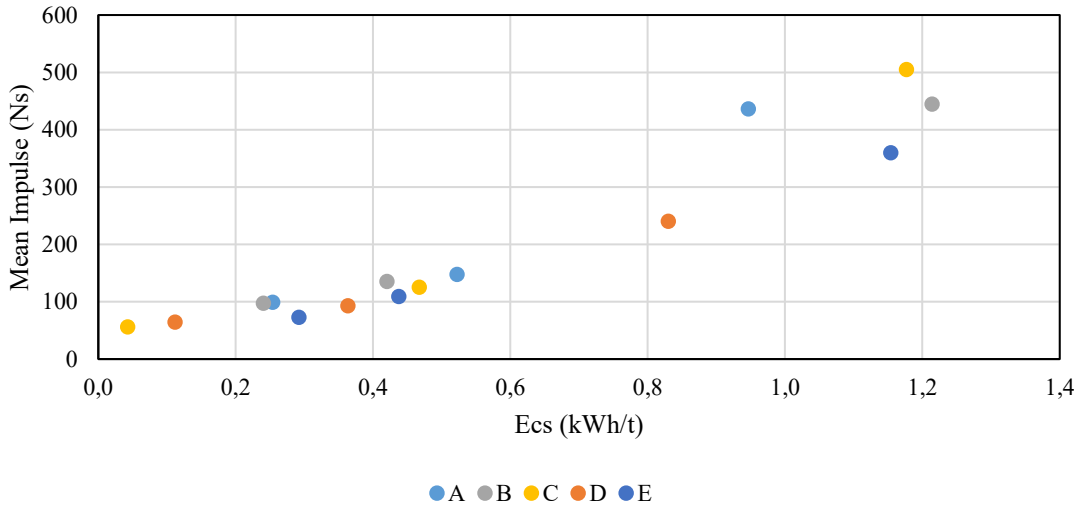

Figure 22 Mean impulse (Ns) vs Specific energy (kWh/t) for the 22,4x19 particles

The specific comminution energy (Ecs) was calculated as the sum of all the energy events divided into the total mass of the set, as is shown in Equation 21.

$$Ecs = \frac{\sum Energy}{mass\ set} \tag{21}$$

Table 17 shows the result of the impulse measurement, and there is not a straightforward relationship between the coefficient of variation and the gap opening for the different ore types. For some ores, such as mine A and D the highest variability in the data is presented in the close gap ratio, while ore type C and E present the different values.

Table 17 Results of the impulse measurements for the five mines

	Energy level	Mean (Ns)	Std dev (Ns)	Coeff. Of var. (%)
A	Close	436,0	330,1	75,7
	Medium	147,4	65,3	44,3
	Open	99,1	61,7	62,3
B	Close	444,4	218,5	49,2
	Medium	135,0	73,8	54,7
	Open	39,8	28,0	70,3
C	Close	504,6	243,8	48,3
	Medium	125,5	83,6	66,6
	Open	56,2	28,2	50,2
D	Close	190,0	101,2	53,2
	Medium	92,9	43,4	46,7
	Open	64,6	31,5	48,7
E	Close	359,5	217,0	60,4
	Medium	153,3	110,3	72,0
	Open	72,5	26,5	36,5

Peak force values range from 25707 N to 7387 N. The analysis of possible relationships between peak force, and uniaxial compressive strength was not with the scope of this thesis, but it should be investigated in the future. The possibility of deriving rock mechanics parameters, such as UCS, in addition to comminution parameters, is an attractive opportunity of research. In the context of having comminution tests with decoupled information about the particle composition and the behaviour in a mechanical environment for a better simulation of the downstream process (Lois-Morales et al., 2020) (Powell & Morrison, 2007)

Additionally, the peak force was recorded for each breakage event, and the mean values are presented in Table 18. As for the impulse, there is no correlation between the data dispersion and the gap opening for the tests performed in the five ore types, as is shown in Table 18.

Table 18 Results of the force measurements for the five mines

	Energy level	*Mean (N)*	*Std dev (N)*	*Coeff. Of var. (%)*
A	High	22 079	9 331	42,3
	Mid	17 515	7 026	40,1
	Low	15 117	9 838	65,1
B	High	22 944	8 066	35,2
	Mid	15 929	6 204	38,9
	Low	16 586	6 360	38,3
C	High	25 707	9 236	35,9
	Mid	13 507	6 840	50,6
	Low	10 246	5 149	50,3
D	High	12 877	6 167	47,9
	Mid	11 187	4 569	40,8
	Low	9 111	3 772	41,4
E	High	18 872	11 349	60,1
	Mid	10 161	5 688	56,0
	Low	7 387	2 321	31,4

The values observed in this section are a first approach to analyse how the prototype is behaving in a range of operating conditions for different ore types. There is a right consistency in the data, and the coefficient of variation presents a limited range of values. However, there is no trend between different energy levels and variability.

Consistent results confirmed the excellent precision of energy measurements. However, in order to analyse the accuracy of these values is essential to benchmark it against results from other standard tests used in industry nowadays.

4.2 Breakage distribution validation

Using Equation 22 with the A and b parameters from the JKDWT and SMC Tests reported by JKTech (Appendix C), t_{10} values were calculated for the Ecs measured with the Geopyörä. The calculated t_{10} values are presented in Table 19 in comparison with those obtained in the Geopyörä for the same Ecs. The highest variations between the measured and calculated t_{10} was for ore type A in the 75% gap ratio (low energy level). This difference can be explained due to the shape of the rocks. Even though the procedure was to discard flat particles, these particles were elongated, meaning that for the highest gap opening (lowest energy) some particle pass thought the wheels, without a full-body breakage, only chipping.

$$t_{10} = A \cdot (1 - exp^{-b \cdot Ecs}) \quad (22)$$

Table 19 Comparison of the calculated JKDWT and SMC Test® t10 and the measure t10 of Geopyorä test

Mine	Size (mm)	Ecs (kW/t)	JKDWT t10 (%)	SMC Test® t10 (%)	Geopyörä t10 (%)
A	22,4x19	0,95	23,5	23,4	26,7
		0,52	14,5	14,0	15,7
		0,25	7,6	7,2	4,1
B	22,4x19	1,21	31,9	33,9	32,8
		0,42	13,3	13,8	11,5
		0,24	7,9	8,2	5,2
C	22,4x19	1,18	29,4	29,7	29,1
		0,47	13,3	13,0	11,2
		0,04	1,3	1,3	1,0
D	22,4x19	0,71	31,7	32,9	33,5
		0,36	18,7	19,3	16,2
		0,11	6,3	6,5	5,6
E	22,4x19	1,15	52,8	53,6	51,5
		0,44	29,6	30,9	29,6
		0,29	21,6	22,7	18,7

Despite the problem observed in the lowest energy level, there is an excellent correlation between the calculated JKDWT and the measured Geopyörä t_{10}, as is shown in Figure 23. The value of the coefficient of determination is 0,97, confirm the strong correlation.

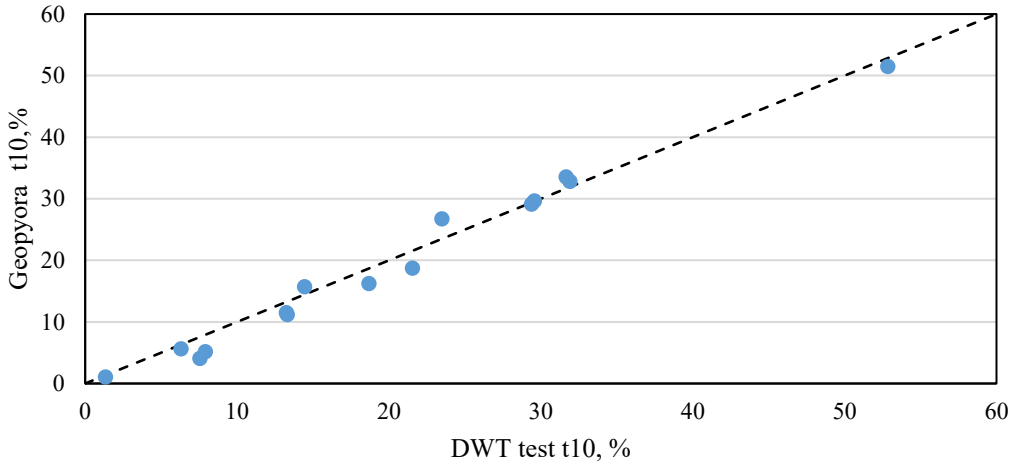

Figure 23 Comparison between the JKDWT t10 vs Measured Geopyörä t10

The same analysis was conducted using the SMC Test® A and b parameters in equation 19. Although there is a higher dispersion in the data, a strong correlation was achieved, as shown in Figure 24.

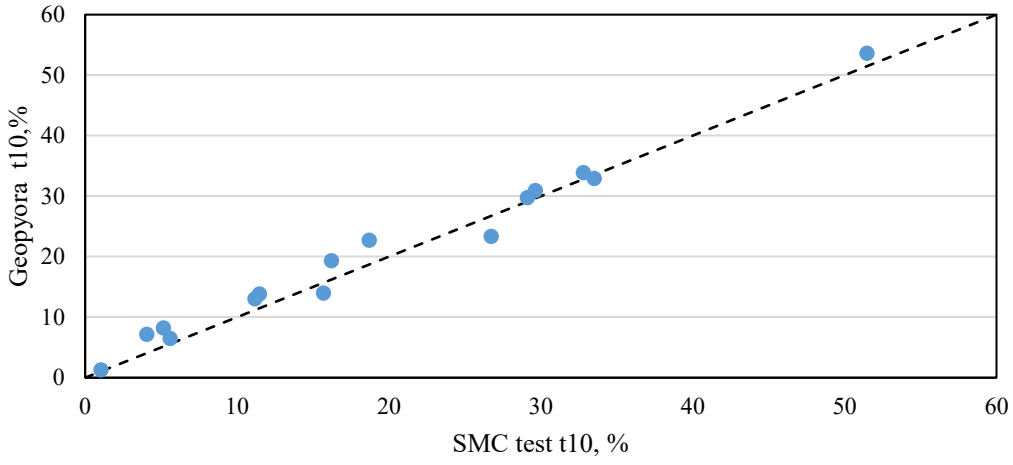

Figure 24 Comparison between the SMC Test® t10 vs Measured Geopyörä t10

The comparison of the measure t_{10} after the breakage tests using the Geopyörä with both the SMC Test® and JKDWT calculated t_{10} shows an excellent correlation. Thus, the Axb parameters correlate appropriately with the results of the Geopyörä test, within a relative error of ± 10% across all samples.

4.3 Energy validation

A different approach to validate the Geopyörä test is to do the opposite exercise with the breakage equation, meaning that with the t_{10} values recorded after each Geopyörä test. Equation 23 describes how the specific comminution energy (Ecs) was calculated by using the same t_{10} values of the Geopyörä tests.

$$Ecs = -\frac{ln\left(1 - \frac{t_{10}}{A}\right)}{b} \tag{23}$$

Table 20 shows the calculated Ecs values using the JK Drop Weight Test and SMC Test® A and b parameters, with the relative error of both measurements.

Table 20 Comparison of error between the Geopyörä Ecs and the calculate specific energy of the JKDWT and SMC Test®

		Ecs (kWh/t)			*Error (%)*	
Mine	Size (mm)	Geopyörä	JKDWT	SMC Test®	JKDWT	SMC Test®
A	22,4x19	0,95 0,52 0,25	1,13 0,57 0,13	1,12 0,59 0,14	16 9 92	15 12 81
B	22,4x19	0,71 0,36 0,11	0,77 0,31 0,10	0,73 0,30 0,09	8 18 15	2 22 19
C	22,4x19	1,21 0,42 0,24	1,26 0,36 0,15	1,16 0,34 0,15	4 17 57	4 22 63
D	22,4x19	1,18 0,47 0,04	1,16 0,39 0,03	1,15 0,40 0,03	1 21 29	3 18 24
E	22,4x19	1,15 0,44 0,29	1,09 0,44 0,25	1,04 0,41 0,23	6 0 18	10 6 27

The relative error increased at lowest energies, i.e. the largest gap opening. This is in accordance with the shape of the particles. Ore type A and C are the ones which present the most non-cubic shape, increasing the probability of passing through the wheels without recording an energy value or recording just the nipping of the wheels.

The Geopyörä design aimed for a single impact, allowing for fragments of broken particles to pass freely through the gap without further breakage. This has been confirmed by this data analysis, where the highest value recorded was 1,21 kWh/t.

Values in this order of magnitude is an indication that the high energy levels used in the JKDWT and SMC Test® are providing more energy than it is required to break the particle. Previous studies have shown that at high energy levels (2,5 kWh/t), the JKDWT is causing secondary breakage or even compressing the fragments into a cake (Chandramohan et al., 2015).

4.4 Comparison of measuring 3 or 2 energy levels

There is a possibility to simplify the Geopyörä procedure by using two energy levels rather than 3. To evaluate the impact of this simplification three cases where proposed;

a. Case 1 represents the three energy values, obtained with the gap ratio of 75%, 50% and 25%.
b. Case 2 represents two energy levels, using the high and low gap ratios of 75% and 25%.
c. Case 3 represents two energy levels, using the gap ratios of 50% and 25%.

The three cases were analysed according to the Axb parameter results obtained from the JKDWT, and SMC Tests against those calculated using the Geopyörä Test.

4.5 Axb comparison.

The Axb parameter represents the ore competence, meaning the ore resistance to breakage. This A and b are fitted parameters from the breakage equation that describes the breakage distribution parameter (t_{10}) as a function of the applied specific energy (Ecs). This parameter is used to predicts the power draw and power size distribution of an AG/SAG mill for a given feed size distribution and feed rate (Morrell & Morrison, 1996).

The JKDWT Axb is a recognised metric widely used in comminution modelling. This parameter is a qualitative measure that inversely proportional to the impact resistance, and this relationship is non-linear (Matei et al., 2015). The Axb results from JKDWT were compared with the A and b parameters fitted to the specific energy (kWh/t) versus t_{10} (%) relationship measured with the Geopyörä prototype. Table 21 shows the results of the individual parameters A and b for the three cases, while the results of the parameter Axb are presented in Table 22.

Table 21 A and b parameters values for the three fitting cases

	Case 1		*Case 2*		*Case 3*	
	A	b	A	b	A	b
A	100,0	0,32	100,0	0,31	100	0,33
B	100,0	0,32	100,0	0,32	100	0,32
C	100,0	0,29	100,0	0,29	100	0,29
D	98,5	0,51	78,3	0,67	100	0,55
E	68,9	1,20	77,5	0,95	63,7	1,43

Table 22 Axb of the JKDWT, SMC Test® and Geopyörä cases

	A x b				
	JKDWT	SMC Test®	Case A	Case B	Case C
A	31,9	29,8	31,6	32,0	32,8
B	34,9	36,0	31,5	32,9	32,1
C	31,3	30,0	28,5	30,1	28,5
D	60,2	61,8	50,1	50,4	55,0
E	88,8	95,3	82,7	75,4	91,2

Figure 25 shows the comparison of the Axb results in case 1, with three energy points. For the less competent ores, the values of Axb are lower than the one reported for the JKDW and SMC tests.

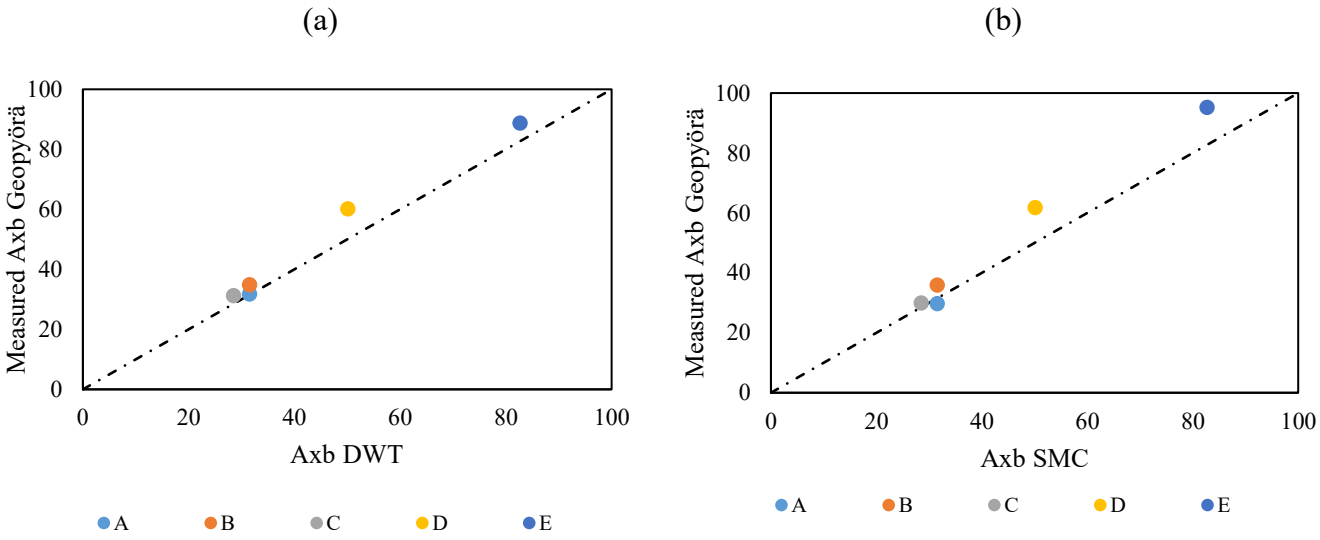

Figure 25 Case 1: Comparison of the calculated Axb for (a) JKDWT (b) SMC Test®

Figure 26 shows the Axb parameter for case 2, using gap ratios of 4:1 and 4:3. It can be observed that for the ore type E, the value is significantly lower than the one reported in the JKDW and SMC tests. This value is concordant with the highest error presented in Ecs comparison for the 4:3 gap ratio.

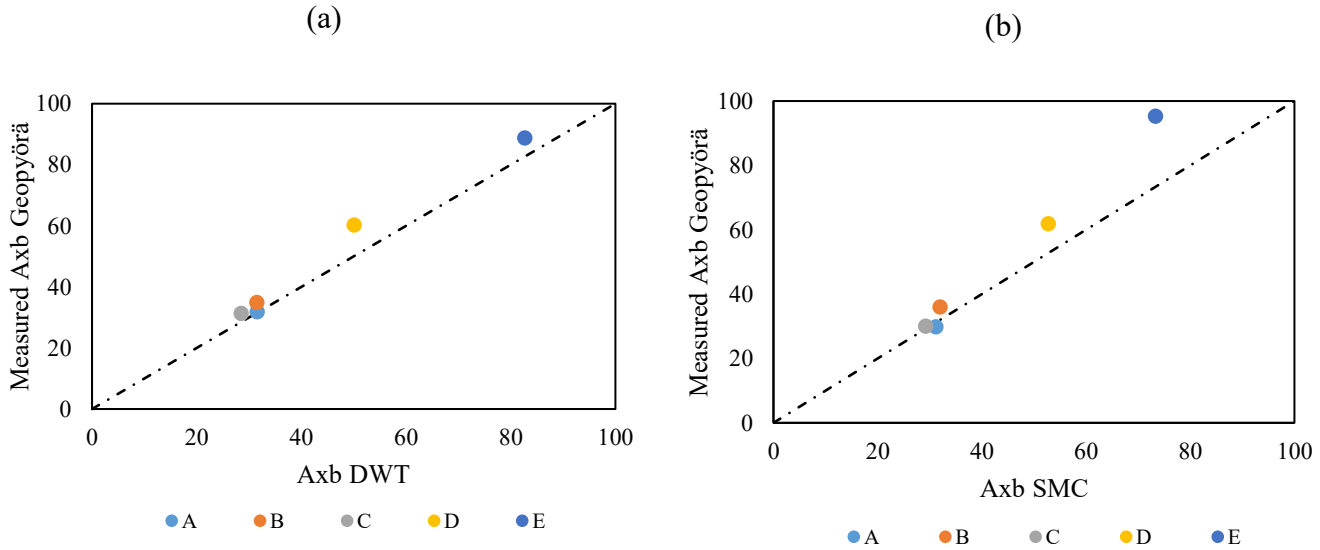

Figure 26 Case 2: Comparison of the calculated Axb for (a) JKDWT (b) SMC Test®

The comparison for case 3, which uses the two lowest gap ratios, is shown in Figure 27. A better agreement with Geopyörä Axb results can be observed in this case.

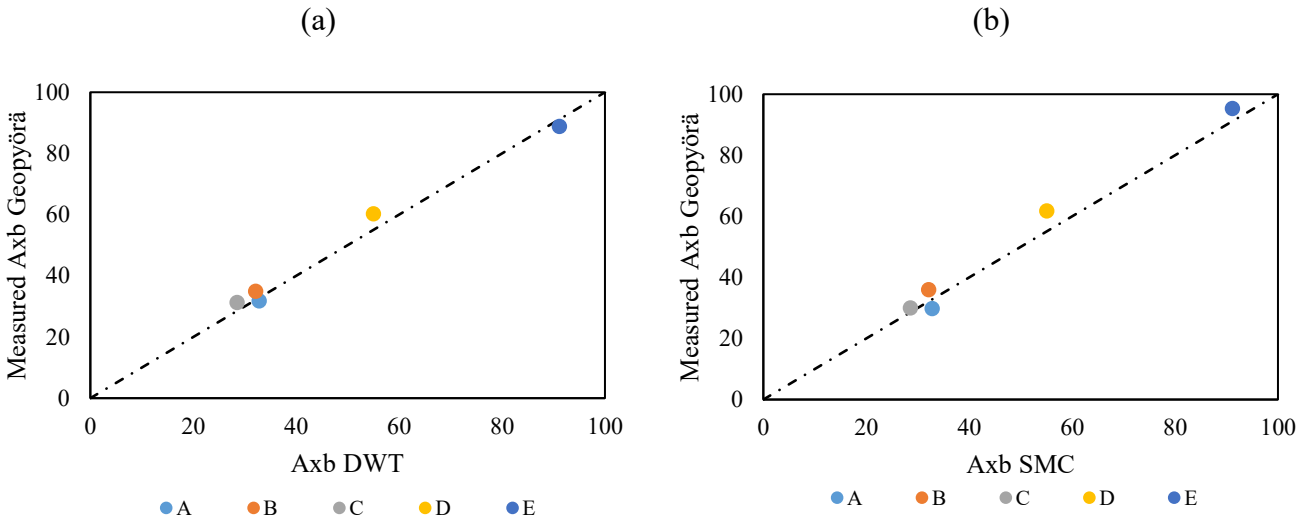

Figure 27 Case 3: Comparison of the calculated Axb for (a) JKDWT (b) SMC Test®

Table 23 shows the results of the three scenarios compared to the JKDWT Axb. The average relative error of the Axb fitted using three energy levels (case 1) is 1% lower than using case 3. However, the best scenario was achieved in case 3, which used the two highest energies levels to fit A and b parameters, with an average relative error of 6,2%.

Table 23 Relative error for the comparison between the three scenarios and the JKDWT Axb

	JKDWT Relative Error (%)		
	Case 1	Case 2	Case 3
A	0,8	2,0	3,2
B	9,6	8,3	8,0
C	8,9	6,6	8,9
D	16,8	12,4	8,6
E	6,9	17,4	2,7
Average error (%)	8,6	9,4	6,2

From this analysis, it can be concluded that the Geopyörä test can derive reliable Axb parameters by using only two breakage energy levels and single-particle size, in comparison to the full JKDWT.

Table 24 shows the relative error of the Axb parameter obtained with the Geopyörä test against the SMC Test® values, confirming that a better agreement is obtained in case 3, where the average error is 8,2%.

Table 24 Relative error for the comparison between the three scenarios and the SMC Test® Axb

	SMC Test® Relative Error (%)		
	Case 1	Case 2	Case 3
A	5,9	4,6	10,1
B	12,4	11,1	10,8
C	5,0	2,6	4,9
D	18,9	14,7	10,9
E	13,2	23,1	4,3
Average error (%)	11,1	11,2	8,2

These results are in line with the errors in energy measurements reported in section 4.2. For larger gap apertures (75%), i.e. low energy, flaky particles do not fully break and tend to either pass freely through the gap or only be chipped.

Although the specific energy in Geopyörä cannot be select at nominal levels and it cannot reach the same high levels as in the JKDWT and SMC Tests, the Axb parameters obtained both tests were in good agreement. While the JKDWT uses five particle sizes and three energy levels, the Geopyörä using only one particle size two energy levels could provide a reasonably good fit of A and b parameters.

Table 25 shows the experimental data points, and the fitted model curve to the five ore types analysed. In terms of the shape of the curve, the more significant discrepancies can be observed in the ore type A, and D. This two are types are not the one that shows the most significant error in the comparison between the Axb parameter, and they represent a very hard and very soft ore respectively.

Table 25 Ecs vs t10 for JKDWT, SMC Test® and Geopyörä for (a) Mine A (b) Mine b (c) Mine C (d) Mine D (e) Mine E

(a)

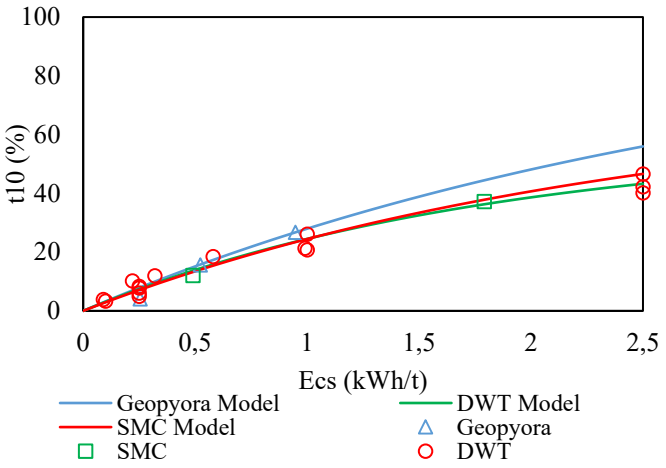

(b)

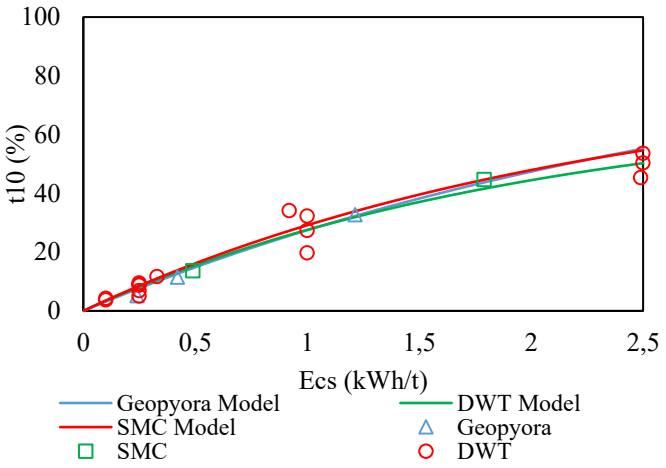

(c)

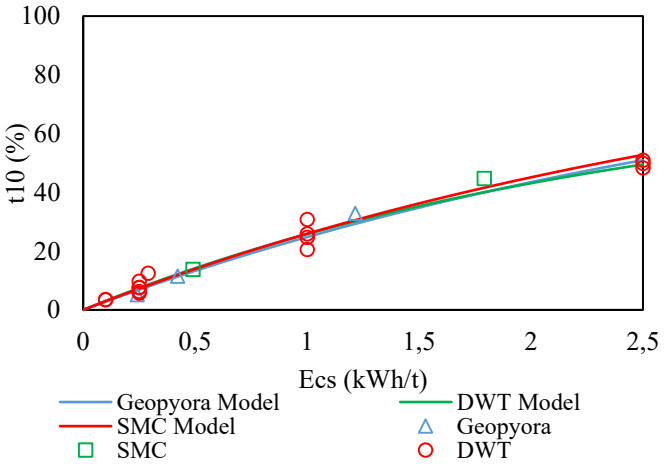

(d)

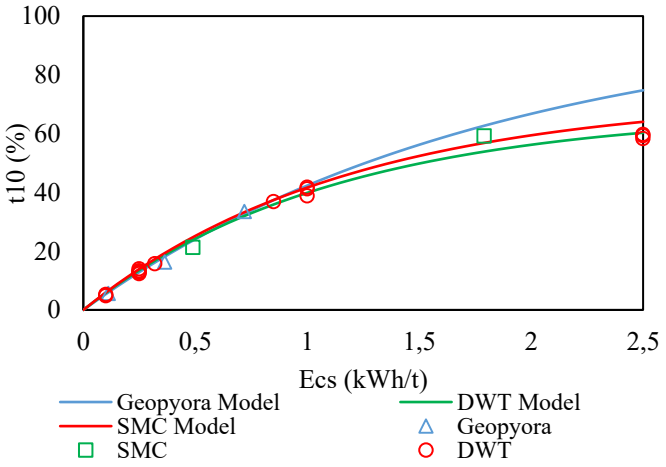

(e)

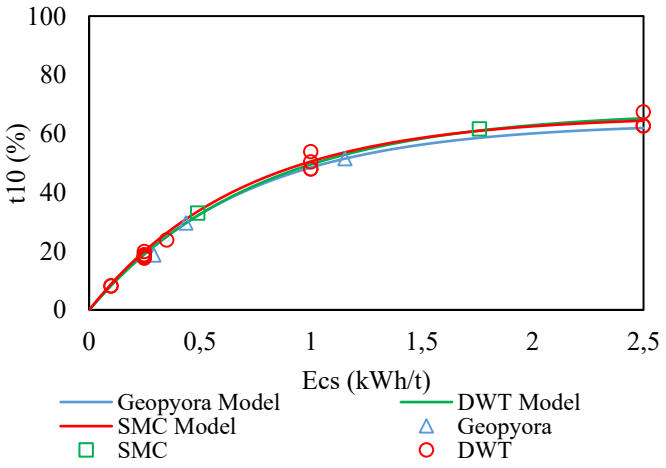

4.6 SMC Test® Drop Weight Index

Another widely used metric to measure competency is the Drop Weight Index DWi, obtained from the SMC Test®. This test has more than 35.000 measured data in over 1.300 ore bodies (Morrell, 2015). The DWi can be calculated by using the empirical Equation 24 (Doll, 2016) with the Axb calculated in the past subchapter.

$$DWi = \frac{SG \cdot 96{,}703}{(Axb)^{0{,}992}} \tag{24}$$

Figure 28 shows consistency between the Geopyörä estimated DWi the actual results from SMC Test®. Dashed lines show a dispersion range of ± 15%; four of the five samples are within this range. A good agreement between the estimated value using the Geopyörä test and the measured DWi can be observed, with an average error of 5,4%. These results are consistent with the Axb parameter validation.

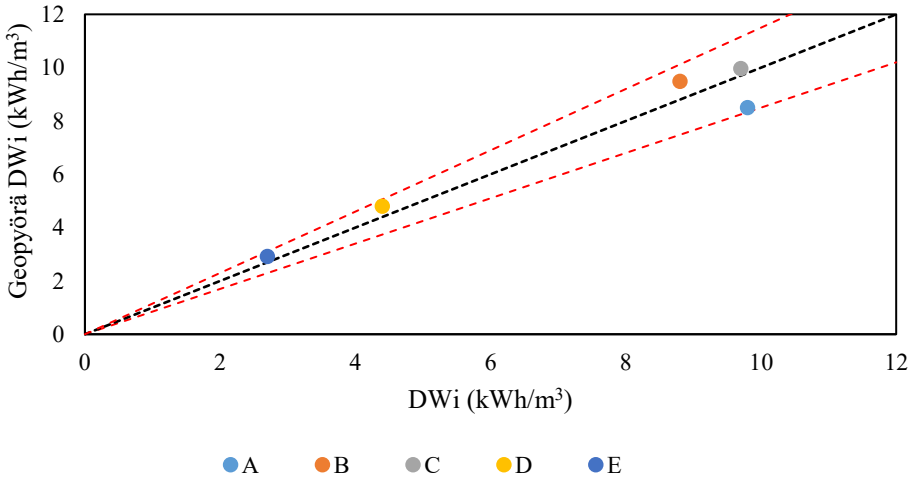

Figure 28 Comparison between DWi and Geopyörä calculated DWi

4.7 Bond Ball Mill Work Index

Standard Bond ball mill tests were performed to determine the Bond ball mill work Index (BBMWi) for each sample. The results were compared to BBMWi values estimated using the Geopyörä data. The BBMWi was estimated using the measured specific breakage energy, i.e. the amount of net product passing on closing screen aperture used in Bond test (150 µm) per applied kWh. Equation 25 shows the relationship used to calculate the Wi parameter as an average of the results for every energy value obtained for a specific ore type in particle size.

$$Wi_{GP} = \frac{\sum_1^n \frac{Ecs}{P_{150}}}{n} \tag{25}$$

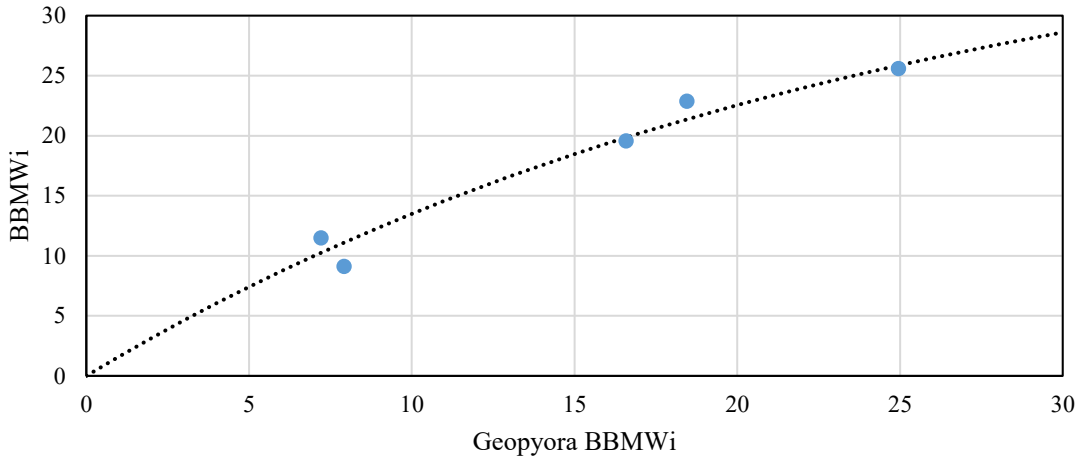

Equation 26 shows how the Geopyörä BBMWi is calculated by using the specific energy of the sample test, and the 150 µm percentage passing, α and β are fitted parameters.

$$BBMWi = \alpha \cdot (1 - exp^{-\beta \cdot Wi_{GP}}) \tag{26}$$

The values of the Geopyörä and the BBMWi are presented in Table 26. The highest error is registered in the softer ore type. The average error is 9,6%.

Table 26 Error between BBMWi and Geopyörä results

Mine	*Geopyörä*	*BBMWi*	*Error (%)*
A	25,6	26,1	2,1
B	19,6	20,0	2,2
C	22,9	21,3	6,7
D	11,5	9,9	14,0
E	9,1	11,4	24,9

Figure 29 shows a comparison between the BBMWi measured using the standard procedure and the BBMWi estimated using the Geopyörä data. A satisfactory correlation can be observed with four out of the five results within a relative error range of ± 15% (dashed lines), which is a sign that the Geopyörä can also provide a reasonable estimation of ore grindability.

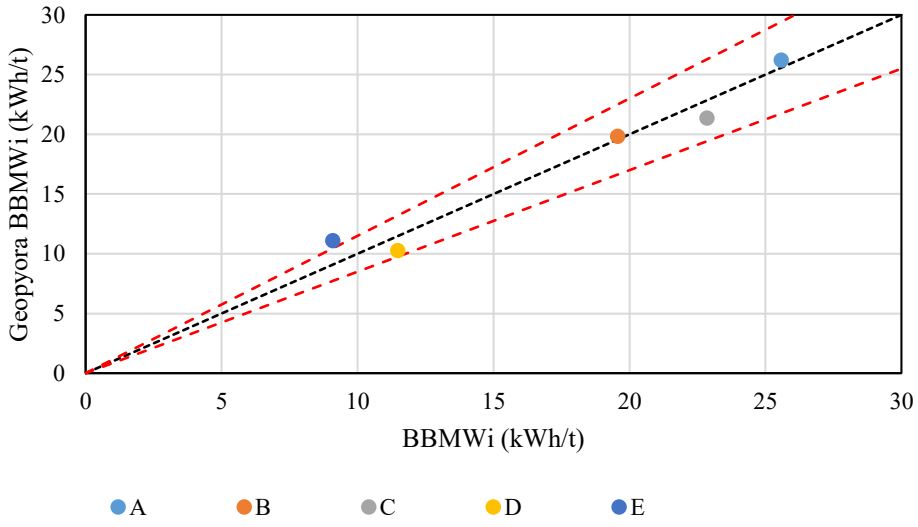

Figure 29 Comparison of BBMWi and the Geopyörä estimated BBMWi

This analysis contemplates a validation of parameters using a screen aperture of 150 micrometres, for both the estimated and measured BBMWi. Although the same principle could be applied for different closing screen apertures, it would have to be validated. It is also possible to obtain correlations with correction factors in case of comparing the Geopyörä estimation with other screen apertures of the Bond Ball Mill test. Nonetheless, these possibilities were not investigated in this thesis work.

4.8 Geopyörä testing procedure

To develop a methodology for the Geopyörä test; sets of 30 and 20 particles from 31,5 mm to 8 mm size were prepared. The samples were tested using three or two energy levels, which can be modified by simply adjusting the gap opening as a ratio of the average particle size. The particle selection procedure used was similar to that in the JKDWT, i.e. randomly selected and manually picked from narrow size fractions.

Each set of 30 particles selected for the test are placed in the automatic feeder, which releases one at a time to be broken between the wheels. During each breakage event, the force, impulse and energy applied to the particle are recorded. The broken product from all particles in the set is collected in a tray at the bottom of the device. Samples were tested using 3 or 2 energy levels. The energy levels can be modified by setting the gap opening as a percentage of the geometric mean of the passing size of the selected particles. The tests with three energy levels represent a gap to particle ratio of 25%, 50% and 75%. The last step of the test procedure is the sieving of the collected, crushed material of each set to determine the t_{10} parameter.

The best suited particle sizes to conducted Geopyörä tests are the following: -22,4 + 19 mm, -19 + 16 mm and -16 + 13,2 mm. Two sets of 30 or 20 particles, depending on the material availability, should be prepared for high and low energy levels.

The gap adjustment should ideally be in a ratio of 25% and 50%. For example, a particle in the size class of -16 + 13,2 mm has a geometric mean of 14,5 mm, and the gap should be set at 3,5 mm and 7 mm respectively for high and low energy.

The first step of the Geopyörä test is an initial calibration. This procedure must be done at the beginning of every test session to account for the rotational speed of the wheels impact on friction losses.

The individual mass of each particle in a set should be recorded prior to the test if the distribution of specific comminution energy is to be determined instead of an average for

the set. Although this procedure is currently done manually, it will be automated in the future.

This procedure should be followed for the two or three energy levels by adjusting the gap and using one set of particles for each set. The final product of each set is collected for particle size analysis using a stack of sieves containing the t_{10} aperture size and the 150 μm (for the Bond Work Index) as a minimum.

With results of the two energy levels (two sets of particles), two values of t_{10} and specific comminution energy are obtained. This data is sufficient to determine an Axb value with relatively good accuracy compared to the JK Drop Weight Test. Using the measured Ecs values and the percentage passing 150 μm, the Bond Work Index can also be estimated with accuracy.

5 CONCLUSIONS AND RECOMMENDATIONS

The Geopyörä breakage test was developed to achieve the goals of ideal comminution for geometallurgy test. It uses small discrete samples of approximately a half kilogram for bulk samples or halves of a one-meter long section of drill core. The test procedure is fast, requiring approximately 10 minutes per sample, which ultimately results in a low-cost operation. Two energy levels proved to be sufficient for estimating both ore competency (Axb and DWi) and hardness (BBMWi) parameters with reasonable accuracy.

Bond ball mill tests, JK Drop Weight Test and SMC tests were used to compare and validate the results of the competence and hardness parameters obtained with the Geopyörä test. There was a good correlation between the t_{10} measured using the Geopyörä and those calculated using the breakage equation with Axb determined with JKDWT and SMC Tests. Thus, the SMC Test® DWi parameters correlate appropriately with the results of the Geopyörä test, within a relative error of ± 15% across all samples.

The estimation of BBMWi was considered adequate for geometallurgical modelling purposes, and future models with a more extensive database can undoubtedly increase the estimate accuracy. A strong correlation can be obtained by calculating a Work Index value from the specific energy and the breakage distribution of the Geopyörä test, with an average relative error of 9,6% between the BBMWi and the Geopyörä Work Index.

The results were in good agreement to present a device as a feasible option to increase the understanding of ore variability from the comminution perspective. The proposed methodology showed the potential of using a method that can work with drill core logging and geochemical analysis to characterise breakage properties for ore bodies at an industrial scale.

The gap ratio is the operational parameter that allows adjusting the energy levels in order to fit the A and b parameters in the breakage curve. This parameter is calculated as the proportion of geometric mean and the gap opening. A gap ratio of 75% was probed as not adequate. The reason to conclude this was due to depending on the shape of the rock, the breakage event can be not correctly recorded or not documented at all.

Better results of the Axb parameter were obtained by using gap ratios of 25% and 50% This criterion eliminates the possibility to record errors related to the shape of the specimen.

The Geopyörä device measures impulse, force and energy values for each broken particle. Additionally, there are possibilities for improvement with automated features. Individual mass of each particle could be measured to obtaining a distribution of the specific comminution energy rather than a single averaged value. Future image analysis tools can be used to measure the t_{10} values online as the product free falls after the breakage event.

Due to the nature of this equipment, with dynamic measurements, the possibility of having online measurements in industrial plants is high if more automation is integrated. Online measurements would allow constant inputs for comminution models and an opportunity to have enough ore characterization data to use artificial intelligence in the analysis and forecasting of the process.

In the scope of this thesis, the effect of the particle size was not analysed in the validation of the method. The JKDWT and SMC Tests analyse the variation of Axb parameters is the different size class to correct the variations, as is shown in Appendix B. This analysis was not part of this work, mainly because of delays due to the current global pandemic situation.

To analyse the precision of the test, the exact values of specific energy measured in the Geopyörä device should be replicated in a JK Drop Weight Test equipment, in order to compare the t_{10} values obtained with both. This test had originally been planned for this thesis work but was also delayed due to the ongoing, and it is expected to be conducted in the near future.

Analysis between the results of the Geopyörä test and the rock mechanics properties has a strong potential for future research, and further work in this area is recommended.

6 SUMMARY

Comminution is the most energy-demanding stage of the mining process, making its optimisation one of the biggest challenges in the industry. Ore variability must be understood in order to achieve this goal. Geometallurgy address this issue from a multidisciplinary perspective, however lack of fast and reliable comminution tests is a current issue to allow a better understanding of the rock properties in an ore deposit.

This thesis introduces Geopyörä, a new testing device which is capable of measuring forces and energy applied to rock particles during the breakage process. The new testing method is faster and uses smaller samples than most of the other comminution tests in the market (e.g. JKDWT, JKRBT, SMC Test® and SPI). To Geopyörä test have been benchmarked against the industry standard JKDWT, SMC Test®, as well as Bond ball mill grinding test.

The methodology developed in this thesis work requires 10 minutes per sample and use less than 0,5 kg of bulk sample or one-meter drill core halve sample. In the case of using a drill core sample, a pre-crushing stage must be done to obtain the necessary particle requirements. The test is performed with particles within the –22,4 and +13,2 mm range.

The validation of the test was done using three sets of thirty particles in the –22,4 + 19 mm size fraction, using gap ratios of 25%, 50% and 75%. Two energy levels proved to be enough for estimating both ore competency and hardness parameters. Gap ratios of 25% and 50% were the optimal operational condition to obtain those parameters.

Ore competency values obtained in the Geopyörä test were validated comparing it with the Axb and DWi parameters. An average error of 6,2% and 8,2% was calculated between the Geopyörä Axb parameter and the Axb reported by the JK Drop Weight Test and the SMC Test® respectively. Geopyörä ore hardness values were compared with the Bond Ball Mill Index with an average error of 9,6% for the five ore types.

The results were in good agreement to present the Geopyora test as a feasible option to increase the understanding of ore variability from the comminution perspective.

7 REFERENCES

Allaire, A., Live, P., Yassa, A., & Major, M. (2013). *Preliminary Feasibility Study of the West and East Pit Deposits of the Fire Lake North Project*.

Alruiz, O. M., Morrell, S., Suazo, C. J., & Naranjo, A. (2009). A novel approach to the geometallurgical modelling of the Collahuasi grinding circuit. *Minerals Engineering*, *22*(12), 1060–1067. https://doi.org/10.1016/j.mineng.2009.03.017

Altman, K., Liskowich, M., Kanti, D., & Shoemaker, S. (2014). *Canadian National Instrument 43-101 Technical Report Çöpler Sulfide Expansion Project Feasibility Study Erzincan Province, Turkey*.

ASTM. (2008). Standard Test Method for Determination of the Point Load Strength Index of Rock and Application to Rock Strength Classifications. *ASTM International, West Conshohocken, PA, 22*(2), 51–60. https://doi.org/10.1520/D5731-08.2

Azadi, M., Northey, S. A., Ali, S. H., & Edraki, M. (2020). Transparency on greenhouse gas emissions from mining to enable climate change mitigation. *Nature Geoscience*, *13*(2), 100–104. https://doi.org/10.1038/s41561-020-0531-3

Bearman, R. A., Briggs, C. A., & Kojovic, T. (1997). The application of rock mechanics parameters to the prediction of comminution behaviour. *Minerals Engineering*, *10*(3), 255–264. https://doi.org/10.1016/s0892-6875(97)00002-2

Bergeron, Y., Kojovic, T., Gagnon, M.-D.-N., & Okono, P. (2017). Applicability of the HIT for evaluating comminution and geomechanical parameters from drill core samples-the odyssey project case study. *COM2017 The Conference of Metallurgists*. www.metsoc.org

Bond, F. (1946). Crushing Tests by Pressure and Impact. *Trans SME/AIME*, 484–494.

Bond, F. (1952). The third theory of comminution. *Trans SME/AIME*, *193*, 484–494.

Bond, F. (1961). *Crushing and Grinding Calculations.* WI: Allis-Chalmers Manufacturing.

Bueno, M., Foggiato, B., & Lane, G. (2015). Geometallurgy applied in comminution to minimize design risks. *SAG Conference*.

Bueno, M., Torvela, J., & Chandramohan, R. (2020). *Test arrangement and method for testing breakage and mechanical properties of rock particles.* (Patent No. PCT/FI2020/050100).

Calvo, G., Mudd, G., Valero, A., & Valero, A. (2016). Decreasing ore grades in global metallic mining: A theoretical issue or a global reality? *Resources*, *5*(4). https://doi.org/10.3390/resources5040036

Chandramohan, R., Lane, G., Foggiatto, B., & Bueno, M. (2015). Reliability of some ore characterization tests. *SAG Conference*. https://www.researchgate.net/publication/323218453

David, D. M. (2019). Geometallurgy. In S. Kawatra & C. Young (Eds.), *SME Mineral Processing and Extractive Metallurgy Handbook* (pp. 173–185).

Dobby, G., Bennett, C., Bulled, D., & Kosick, X. (2004). Geometallurgical modeling - the new approach to plant design and production forecasting/planning, and mine/mill optimization. *36th Annual Canadian Mineral Processors Conference*.

Dobby, G., Bennett, C., & Kosick, G. (2001). Advances in SAG circuit design and simulation applied to the mine block model. *International Autogenous and Semiautogenous Grinding Technology*.

Doll, A. (2016). *Calculating DWi from a drop weight test result*. www.sagmilling.com

Dominy, S. C., O'connor, L., Parbhakar-Fox, A., Glass, H. J., & Purevgerel, S. (2018). Geometallurgy—A route to more resilient mine operations. In *Minerals* (Vol. 8, Issue 12). MDPI AG. https://doi.org/10.3390/min8120560

Fahernwald, A., Newton, J., & Herkernhoff, E. (1937). Velocity of hit in rock crushing. *Eng Min*, *138*, 45–48.

Gaudin, A., & Hukki, R. (1946). *Trans SME/AIME*. *169*.

Gupta, A., & Yan, D. (2016). Mathematical Modelling of Comminution Processes. In *Mineral Processing Design and Operations* (pp. 317–355). Elsevier. https://doi.org/10.1016/b978-0-444-63589-1.00011-3

Haldar, S. K. (2018). Sampling Methods. In *Mineral Exploration* (pp. 123–144). Elsevier. https://doi.org/10.1016/B978-0-12-814022-2.00007-1

Heiskari, H. (2017). *Development of comminution test method for small drill core sample*. University of Oulu.

Heiskari, H., Kurki, P., Luukkanen, S., Sinche Gonzalez, M., Lehto, H., & Liipo, J. (2019). Development of a comminution test method for small ore samples. *Minerals Engineering*, *130*, 5–11. https://doi.org/10.1016/j.mineng.2018.10.005

Hukki, R. T. (1961). Proposal for a solomonic settlement between the theories of von Rittinger, Kick and Bond. *Trans. AIME*, *220*(5), 4.

JKTech. (2017a). *JK Bond Ball Mill Test*. www.jktech.com.au

JKTech. (2017b). *JK Rotary Breakage Test* (pp. 1–2).

JKTech. (2017c). *JKTech Laboratory Services Bond Rod Mill Index Test (BRMWI) Bond Rod Mill Index Test (BRMWI)*. www.jktech.com.au

Kham, P., Bennett, D., Tordoir, A., Walker, P., Rosa, L., Valery, W., & Duffy, K. (2014). Throughput Forecasting and Optimisation at the Phu Kham Copper-Gold Operation. *AusIMM Mill Operators Conference*.

Kojovic, T. (2016). HIT-a Portable Field Device for Rapid Testing at Site. *13th AusIMM Mill Operators Conference*.

Kojovic, T., Bergeron, Y., & Leetmaa, K. (2019). The value of daily HIT ore hardness testing of sag feed at the meadowbank gold mine. *SAG Conference*.

Lishchuk, V., & Pettersson, M. (2020). The mechanisms of decision-making when applying geometallurgical approach to the mining industry. *Mineral Economics*, 1–10. https://doi.org/10.1007/s13563-020-00220-9

Lois-Morales, P., Evans, C., Bonfils, B., & Weatherley, D. (2020). The impact load cell as a tool to link comminution properties to geomechanical properties of rocks. *Minerals Engineering*, *148*. https://doi.org/10.1016/j.mineng.2020.106210

Lund, C., & Lamberg, P. (2014). Geometallurgy-A tool for better resource efficiency. *European Geologist*, 39–43.

Manouchehri, H., Christoffersson, A., & Nillson-Wullf, T. (2016). Energy efficiency in comminution-getting more from the crushing stage. *International Mineral Processing Congress*.

Matei, V., Bailey, C., & Morrell, S. (2015a). A new way of representing A and b parameters from JK Drop-Weight and SMC Test: The "SCSE." *SAG Conference*.

Matei, V., Bailey, C. W., & Morrell, S. (2015b). A new way of representing A and b parameters from JK Drop-Weight and SMC Tests: The "SCSE." *SAG Conference*.

McKay, N., Vann, J., Ware, W., Morley, C., & Hodkiewicz, P. (2016). Strategic and

Tactical Geometallurgy – a Systematic Process to Add and Sustain Resource Value - AusIMM. *Third AusIMM International Geometallurgy Conference (GeoMet)*, 29–36.

Michaux, S., & O'connor, L. (2019). *How to set up and Develop a Geometallurgical Program*.

Morrell, S. (2004). Predicting the specific energy of autogenous and semi-autogenous mills from small diameter drill core samples. *Minerals Engineering*, *17*(3), 447–451. https://doi.org/10.1016/j.mineng.2003.10.019

Morrell, S. (2006). AG/SAG Mill Circuit Grinding Energy Requirement—How to Predict It from Small-Diameter Drill Core Samples Using the SMC TestStephen MLA (Modern Language Assoc.) Kawatra, S. K. Advances in Comminution. Society for Mining, Metallurgy, and Exploration, Inc. In *Advances in Comminution* (Vol. 2006, pp. 3–14). Society for Mining, Metallurgy, and Exploration, Inc.

Morrell, S. (2009). Predicting the overall specific energy requirement of crushing, high pressure grinding roll and tumbling mill circuits. *Minerals Engineering*, *22*(6), 544–549. https://doi.org/10.1016/j.mineng.2009.01.005

Morrell, S. (2010). Predicting the specific energy required for size reduction of relatively coarse feeds in conventional crushers and high pressure grinding rolls. *Minerals Engineering*, *23*(2), 151–153. https://doi.org/10.1016/j.mineng.2009.10.003

Morrell, S. (2011). *Mapping orebody hardness variability for AG/SAG/Crushing and HPGR circuits*.

Morrell, S. (2014). Innovations in comminution modelling and ore characterisation. In *Mineral Processing and Extractive Metallurgy: 100 Years of Innovation* (pp. 77–88).

Morrell, S. (2015). Global Trends in Ore Hardness. *SAG Conference*.

Morrell, S. (2019). Testing and Calculations for Comminution Machines. In S. Kawatra & C. Young (Eds.), *SME Mineral Processing and Extractive Metallurgy Handbook* (pp. 529–563).

Morrell, S., & Morrison, R. (1989). Ore charge, ball load and Material Flow effects on an energy based SAG Mill model. *SAG Conference*.

Morrell, S., & Morrison, R. (1996). AG and SAG mill circuit selection and design by simulation. *SAG Conference*.

Mwanga, A. (2016). *Test Methods for Characterising Ore Comminution Behavior in Geometallurgy*. Luleå University of Technology.

Mwanga, A., Lamberg, P., & Rosenkranz, J. (2015). Comminution test method using small drill core samples. *Minerals Engineering*, *72*, 129–139. https://doi.org/10.1016/j.mineng.2014.12.009

Mwanga, A., Rosenkranz, J., & Lamberg, P. (2015). Testing of ore comminution behavior in the geometallurgical context—A review. In *Minerals* (Vol. 5, Issue 2, pp. 276–297). MDPI AG. https://doi.org/10.3390/min5020276

Napier-Munn, T., Morrell, S., Morrison, R., & Kojovic, T. (1996). *Mineral Comminution Circuits Their operation and optimization*. Julius Kruttsnitt Mineral Research Center.

Napier-Munn, T., Whiten, W., & Faramarzi, F. (2020). Bias in manual sampling of rock particles. *Minerals Engineering*, *153*. https://doi.org/10.1016/j.mineng.2020.106260

Narayanan, S., & Whiten, W. (1988). *Determination of comminution characteristics from single particle breakage tests and its application to ball mill scale-up.* (Trans. Ins).

Niitti, T. (1970). Rapid evaluation of grindability by a simple batch test. *International Mineral Processing Congress Proceedings*, 41–46.

Powell, M. S., & Morrison, R. D. (2007). The future of comminution modelling. *International Journal of Mineral Processing*, *84*(1–4), 228–239. https://doi.org/10.1016/j.minpro.2006.08.003

Putland, B., Sciberras, R., & Giblett, A. (2019). Grinding Circuit Performance Optimization. In S. Kawatra & C. Young (Eds.), *SME Mineral Processing and Extractive Metallurgy Handbook* (pp. 499–505). Society for Mining, Metallurgy, and Exploration.

Radziszewski, P. (2013). Energy recovery potential in comminution processes. *Minerals Engineering*, *46–47*, 83–88. https://doi.org/10.1016/j.mineng.2012.12.002

Sahoo, R. K., Weedon, D. M., & Roach, D. (2004). Single-particle breakage tests of Gladstone Port Authority's coal by a twin pendulum apparatus. *Advanced Powder Technology*, *15*(2), 263–280. https://doi.org/10.1163/156855204773644472

SGS. (2005). *SPI -A decade later why was the SPI Test created?*

Shi, F., & Kojovic, T. (2007). Validation of a model for impact breakage incorporating particle size effect. *International Journal of Mineral Processing*, *82*(3), 156–163. https://doi.org/10.1016/j.minpro.2006.09.006

Shi, F., Kojovic, T., Larbi-Bram, S., & Manlapig, E. (2009). Development of a rapid particle breakage characterisation device - The JKRBT. *Minerals Engineering*, *22*(7–8), 602–612. https://doi.org/10.1016/j.mineng.2009.05.001

Tolosana-Delgado, R., & van den Boogaart, K. G. (2018). Predictive geometallurgy: An interdisciplinary key challenge for mathematical geosciences. In *Handbook of Mathematical Geosciences: Fifty Years of IAMG* (pp. 673–686). Springer

International Publishing. https://doi.org/10.1007/978-3-319-78999-6_33

Toraman, O. Y., Kahraman, S., & Cayirli, S. (2010). Predicting the crushability of rocks from the impact strength index. *Minerals Engineering*, *23*(9), 752–754. https://doi.org/10.1016/j.mineng.2010.04.004

Torvela, J. (2020). *Double wheel crusher prototype*. University of Oulu.

Torvela, J., Bueno, M., Liedes, T., & Luukkanen, S. (2020). *The Double Wheel Breakage Test*.

Valery, W., Duffy, K., & Jankovic, A. (2019). Mine to Mill optimization. In S. Kawatra & C. Young (Eds.), *SME Mineral Processing and Extractive Metallurgy Handbook* (pp. 335–343). Society for Mining, Metallurgy, and Exploration.

Walker et al. (1937). *Principles of chemical engineering*.

Weedon, D. M., & Wilson, F. (2000). Modelling iron ore degradation using a twin pendulum breakage device. *International Journal of Mineral Processing*, *59*(3), 195–213. https://doi.org/10.1016/S0301-7516(99)00066-6

Wills, B. A., & Finch, J. A. (2016). Comminution. In *Wills' Mineral Processing Technology* (pp. 109–122). Butterworth-Heinemann. https://doi.org/10.1016/B978-0-08-097053-0.00005-4

Yashima, S., Saito, F., & Horita, H. (1981). Single particle testing by double pendulum type impact testing apparatus. *Kogaku Robunshui*, *7*(83–89).

APPENDIX A

The details of the Bond Ball Mill tests are presented in the following tables.

Table 27 Bond Ball Mill Test Details for ore A

Test Details		
Ore Source	A	
Closing Screen	150	µm
Product in Feed	7,52	%
Weight of Feed	1211,2	g
Volume of Feed in Mill	700	ml
Target recirculating Load	250	%
Prod for 250% Circ. Load	346	g
Last 3 Grindabilities	0,632	g/rev
	0,622	g/rev
	0,618	g/rev
Average of last 3 cycles	0,624	g/rev
Last 3 Circulating Load	249	%
	255	%
	252	%
Average of last 3 cycles	252	%
Feed 80% passing	2534	µm
Product 80% passing	84	µm

Table 28 Bond Ball Mill Test Details for ore B

Test Details		
Ore Source	B	
Closing Screen	150	µm
Product in Feed	11,93	%
Weight of Feed	1400,5	g
Volume of Feed in Mill	700	ml
Target recirculating Load	250	%
Prod for 250% Circ. Load	400	g
Last 3 Grindabilities	1,073	g/rev
	1,075	g/rev
	1,09	g/rev
Average of last 3 cycles	1,079	g/rev
Last 3 Circulating Load	247	%
	249	%
	246	%
Average of last 3 cycles	247	%
Feed 80% passing	2205	µm
Product 80% passing	109	µm

Table 29 Bond Ball Mill Test Details for ore C

Test Details		
Ore Source	C	
Closing Screen	150	µm
Product in Feed	10,73	%
Weight of Feed	1301,9	g
Volume of Feed in Mill	700	ml
Target recirculating Load	250	%
Prod for 250% Circ. Load	372	g
Last 3 Grindabilities	0,831	g/rev
	0,856	g/rev
	0,841	g/rev
Average of last 3 cycles	0,842	g/rev
Last 3 Circulating Load	256	%
	241	%
	255	%
Average of last 3 cycles	251	%
Feed 80% passing	2276	µm
Product 80% passing	102	µm

Table 30 Bond Ball Mill Test Details for ore D

Test Details		
Ore Source	D	
Closing Screen	150	µm
Product in Feed	12,87	%
Weight of Feed	1366,3	g
Volume of Feed in Mill	700	ml
Target recirculating Load	250	%
Prod for 250% Circ. Load	290	g
Last 3 Grindabilities	2,1	g/rev
	2,103	g/rev
	2,157	g/rev
Average of last 3 cycles	2,12	g/rev
Last 3 Circulating Load	254	%
	250	%
	242	%
Average of last 3 cycles	249	%
Feed 80% passing	2226	µm
Product 80% passing	113	µm

Table 31 Bond Ball Mill Test Details for ore E

Test Details		
Ore Source	E	
Closing Screen	150	µm
Product in Feed	13,36	%
Weight of Feed	1300,03	g
Volume of Feed in Mill	700	ml
Target recirculating Load	250	%
Prod for 250% Circ. Load	371	g
Last 3 Grindabilities	2,871	g/rev
	2,8	g/rev
	2,712	g/rev
Average of last 3 cycles	2,828	g/rev
Last 3 Circulating Load	244	%
	257	%
	249	%
Average of last 3 cycles	250	%
Feed 80% passing	2225	µm
Product 80% passing	113	µm

APPENDIX B

Table 32 Normalised values of Axb (JKDWT) for: (a) Ore A (b) Ore b (c) Ore C (d) Ore D (e) Ore E

(a)

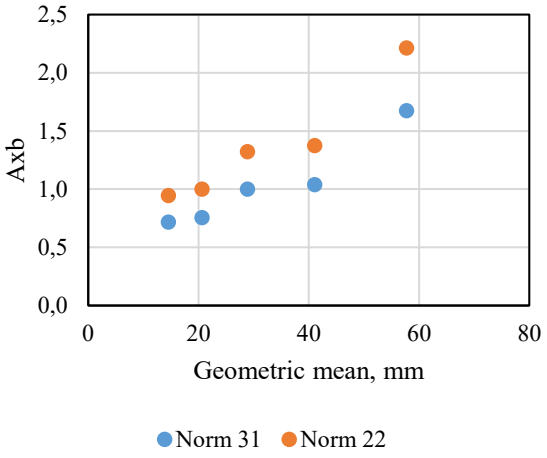

(b)

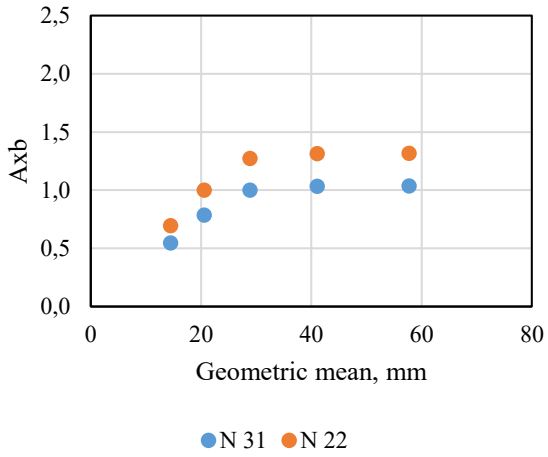

(c)

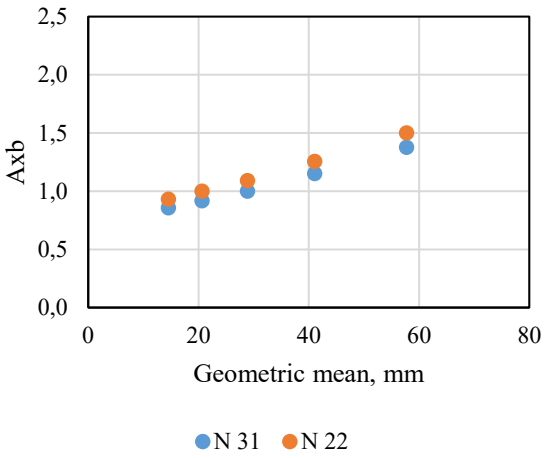

(d)

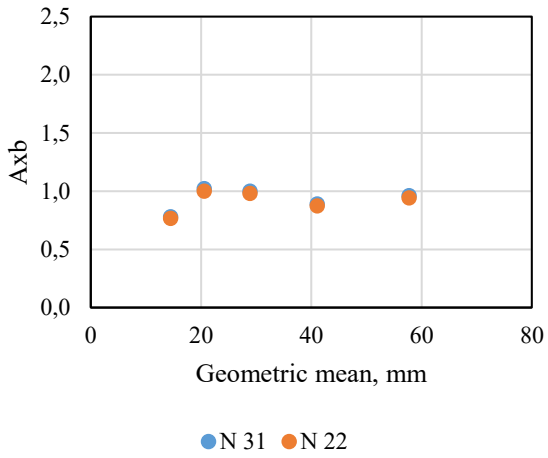

(e)

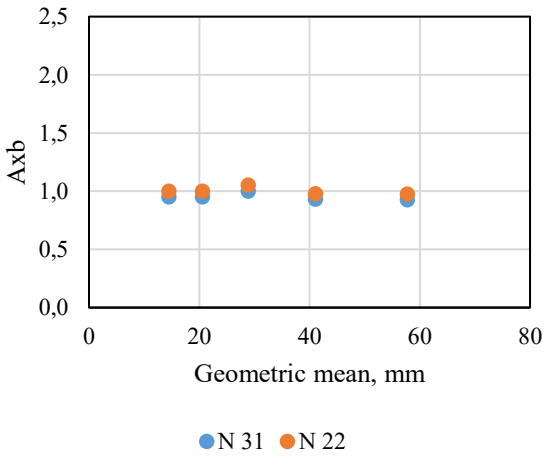

APPENDIX C

Appendix C consists in the attached JK Drop Weight Test and SMC Test® report provided by Wardell Armstrong Centre.

INTEGRATED JKDW AND SMC TEST® REPORT

University of Oulu

Tested by: Wardell Armstrong

Truro, Cornwall, UK

Prepared by: Matt Weier

JKTech Job No: 20027/P1
Testing Date: December 2019

TABLE OF CONTENTS

Page No

APPENDICES

Page No

LIST OF FIGURES

Page No

LIST OF TABLES

Page No

1 EXECUTIVE SUMMARY

1.1 JKDW Results Summary

Table 1 - Parameters from JKDW Test Results

Sample Designation	*A*	*b*	*A*b*	*SCSE (kWh/t)*	*SG*
Mine B	71.2	0.49	34.9	11.7*	3.20
Mine A	57.9	0.55	31.8	11.72*	2.95
Mine D	67.6	0.89	60.2	8.56*	2.90
Mine F	80.1	3.83	306.8	4.59*	4.22
Mine C	78.3	0.40	31.3	11.92*	2.98
Mine E	67.8	1.31	88.8	7.2*	2.80

*Sample parameters are outside the range of parameteres used when developing the SCSE model. As such SCSE values for flagged samples should be treated with caution.

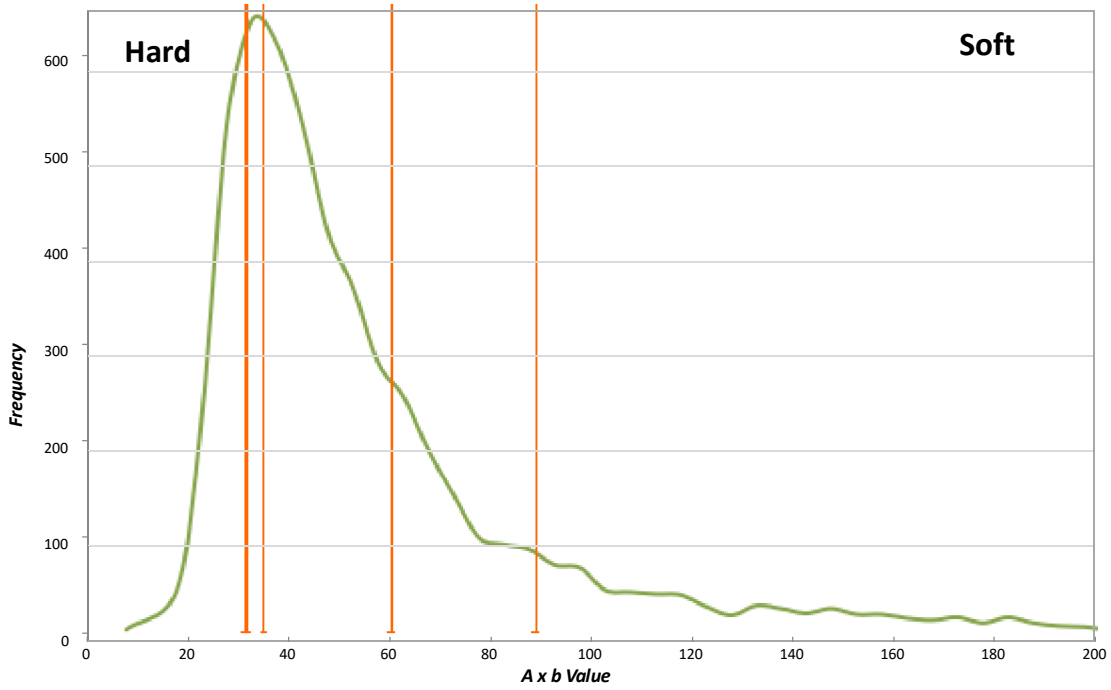

Figure 1 - Frequency Distribution of $A*b$ in the JKTech Database

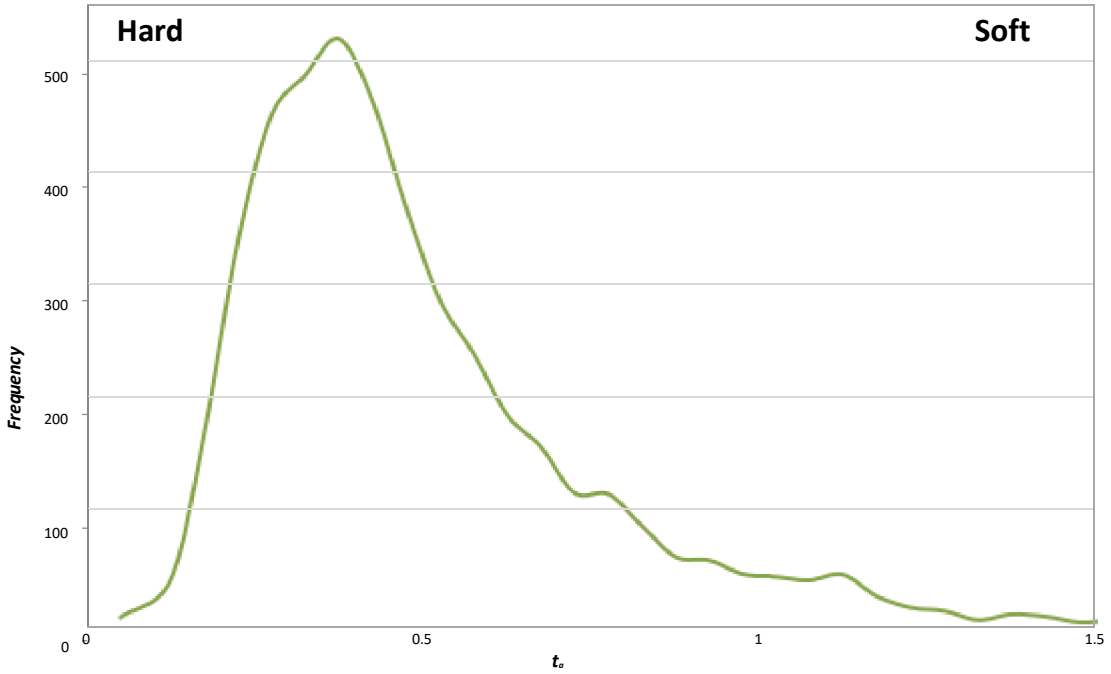

Figure 2 - Frequency Distribution of t_a in the JKTech Database

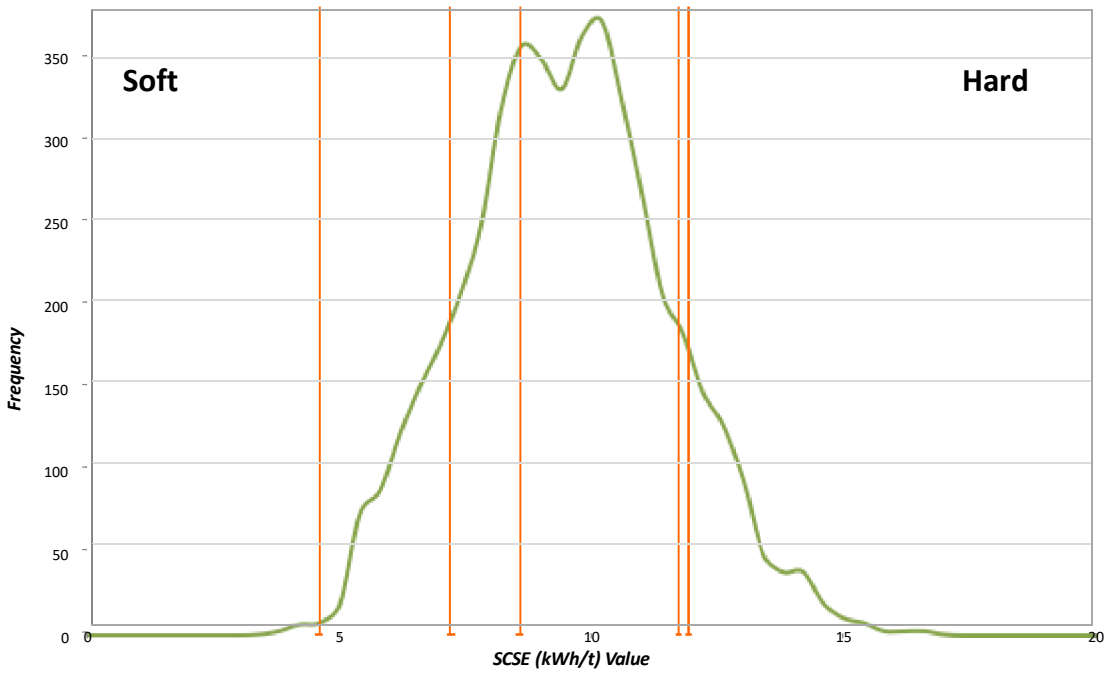

Figure 3 - Frequency Distribution of SCSE in the JKTech Database

1.2 SMC Results Summary

Table 2 - SMC Test® Results

Sample Designation	*DWi* (kWh/m³)	*DWi* (%)	*Mi* Parameters (kWh/t)			SG
			Mia	Mih	Mic	
Mine B	8.8	77.0	20.4	16.0	8.3	3.20
Mine A	9.8	86.0	24.2	19.3	10.0	2.95
Mine D	4.4	22.0	12.9	8.8	4.5	2.90
Mine F	1.4	3.0	3.5	1.9	1.0	4.22
Mine C	9.7	85.0	23.8	18.9	9.8	2.98
Mine E	2.7	9.0	9.2	5.7	2.9	2.80

Table 3 – Parameters derived from the SMC Test® Results

Sample Designation	A	b	A*b	t_a	SCSE (kWh/t)
Mine B	81.9	0.44	36.0	0.29	11.5
Mine A	72.7	0.41	29.8	0.26	12.13
Mine D	72.7	0.85	61.8	0.55	8.46
Mine F	78.8	3.95	311.3	1.91	4.58
Mine C	100.0	0.30	30.0	0.26	12.18
Mine E	66.2	1.44	95.3	0.88	7.02

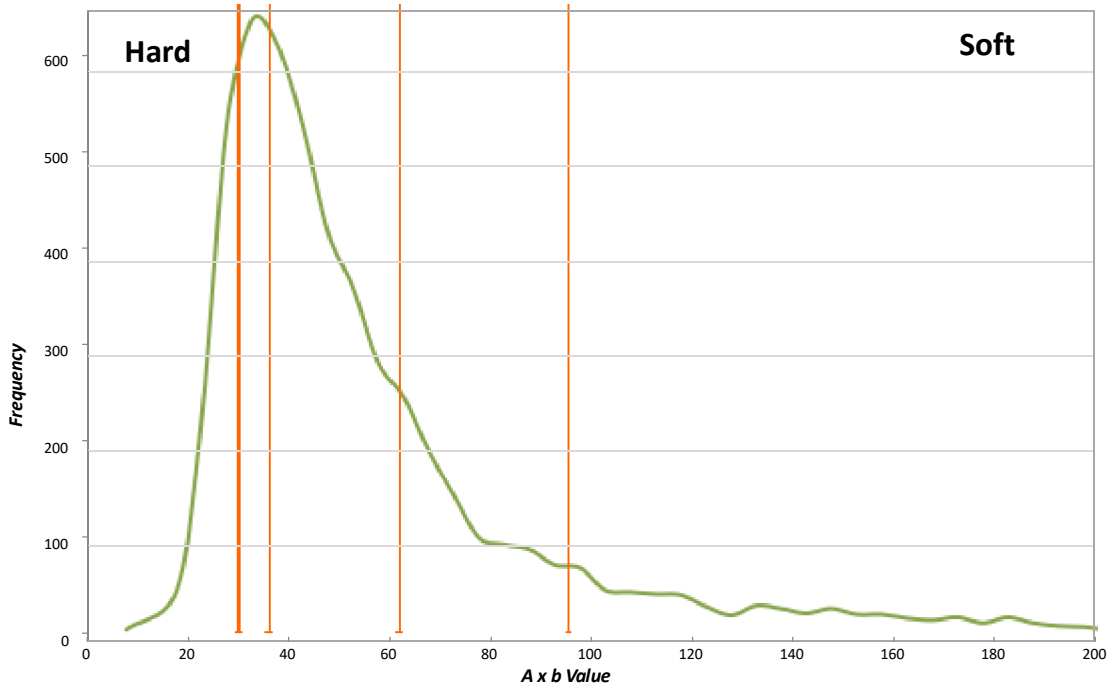

Figure 4 - Frequency Distribution of $A*b$ in the JKTech Database

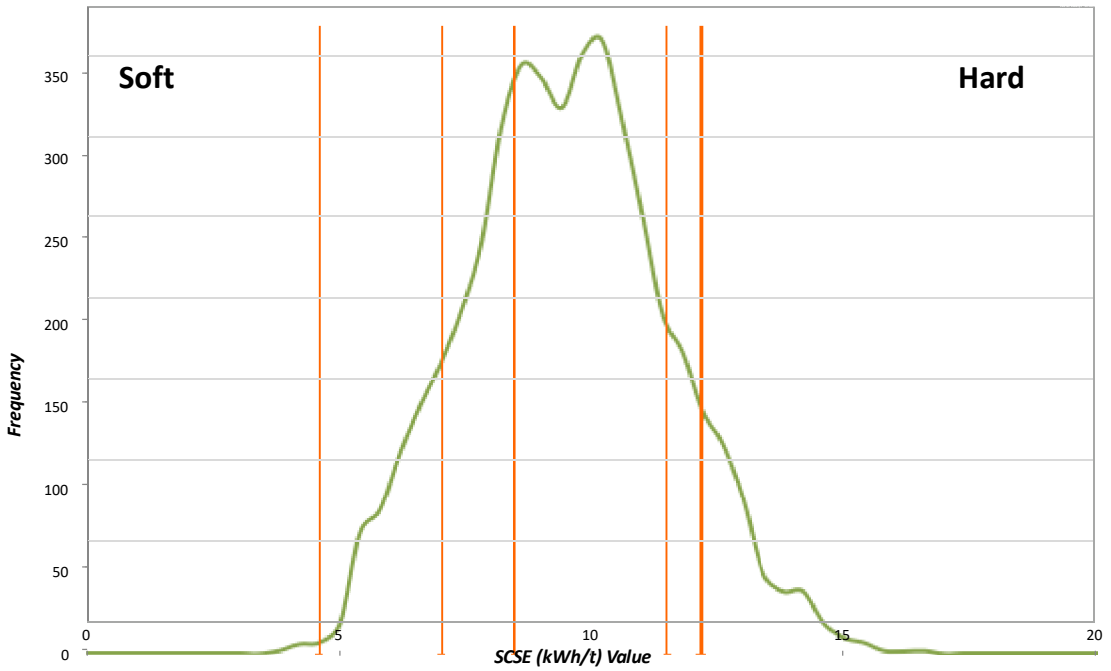

Figure 5 - Frequency Distribution of SCSE in the JKTech Database

2 INTRODUCTION

Integrated JKDW and SMC data for six samples from University of Oulu Project were received from Wardell Armstrong on January 06, 2020, by JKTech for JKDW and SMC test analysis. The samples were identified as Mine B, Mine A, Mine D, Mine F, Mine C and Mine E. The data were analysed to determine the JKSimMet and SMC Test comminution parameters. SMC Test results were forwarded to SMC Testing Pty Ltd for the analysis of the SMC Test data. The samples had been subjected to Integrated JKDW and SMC testing (six). Analysis and reporting were completed on January 10, 2020.

Some samples in this report have been previously reported as JKTech job 19027/P4, these have been included in this report at Wardell Armstrong's request.

3 THE JK DROP-WEIGHT TEST

3.1 Introduction

The JKTech Drop-Weight test provides ore specific parameters for use in the JKSimMet Mineral Processing Simulator software. In JKSimMet, these parameters are combined with equipment details and operating conditions to analyse and/or predict SAG/autogenous mill performance. The same test procedure also provides ore type characterisation for the JKSimMet crusher model. These ore specific parameters have been calculated from the test results and are supplied to University of Oulu in this report as part of the standard procedure.

3.2 JK Drop-Weight Test Procedure

Details of the JK Drop-Weight test procedure can be found in APPENDIX B.

3.3 Interpretation of JKDW Test Results

3.3.1 Resistance to Impact Breakage

One of the problems with the functional form used to represent the t_{10} v E_{cs} relationship is that the parameters A and b are not independent and thus cannot be used directly for comparisons between ore types. Two alternative parameters give a better comparison. One of these is the product $A*b$. For this parameter, a smaller number means a greater resistance to impact breakage.

Also included in the derived results are the SAG Circuit Specific Energy (SCSE) values. The SCSE value is derived from simulations of a “standard” circuit comprising a SAG mill in closed circuit with a pebble crusher. For this parameter a larger number means a greater resistance to impact breakage. SCSE is described in detail in APPENDIX A.

3.3.2 Resistance to Abrasion Breakage

Resistance to abrasion is indicated by the t_a parameter. As with parameter $A*b$, a smaller value of t_a indicates more resistance, this time to abrasion breakage. This section was not performed for the samples in this report.

3.3.3 Limitation of Breakage Model with Very Soft Rock Types

It should be noted that the use of A and b parameters derived for very soft rock, in conjunction with the Variable Rates SAG Mill model in JKSimMet may be problematic. This is because the data from which the model was developed did not include ore types in this range.

3.3.4 Effect of Particle Size on Resistance to Impact Breakage

Variation of impact resistance with particle size is important for crusher power draw calculations and SAG/autogenous mill media competency considerations. Some ores exhibit a significant decrease in impact resistance with increasing particle size while others show no variation with size. The opposite trend of increasing impact resistance with increasing particle size is extremely rare.

The trend most frequently observed is for there to be decreasing slope with decreasing energy (E_{cs} values). However, it is both the slope and the absolute values of the low

energy t_{10} values that are of interest for SAG/autogenous milling because these data give an indication of the ability of media particles to survive. If the trend of the t_{10} values with increasing particle size is significantly upwards, it can be inferred by extrapolation that particles in the 100 – 200 mm size range (normal media size) will not be strong enough to survive. The same argument applies if the absolute values of t_{10} at low energy are sufficiently high.

Note that the E_{cs} values in the Specific Comminution Energy table that is given for each DW test in this report, are calculated using the new JKMRC breakage model. A description of this model can be found in Shi and Kojovic (2007). The model has three parameters, one of which accounts for the effect of particle size on impact resistance. The parameters are fitted using the full set of data aquired in the Drop Weight test. This approach avoids the arbitrary method of curve extrapolation used previously on an as needed basis, to correct for data inconsistences. The benefit of using the new model is that the E_{cs} data will behave sensibly when interpolated or extrapolated, either finer or coarser, in JKSimMet crusher simulations.

3.3.5 Density Results

As part of the standard JKTech ore property assessment procedures, the relative density of 30 randomly selected particles in the size range 26.5 mm to 31.5 mm are determined by weighing each particle, suspended initially in air and then in water.

It should be noted that this method measures the density of the particle rather than the density of the solid phase, since any internal porosity will be included in the volume measurement. A more accurate measurement of the solid phase density is possible using a Helium Pycnometer. However, it is the particle density rather than the phase density that is of concern in the assessment of SAG milling properties.

Even at the coarse particle sizes tested, it is normal to find a range of relative densities as the mineralogy of the particles varies. However, of great concern in SAG/autogenous milling is the possibility of a component in the ore that is both high density and resistant to breakage. Such material will concentrate in the load in a SAG/autogenous mill and result in higher than expected power draw.

3.4 JKDW Test Results

3.4.1 Summary of SAG/autogenous Mill Model Parameters

Table 4 shows the SAG/autogenous mill model parameters for the six samples.

Table 4 - SAG/Autogenous Mill Parameters from JKDW Test Results

Ore Type	*A*	*b*	*A * b*	SCSE (kWh/t)
Mine B	71.20	0.49	34.9	11.70*
Mine A	57.90	0.55	31.8	11.72*
Mine D	67.60	0.89	60.2	8.56*
Mine F	80.10	3.83	306.8	4.59*
Mine C	78.30	0.40	31.3	11.92*
Mine E	67.80	1.31	88.8	7.20*

*Sample parameters are outside the range of parameteres used when developing the SCSE model. As such SCSE values for flagged samples should be treated with caution.

The $A*b$, t_a and SCSE values are given for the six samples in Table 5, which also includes the percentage of of samples from the JKTech database which are softer.

Table 5 – Parameters Compared with Population of Values from Database

	$A * b$		SCSE (kWh/t)	
	Value	**%**	**Value**	**%**
Data Base Hardest	12.9	100	16.78	100
Data Base Average (Median)	45.2	50	9.46	50
Data Base Average (Mean)	61.9	28.6	9.48	49.7
Data Base Softest	810.0	0	3.91	0
Mine B	34.9	72.8	11.70*	85.9
Mine A	31.8	80.3	11.72*	86.3
Mine D	60.2	30.1	8.56*	33.3
Mine F	306.8	1.0	4.59*	0.3
Mine C	31.3	81.4	11.92*	88.1
Mine E	88.8	14.3	7.20*	13.7

The frequency distribution of the parameters $A*b$, t_a and SCSE from the JKTech database of ores tested are given in Figure 6 to Figure 8 respectively.

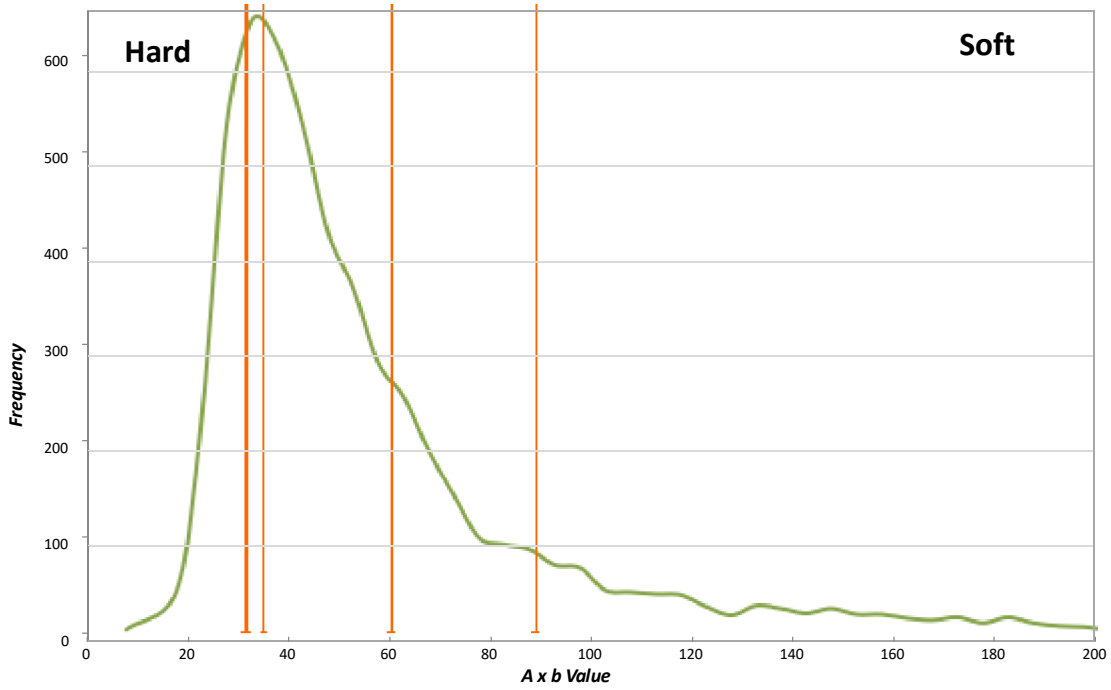

Figure 6 - Frequency Distribution of $A*b$ in the JKTech Database

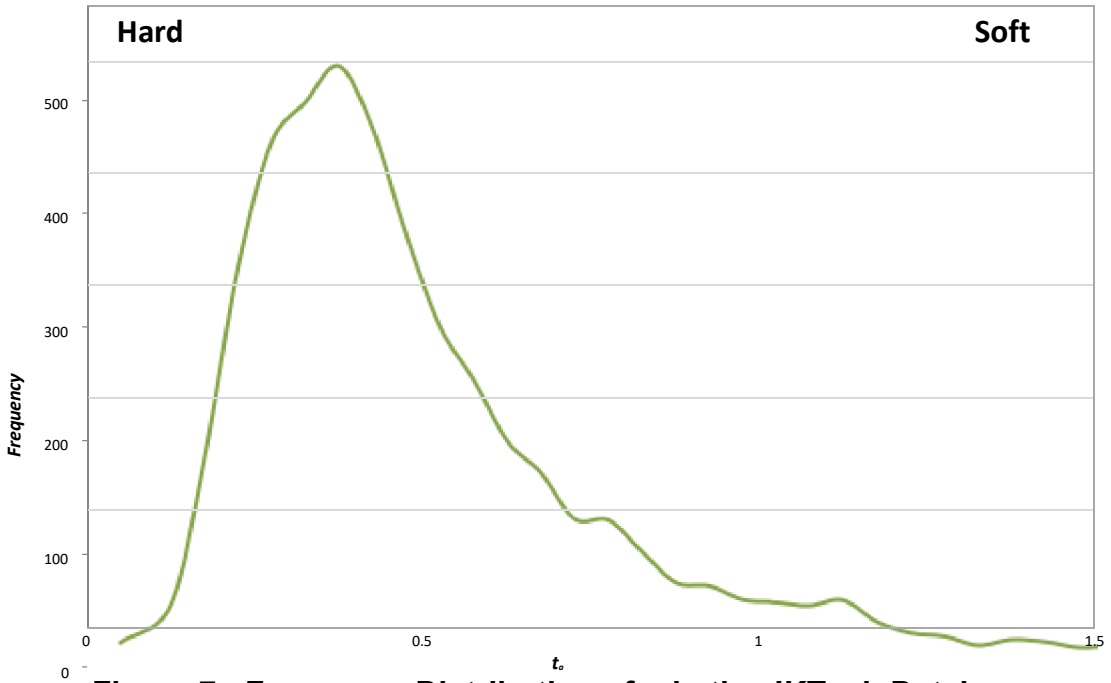

Figure 7 - Frequency Distribution of t_a in the JKTech Database

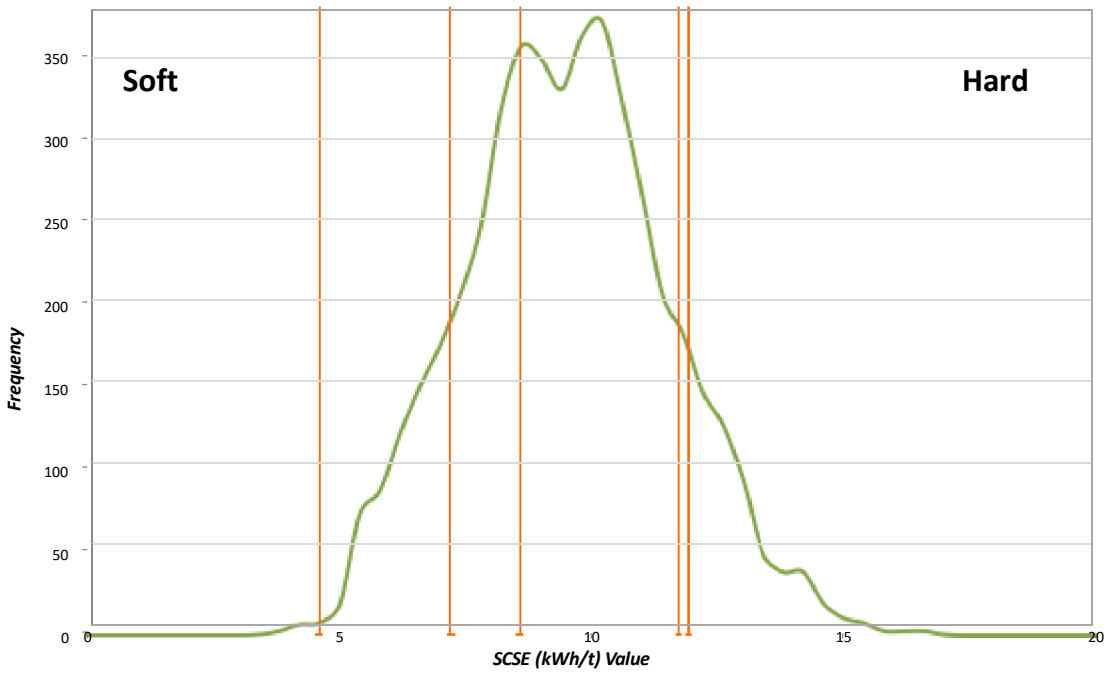

Figure 8 - Frequency Distribution of SCSE in the JKTech Database

3.4.2 JKDW Test Results for Mine B

The t_{10} versus E_{cs} relationship for sample Mine B is given in Figure 9.

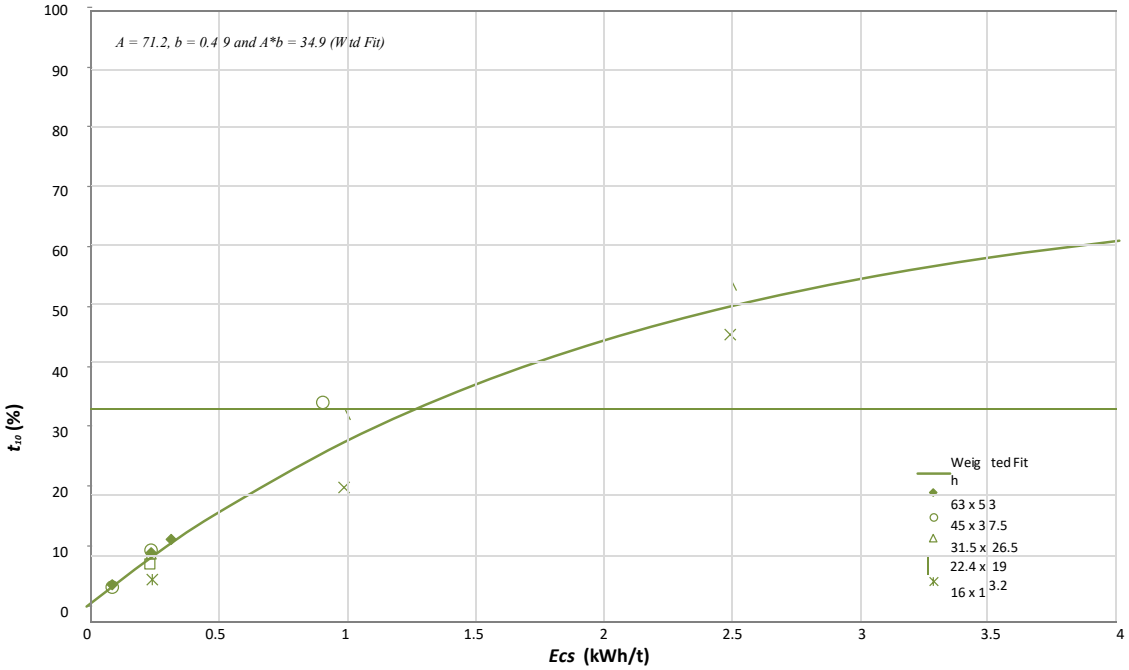

Figure 9 – t_{10} - E_{cs} Relationships for Mine B

Mine B has an $A*b$ value of 34.9. In the JKTech database 72.8% of the 5,200 ore types tested have higher $A*b$ values (refer to Table 5).

The SCSE value for Mine B is 11.70* kWh/t, with 85.9% of samples in the JKTech database having a lower SCSE.

The crusher model parameters for sample Mine B are given in Table 6 below.

The data in Table 6 indicate that for particles of Mine B of up to 63 mm, there is some increase in impact resistance with decreasing particle size.

Table 6 - Crusher Model Parameters for Mine B

	Size Relative to Initial Size				
	t_{75}	t_{50}	t_{25}	t_4	t_2
t_{10}	cumulative percent passing				
10.0	3.02	3.72	5.48	21.82	56.38
20.0	5.73	7.16	10.77	44.64	86.46
30.0	8.58	10.78	16.24	65.69	98.28

Specific Comminution Energy:

	Initial Particle Size, mm				
	+13.2-16.0 14.53	+19.0-22.4 20.63	+26.5-31.5 28.89	+37.5-45.0 41.08	+53.0-63.0 57.78
t_{10}	Ecs, kWh/t				
10	0.43	0.36	0.31	0.27	0.23
20	0.90	0.77	0.66	0.57	0.49
30	1.44	1.23	1.06	0.90	0.78

The values in this table have been adjusted using the Shi-Kojovic model to achieve data smoothing.

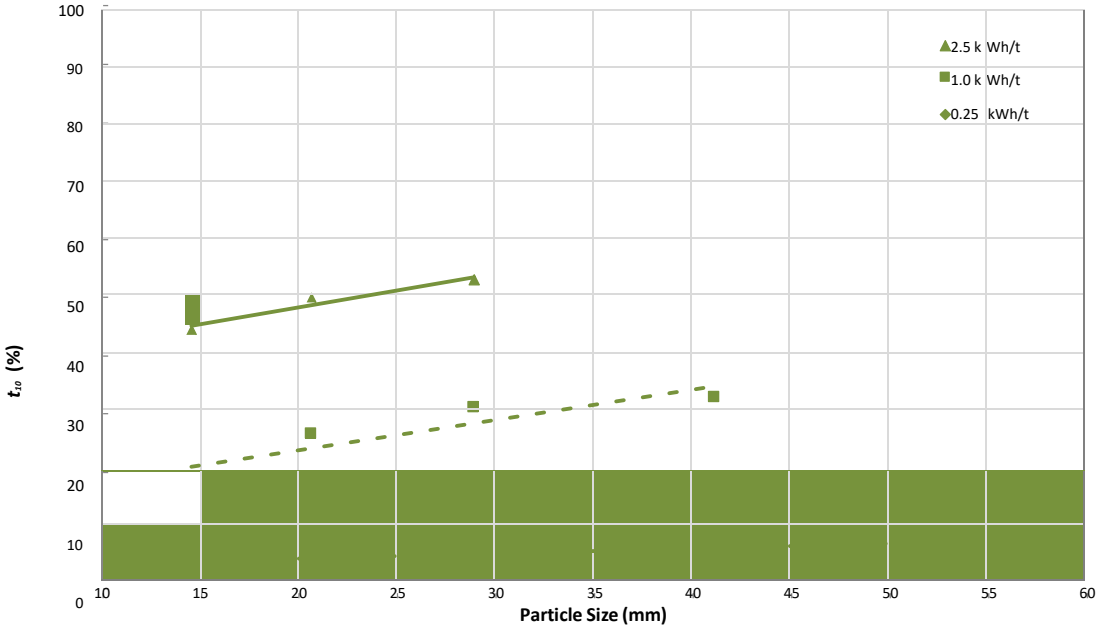

Figure 10 - Variation of Impact Resistance with Particle Size - Mine B

The data graphed in Figure 10 are the t_{10} values for up to 5 different particle sizes from Mine B, all broken with very similar specific comminution energies (0.25 kWh/t, 1.0 kWh/t and 2.5 kWh/t).

The data for Mine B follow the frequently observed trend of decreasing slope with decreasing energy (E_{cs} values).

The density measurements for the 30 particles from Mine B are given in Table 7 below. These results are plotted as a histogram in Figure 11.

Table 7 - Relative Density Measurements for 30 Particles for Mine B

3.06	3.32	3.62	3.18	3.06
3.19	3.22	3.29	3.33	3.14
3.19	3.23	3.11	3.19	2.92
3.11	3.12	3.25	3.14	3.28
3.23	3.19	3.30	3.20	3.02
3.21	3.19	3.28	3.28	3.16
Mean				**3.20**
Standard Deviation				**0.12**
Maximum				**3.62**
Minimum				**2.92**

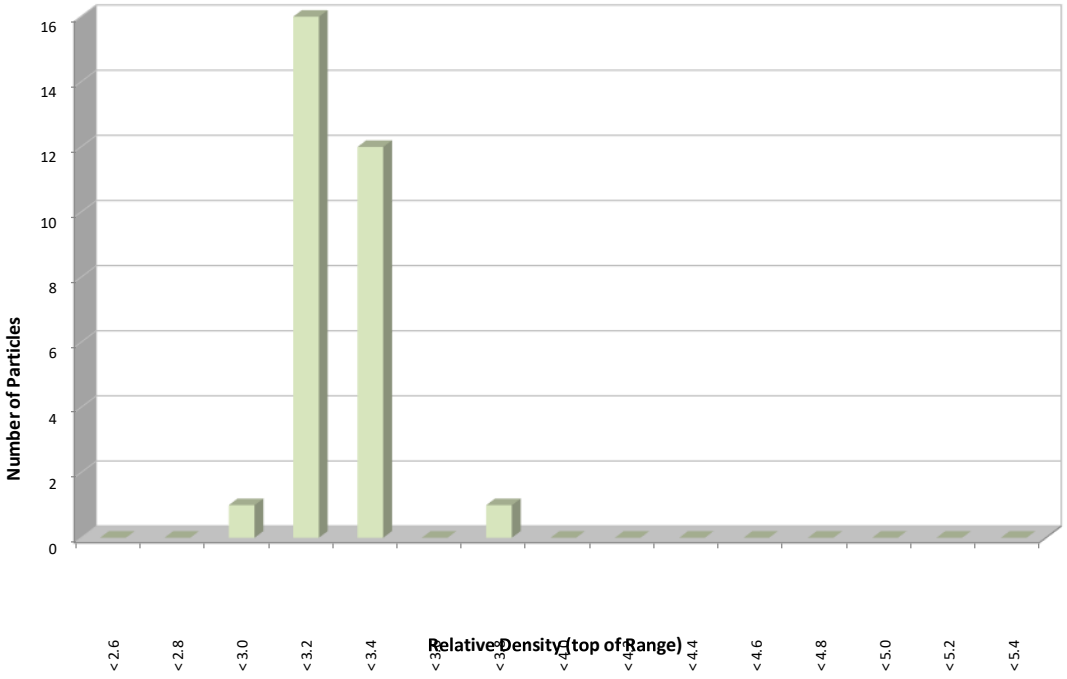

Figure 11 - Histogram of the Relative Density Measurements for 30 Particles for Mine B

The Mine B data contain slight evidence of bimodality in the relative density distribution, that is, slight evidence of a dense component that could concentrate in the mill load and cause power problems, resulting in a loss of throughput.

3.4.3 JKDW Test Results for Mine A

The t_{10} versus E_{cs} relationship for sample Mine A is given in Figure 12.

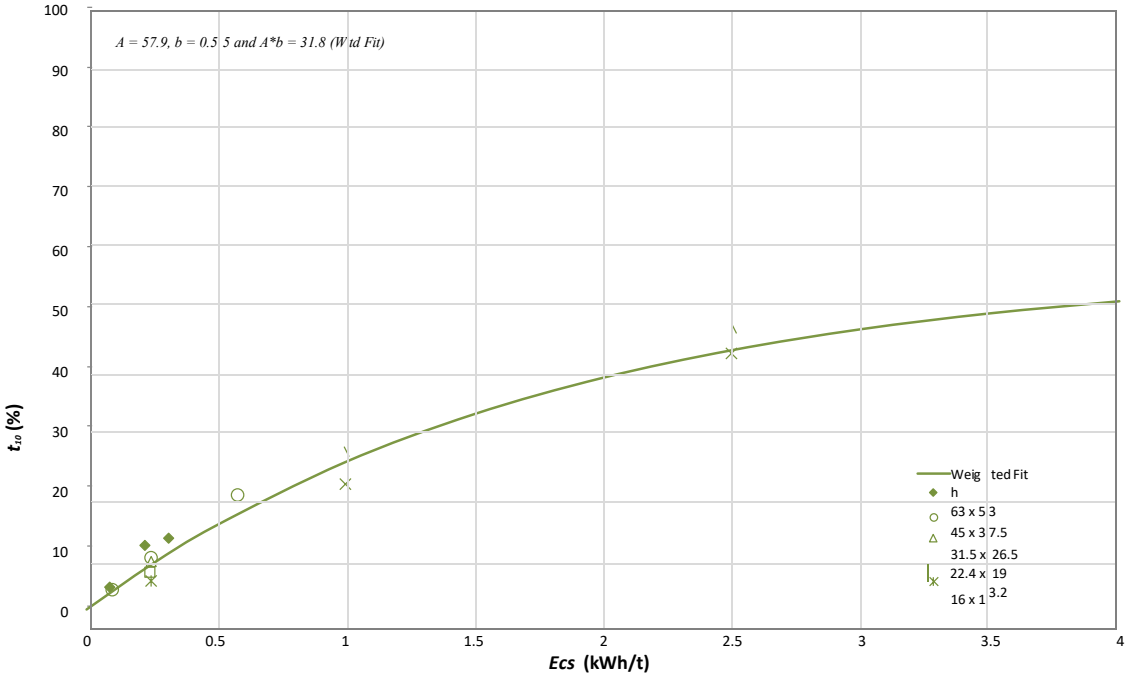

Figure 12 – t_{10} - E_{cs} Relationships for Mine A

Mine A has an $A*b$ value of 31.8. In the JKTech database 80.3% of the 5,200 ore types tested have higher $A*b$ values (refer to Table 5).

The SCSE value for Mine A is 11.72* kWh/t, with 86.3% of samples in the JKTech database having a lower SCSE.

The crusher model parameters for sample Mine A are given in Table 8 below.

The data in Table 8 indicate that for particles of Mine A up to 63 mm, there is some increase in impact resistance with decreasing particle size.

Table 8 - Crusher Model Parameters for Mine A

	Size Relative to Initial Size				
	t_{75}	t_{50}	t_{25}	t_4	t_2
t_{10}	cumulative percent passing				
10.0	2.08	2.77	4.66	24.63	58.46
20.0	4.19	5.60	9.48	46.98	89.25
30.0	6.63	8.80	14.68	66.09	100.00

Specific Comminution Energy:

	Initial Particle Size, mm				
	+13.2-16.0 14.53	+19.0-22.4 20.63	+26.5-31.5 28.89	+37.5-45.0 41.08	+53.0-63.0 57.78
t_{10}	E_{cs}, kWh/t				
10	0.45	0.39	0.34	0.29	0.25
20	0.99	0.85	0.73	0.63	0.54
30	1.65	1.41	1.22	1.05	0.90

The values in this table have been adjusted using the Shi-Kojovic model to achieve data smoothing.

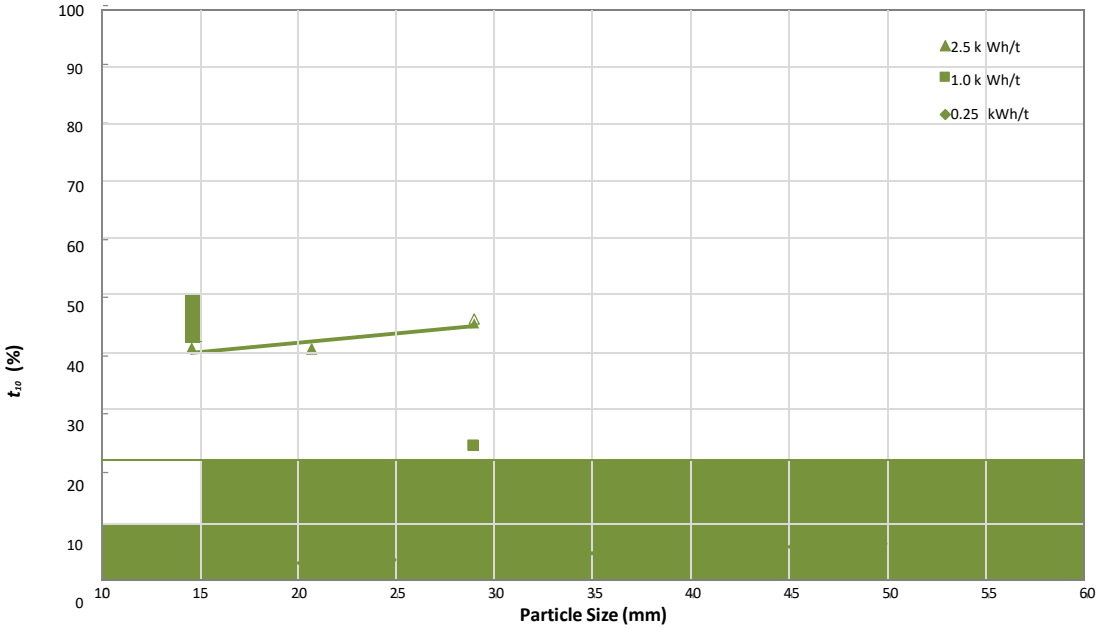

Figure 13 - Variation of Impact Resistance with Particle Size - Mine A

The data graphed in Figure 13 are the t_{10} values for up to 5 different particle sizes from Mine A, all broken with very similar specific comminution energies (0.25 kWh/t, 1.0 kWh/t and 2.5 kWh/t).

The data for Mine A partially follow the frequently observed trend of decreasing slope with decreasing energy (E_{cs} values).

The density measurements for the 30 particles from Mine A are given in Table 9 below. These results are plotted as a histogram in Figure 14.

Table 9 - Relative Density Measurements for 30 Particles for Mine A

2.88	2.92	2.99	3.03	2.83
2.96	2.92	3.04	2.99	3.01
3.02	2.93	2.87	2.85	2.83
3.00	3.00	2.87	2.91	2.92
3.07	2.83	3.14	3.07	2.86
3.07	2.99	2.91	2.84	2.94
Mean				**2.95**
Standard Deviation				**0.08**
Maximum				**3.14**
Minimum				**2.83**

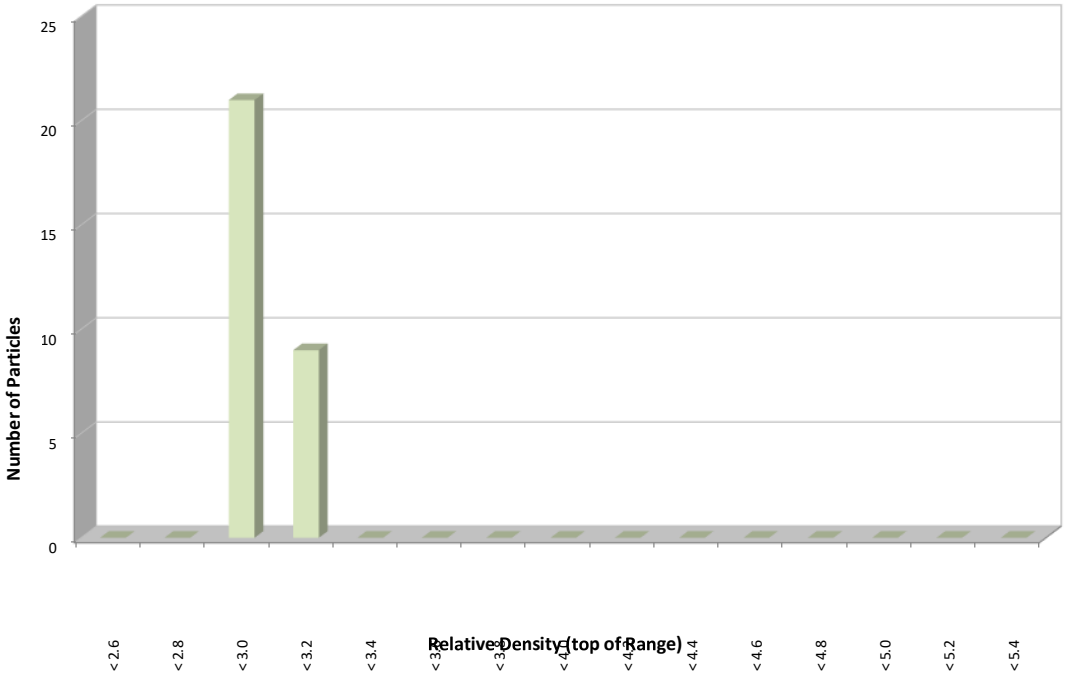

Figure 14 - Histogram of the Relative Density Measurements for 30 Particles for Mine A

The Mine A data contain no evidence of bimodality in the relative density distribution, that is, no evidence of a dense component that could concentrate in the mill load and cause power problems, resulting in a loss of throughput.

3.4.4 JKDW Test Results for Mine D

The t_{10} versus E_{cs} relationship for sample Mine D is given in Figure 15.

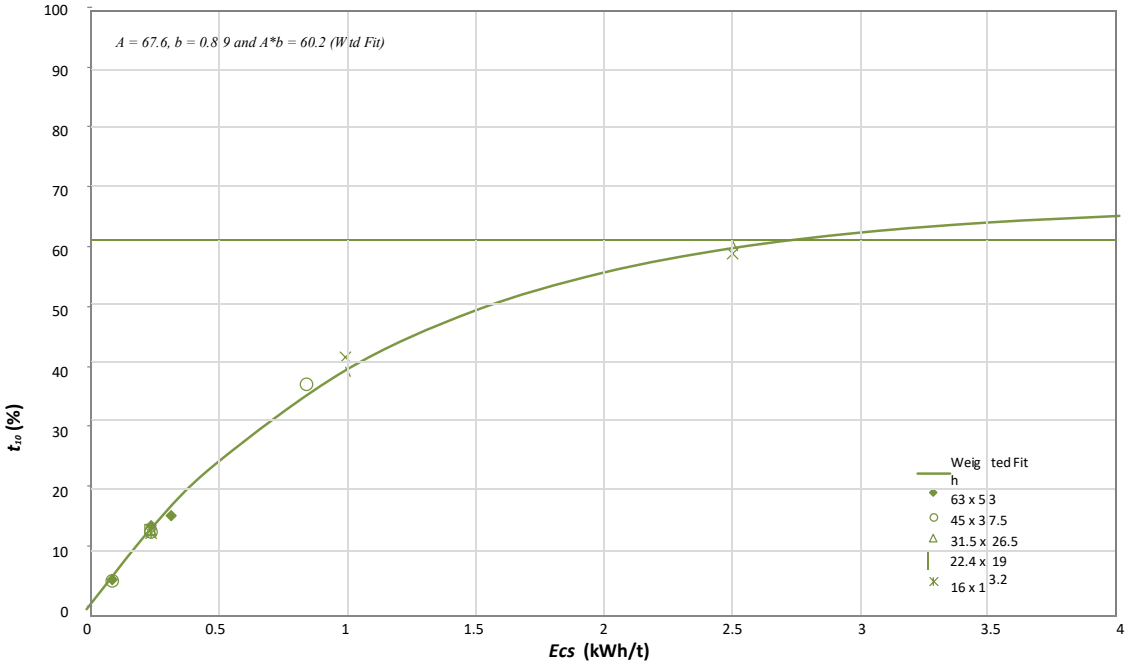

Figure 15 – t_{10} - E_{cs} Relationships for Mine D

Mine D has an $A*b$ value of 60.2. In the JKTech database 30.1% of the 5,200 ore types tested have higher $A*b$ values (refer to Table 5).

The SCSE value for Mine D is 8.56* kWh/t, with 33.3% of samples in the JKTech database having a lower SCSE.

The crusher model parameters for sample Mine D are given in Table 10 below.

The data in Table 10 indicate that for particles of Mine D up to 63 mm, there is no increase in impact resistance with decreasing particle size.

Table 10 - Crusher Model Parameters for Mine D

	Size Relative to Initial Size				
	t_{75}	t_{50}	t_{25}	t_4	t_2
t_{10}	cumulative percent passing				
10.0	4.21	4.83	6.28	20.75	50.78
20.0	8.32	9.63	12.57	41.20	80.73
30.0	12.61	14.64	19.03	60.00	95.25

Specific Comminution Energy:

	Initial Particle Size, mm				
	+13.2-16.0 14.53	+19.0-22.4 20.63	+26.5-31.5 28.89	+37.5-45.0 41.08	+53.0-63.0 57.78
t_{10}	E_{cs}, kWh/t				
10	0.18	0.18	0.18	0.18	0.18
20	0.39	0.39	0.39	0.39	0.39
30	0.66	0.66	0.66	0.66	0.66

The values in this table have been adjusted using the Shi-Kojovic model to achieve data smoothing.

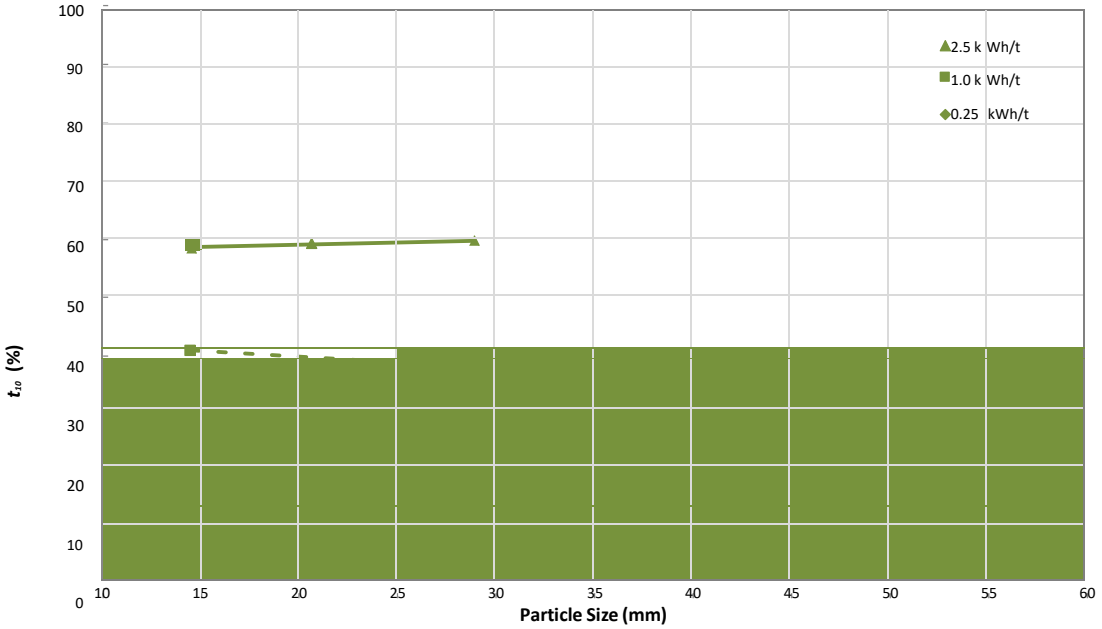

Figure 16 - Variation of Impact Resistance with Particle Size - Mine D

The data graphed in Figure 16 are the t_{10} values for up to 5 different particle sizes from Mine D, all broken with very similar specific comminution energies (0.25 kWh/t, 1.0 kWh/t and 2.5 kWh/t).

The data for Mine D partially follow the frequently observed trend of decreasing slope with decreasing energy (E_{cs} values).

The density measurements for the 30 particles from Mine D are given in Table 11 below. These results are plotted as a histogram in Figure 17.

Table 11 - Relative Density Measurements for 30 Particles for Mine D

2.74	2.83	3.13	2.71	2.87
2.78	2.81	2.66	3.01	3.04
2.79	2.95	3.34	3.02	3.05
2.79	3.06	2.76	3.09	3.35
2.83	2.86	2.76	3.24	2.83
2.71	2.68	2.90	2.73	2.82
Mean				**2.90**
Standard Deviation				**0.19**
Maximum				**3.35**
Minimum				**2.66**

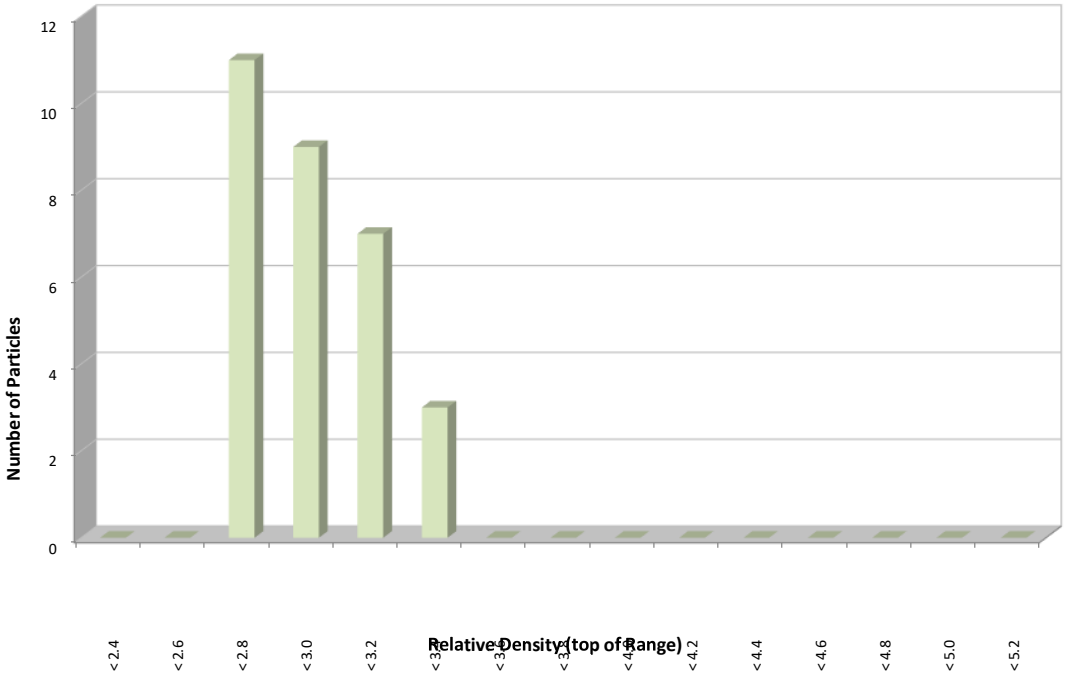

Figure 17 - Histogram of the Relative Density Measurements for 30 Particles for Mine D

The Mine D data contain no evidence of bimodality in the relative density distribution, that is, no evidence of a dense component that could concentrate in the mill load and cause power problems, resulting in a loss of throughput.

3.4.5 JKDW Test Results for Mine F

The t_{10} versus E_{cs} relationship for sample Mine F is given in Figure 18.

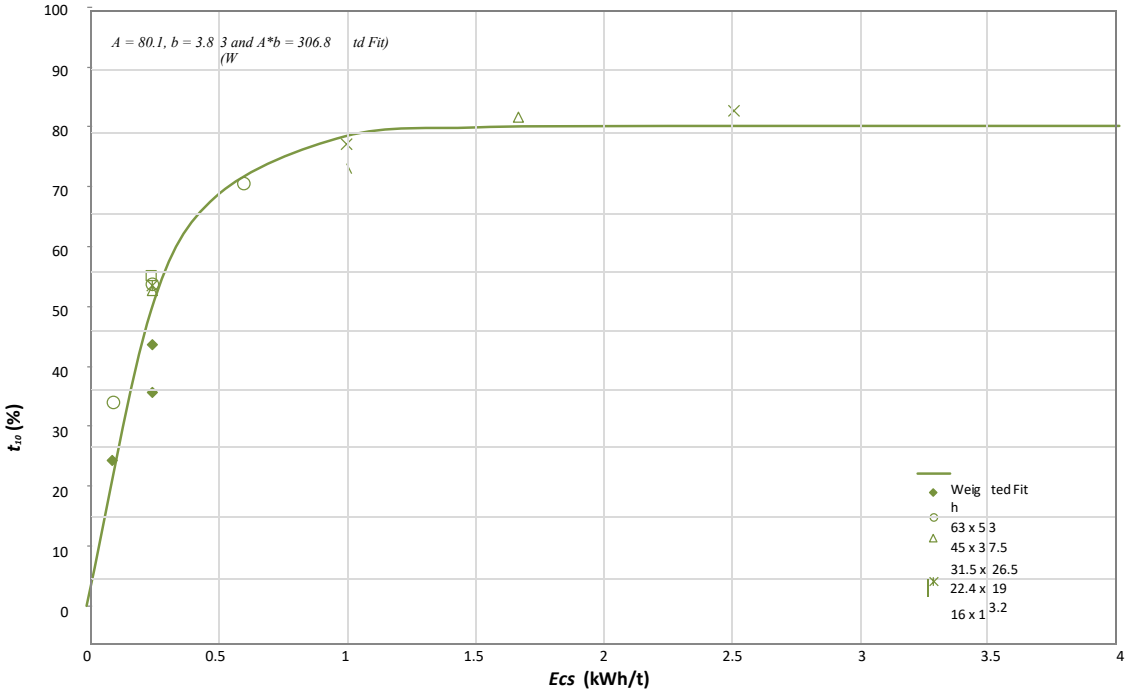

Figure 18 – t_{10} - E_{cs} Relationships for Mine F

Mine F has an $A*b$ value of 306.8. In the JKTech database 1.0% of the 5,200 ore types tested have higher $A*b$ values (refer to Table 5).

The SCSE value for Mine F is 4.59* kWh/t, with 0.3% of samples in the JKTech database having a lower SCSE.

The crusher model parameters for sample Mine F are given in Table 12 below.

The data in Table 12 indicate that for particles of Mine F up to 63 mm, there is no increase in impact resistance with decreasing particle size.

Table 12 - Crusher Model Parameters for Mine F

	Size Relative to Initial Size				
	t_{75}	t_{50}	t_{25}	t_4	t_2
t_{10}	cumulative percent passing				
10.0	4.69	5.86	8.23	14.59	39.33
20.0	7.71	9.84	14.62	30.74	66.53
30.0	9.70	12.65	19.82	47.35	83.83

Specific Comminution Energy:

	Initial Particle Size, mm				
	+13.2-16.0 14.53	+19.0-22.4 20.63	+26.5-31.5 28.89	+37.5-45.0 41.08	+53.0-63.0 57.78
t_{10}	E_{cs}, kWh/t				
10	0.03	0.03	0.03	0.03	0.03
20	0.08	0.08	0.08	0.08	0.08
30	0.12	0.12	0.12	0.12	0.12

The values in this table have been adjusted using the Shi-Kojovic model to achieve data smoothing.

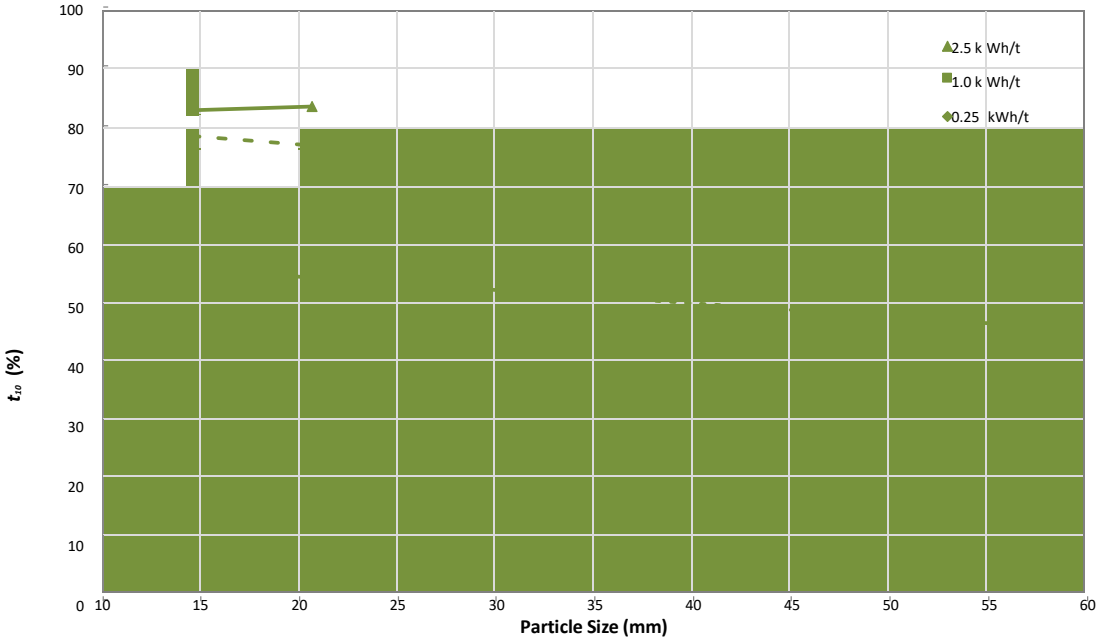

Figure 19 - Variation of Impact Resistance with Particle Size - Mine F

The data graphed in Figure 19 are the t_{10} values for up to 5 different particle sizes from Mine F, all broken with very similar specific comminution energies (0.25 kWh/t, 1.0 kWh/t and 2.5 kWh/t).

The data for Mine F partially follow the frequently observed trend of decreasing slope with decreasing energy (E_{cs} values).

The density measurements for the 30 particles from Mine F are given in Table 13 below. These results are plotted as a histogram in Figure 20.

Table 13 - Relative Density Measurements for 30 Particles for Mine F

4.28	4.67	4.44	4.88	4.88
4.83	2.75	3.16	4.56	3.84
3.84	4.88	4.23	4.40	4.63
3.15	3.60	4.68	4.68	3.81
4.72	4.87	3.85	3.82	4.50
3.95	4.06	3.24	4.70	4.73
Mean				**4.22**
Standard Deviation				**0.60**
Maximum				**4.88**
Minimum				**2.75**

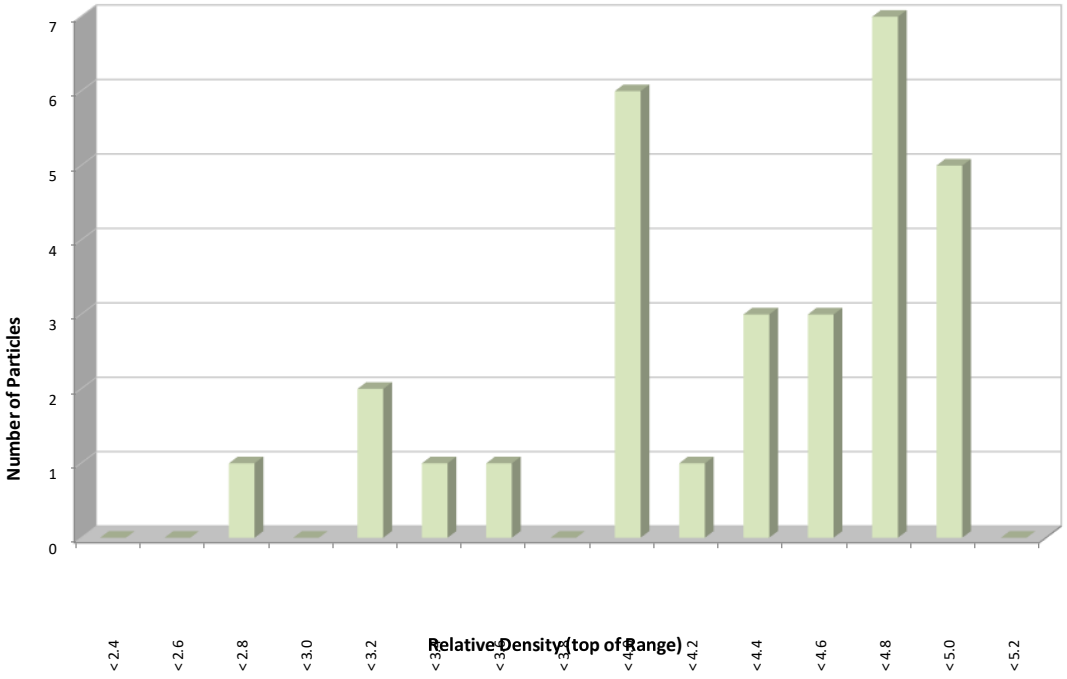

Figure 20 - Histogram of the Relative Density Measurements for 30 Particles for Mine F

The Mine F data contain some evidence of bimodality in the relative density distribution, that is, some evidence of a dense component that could concentrate in the mill load and cause power problems, resulting in a loss of throughput.

3.4.6 JKDW Test Results for Mine C

The t_{10} versus E_{cs} relationship for sample Mine C is given in Figure 21.

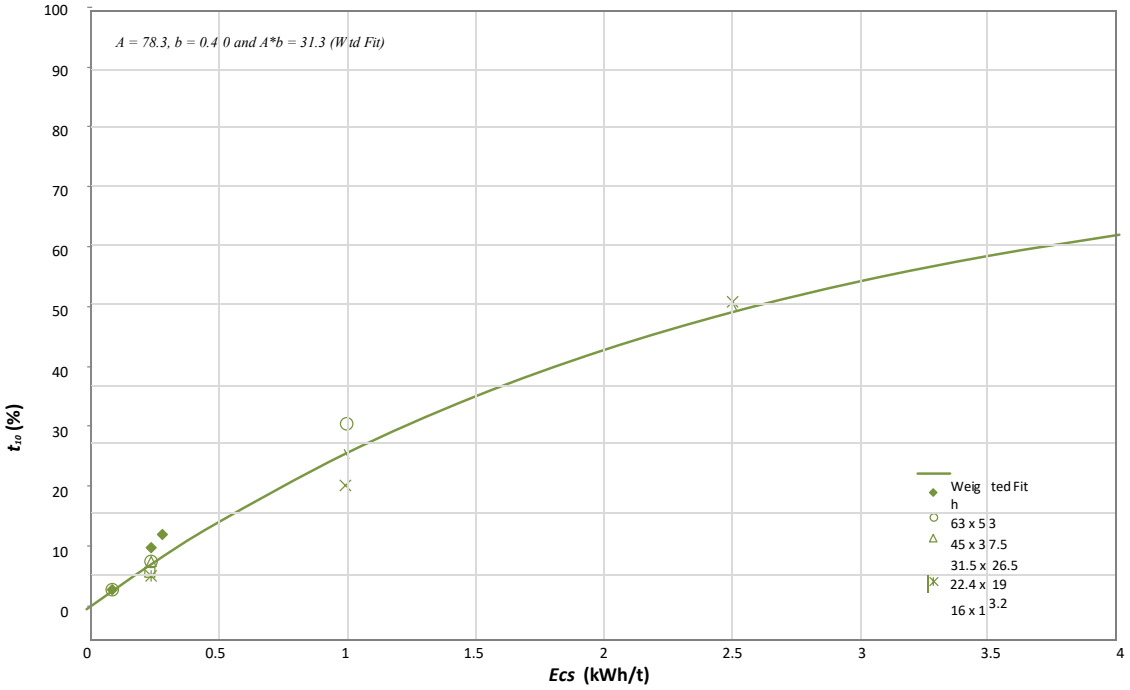

Figure 21 – t_{10} - E_{cs} Relationships for Mine C

Mine C has an $A*b$ value of 31.3. In the JKTech database 81.4% of the 5,200 ore types tested have higher $A*b$ values (refer to Table 5).

The SCSE value for Mine C is 11.92* kWh/t, with 88.1% of samples in the JKTech database having a lower SCSE.

The crusher model parameters for sample Mine C are given in Table 14 below.

The data in Table 14 indicate that for particles of Mine C up to 63 mm, there is some increase in impact resistance with decreasing particle size.

Table 14 - Crusher Model Parameters for Mine C

	Size Relative to Initial Size				
	t_{75}	t_{50}	t_{25}	t_4	t_2
t_{10}	cumulative percent passing				
10.0	2.67	3.37	5.17	21.87	52.55
20.0	5.81	7.22	10.81	44.57	83.75
30.0	9.32	11.48	16.84	65.15	98.67

Specific Comminution Energy:

	Initial Particle Size, mm				
	+13.2-16.0 14.53	+19.0-22.4 20.63	+26.5-31.5 28.89	+37.5-45.0 41.08	+53.0-63.0 57.78
t_{10}	E_{cs}, kWh/t				
10	0.42	0.37	0.33	0.30	0.27
20	0.89	0.79	0.71	0.63	0.56
30	1.43	1.28	1.14	1.02	0.91

The values in this table have been adjusted using the Shi-Kojovic model to achieve data smoothing.

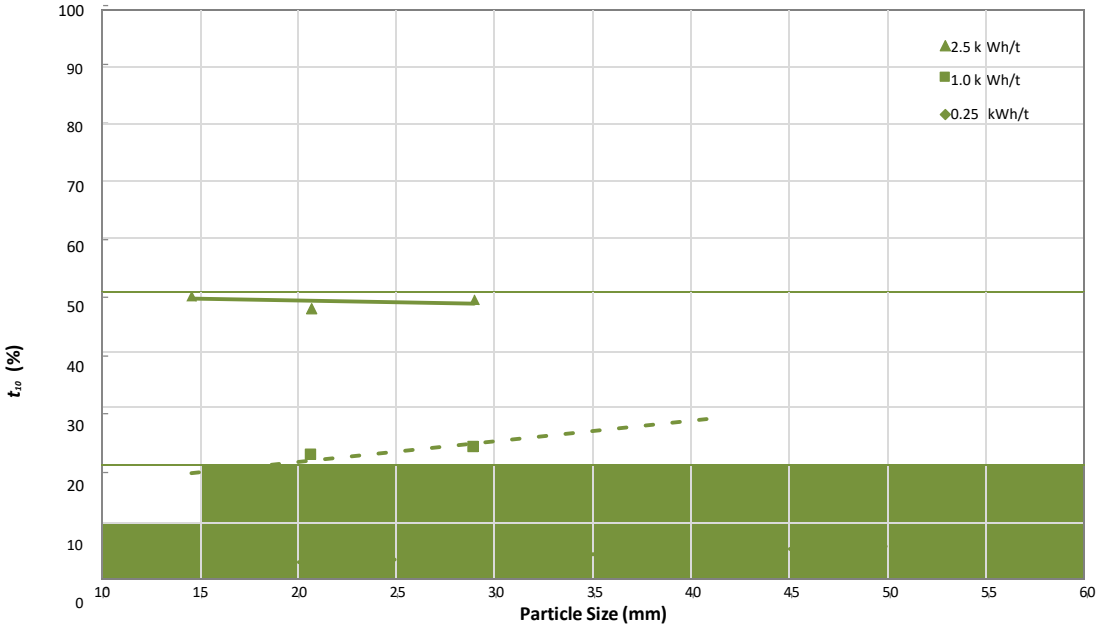

Figure 22 - Variation of Impact Resistance with Particle Size - Mine C

The data graphed in Figure 22 are the t_{10} values for up to 5 different particle sizes from Mine C, all broken with very similar specific comminution energies (0.25 kWh/t, 1.0 kWh/t and 2.5 kWh/t).

The data for Mine C partially follow the frequently observed trend of decreasing slope with decreasing energy (E_{cs} values).

The density measurements for the 30 particles from Mine C are given in Table 15 below. These results are plotted as a histogram in Figure 23.

Table 15 - Relative Density Measurements for 30 Particles for Mine C

3.09	2.85	3.15	3.07	2.86
2.86	2.99	2.85	2.92	2.90
2.93	2.85	2.88	2.87	3.28
2.99	2.82	2.96	3.03	3.03
3.09	2.84	2.83	2.85	2.90
3.33	3.65	2.83	3.05	2.94
Mean				**2.98**
Standard Deviation				**0.18**
Maximum				**3.65**
Minimum				**2.82**

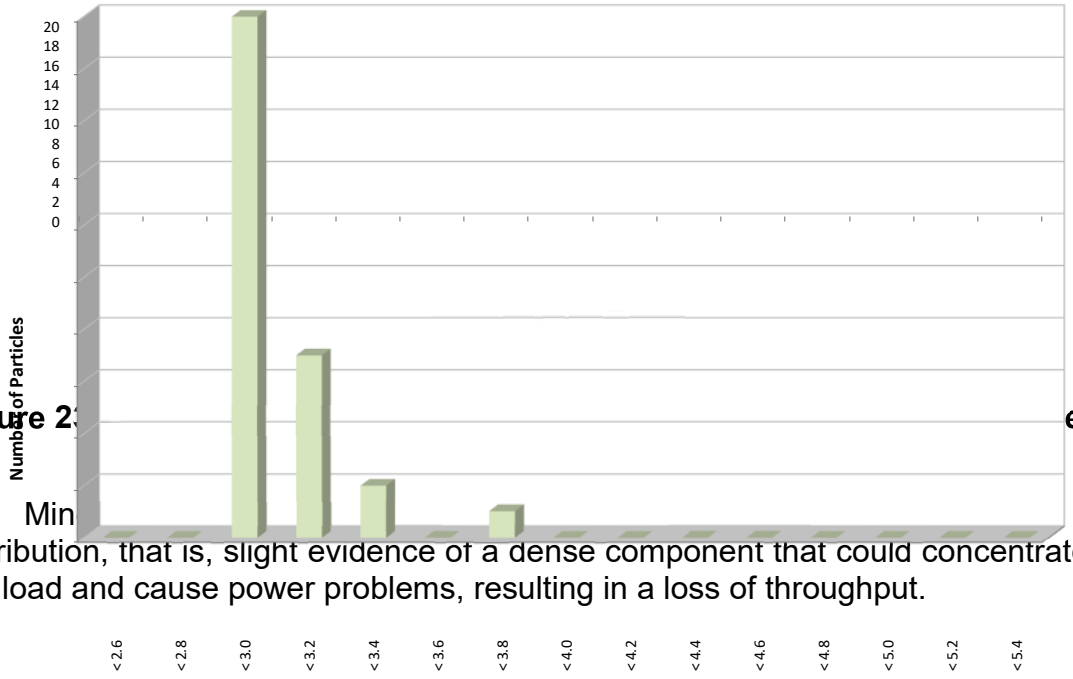

Figure 2 es for

The Min density distribution, that is, slight evidence of a dense component that could concentrate in the mill load and cause power problems, resulting in a loss of throughput.

3.4.7 JKDW Test Results for Mine E

The t_{10} versus E_{cs} relationship for sample Mine E is given in Figure 24.

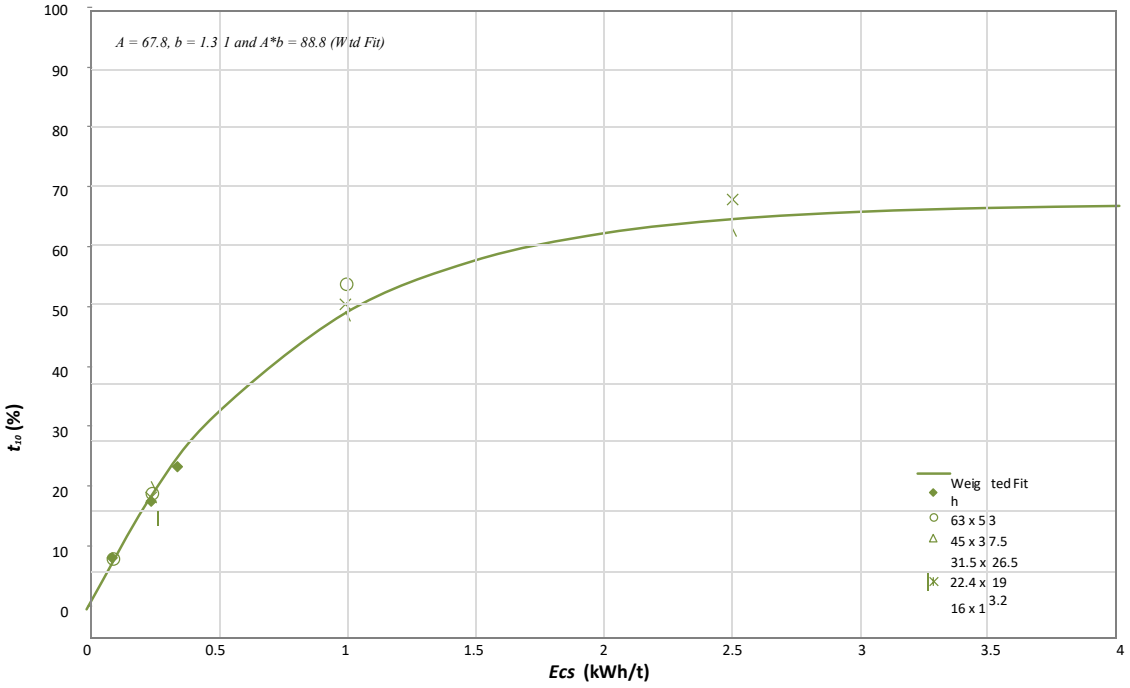

Figure 24 - t_{10} - E_{cs} Relationships for Mine E

Mine E has an $A*b$ value of 88.8. In the JKTech database 14.3% of the 5,200 ore types tested have higher $A*b$ values (refer to Table 5).

The SCSE value for Mine E is 7.20* kWh/t, with 13.7% of samples in the JKTech database having a lower SCSE.

The crusher model parameters for sample Mine E are given in Table 16 below.

The data in Table 16 indicate that for particles of Mine E up to 63 mm, there is no increase in impact resistance with decreasing particle size.

Table 16 - Crusher Model Parameters for Mine E

	Size Relative to Initial Size				
	t_{75}	t_{50}	t_{25}	t_4	t_2
t_{10}	cumulative percent passing				
10.0	3.49	4.31	6.09	21.24	50.83
20.0	7.27	8.93	12.35	40.63	81.11
30.0	11.37	13.92	18.90	57.80	95.92

Specific Comminution Energy:

	Initial Particle Size, mm				
	+13.2-16.0 14.53	+19.0-22.4 20.63	+26.5-31.5 28.89	+37.5-45.0 41.08	+53.0-63.0 57.78
t_{10}	E_{cs}, kWh/t				
10	0.12	0.12	0.12	0.12	0.12
20	0.27	0.27	0.27	0.27	0.27
30	0.45	0.45	0.45	0.45	0.45

The values in this table have been adjusted using the Shi-Kojovic model to achieve data smoothing.

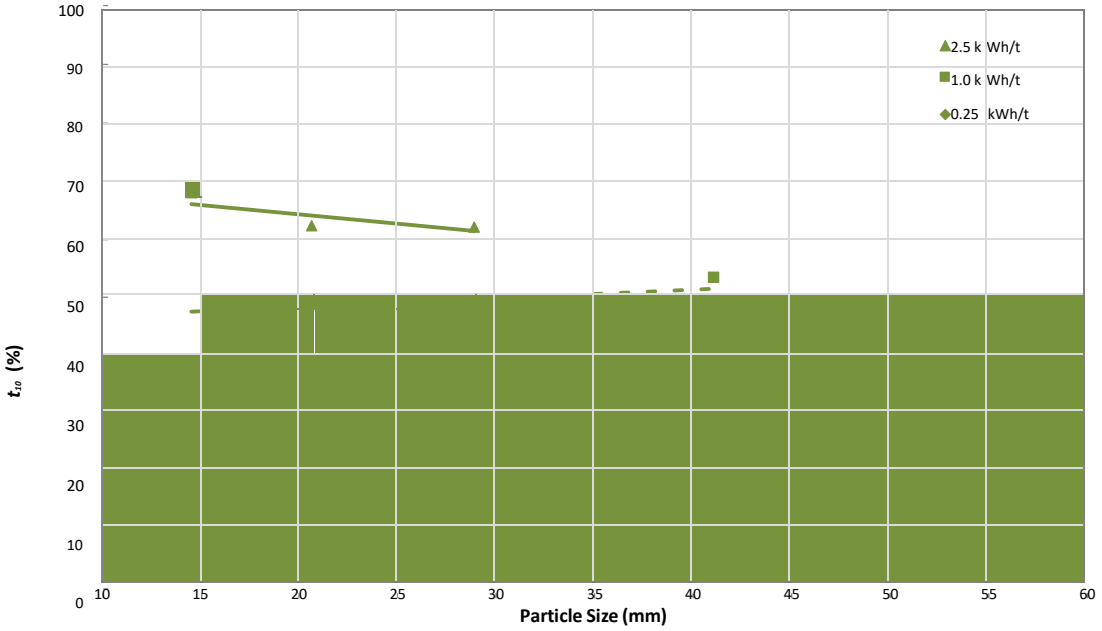

Figure 25 - Variation of Impact Resistance with Particle Size - Mine E

The data graphed in Figure 25 are the t_{10} values for up to 5 different particle sizes from Mine E, all broken with very similar specific comminution energies (0.25 kWh/t, 1.0 kWh/t
and 2.5 kWh/t).

The data for Mine E partially follow the frequently observed trend of decreasing slope with decreasing energy (E_{cs} values).

The density measurements for the 30 particles from Mine E are given in Table 17 below. These results are plotted as a histogram in Figure 26.

Table 17 - Relative Density Measurements for 30 Particles for Mine E

2.79	2.76	2.87	2.78	2.92
2.78	2.81	2.78	2.79	2.78
2.77	2.78	2.84	2.77	2.78
2.78	2.80	2.79	2.83	2.75
2.78	2.93	2.77	2.83	2.78
2.86	2.78	2.77	2.79	2.77
Mean				**2.80**
Standard Deviation				**0.04**
Maximum				**2.93**
Minimum				**2.75**

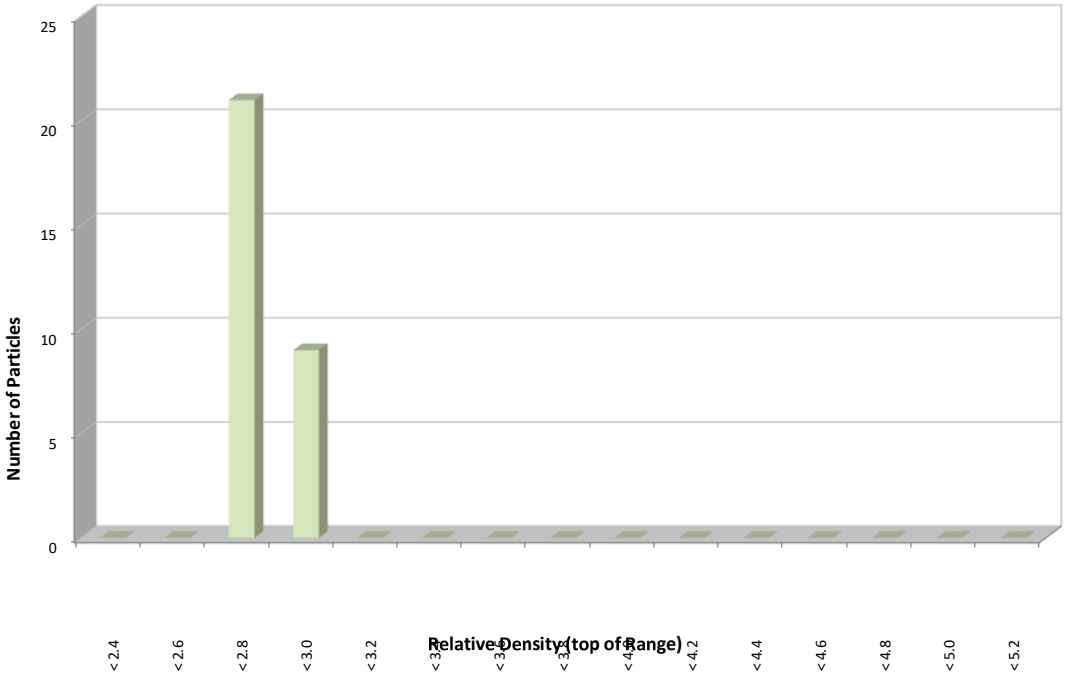

Figure 26 - Histogram of the Relative Density Measurements for 30 Particles for Mine E

The Mine E data contain no evidence of bimodality in the relative density distribution, that is, no evidence of a dense component that could concentrate in the mill load and cause power problems, resulting in a loss of throughput.

4 THE SMC TEST®

4.1 Introduction

The standard JK Drop-Weight test provides ore specific parameters for use in the JKSimMet Mineral Processing Simulator software. In JKSimMet, these parameters are combined with equipment details and operating conditions to analyse and/or predict SAG/autogenous mill performance. The same test procedure also provides ore type characterisation for the JKSimMet crusher model.

The SMC Test was developed by Steve Morrell of SMC Testing Pty Ltd (SMCT). The test provides a cost effective means of obtaining these parameters, in addition to a range of other power-based comminution parameters, from drill core or in situations where limited quantities of material are available. The ore specific parameters have been calculated from the test results and are supplied to University of Oulu in this report as part of the standard procedure

4.2 General Description and Test Background

The SMC Test® was originally designed for the breakage characterisation of drill core and it generates a relationship between input energy (kWh/t) and the percent of broken product passing a specified sieve size. The results are used to determine the so-called JK Drop-Weight index (DWi), which is a measure of the strength of the rock when broken under impact conditions and has the units kWh/m^3. The DWi is directly related to the JK rock breakage parameters A and b and hence can be used to estimate the values of these parameters as well as being correlated with the JK abrasion parameter - t_a. For crusher modelling the t_{10}-E_{cs} matrix can also be derived. This is done by using the size-by-size $A*b$ values that are used in the SMC Test® data analysis (see below) to estimate the t_{10}-E_{cs} values for each of the relevant size fractions in the crusher model matrix.

For power-based calculations, (see APPENDIX C), the SMC Test® provides the comminution parameters M_{ia}, M_{ih} and M_{ic}. M_{ia} is the work index for the grinding of coarser particles (> 750 µm) in tumbling mills such as autogenous (AG), semi-autogenous (SAG), rod and ball mills. M_{ih} is the work index for the grinding in High Pressure Grinding Rolls (HPGR) and M_{ic} for size reduction in conventional crushers.

The SMC Test® is a precision test, which uses particles that are either cut from drill core using a diamond saw to achieve close size replication or else selected from crushed material so that particle mass variation is controlled within a prescribed range. The particles are then broken at a number of prescribed impact energies. The high degree of control imposed on both the size of particles and the breakage energies used, means that the test is largely free of the repeatability problems associated with tumbling-mill based tests. Such tests usually suffer from variations in feed size (which is not closely controlled) and energy input, often assumed to be constant when in reality it can be highly variable (Levin, 1989).

The relationship between the DWi and the JK rock breakage parameters makes use of the size-by-size nature of rock strength that is often apparent from the results of full JK Drop-Weight tests. The effect is illustrated in Figure 27, which plots the normalized values of A*b against particle size. This figure also shows how the gradient of these plots varies across the full range of rock types tested. In the case of a conventional JK Drop-Weight test, these values are effectively averaged and a mean value of A and

b is reported. The SMC Test® uses a single size and makes use of relationships such as that shown in Figure 27 to predict the A and b of the particle size that has the same value as the mean for a JK full Drop-Weight test.

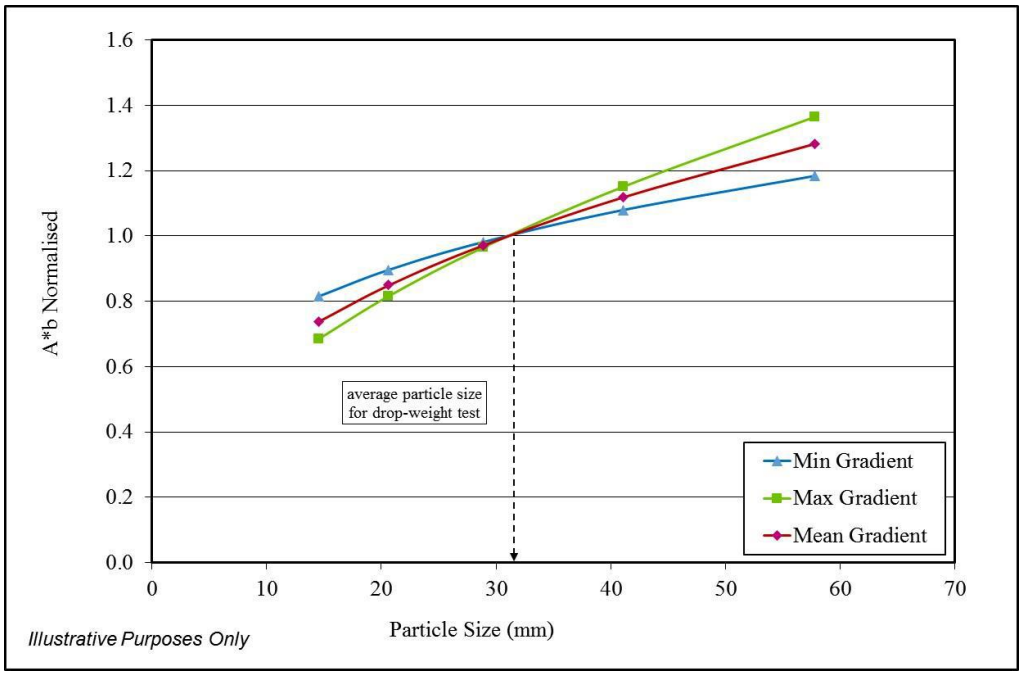

Figure 27 – Relationship between Particle Size and *A*b*

4.3 The Test Procedure

In the SMC Test®, five sets of 20 particles are broken, each set at a different specific energy level, using a JK Drop-Weight tester. The breakage products are screened at a sieve size selected to provide a direct measurement of the t_{10} value.

The test calls for a prescribed target average volume for the particles, with the target being chosen to be equivalent to the mean volume of particles in one of the standard JK Drop-Weight test size fractions.

The rest height of the drop-head (gap) is recorded after breakage of each particle to allow for a correction to the drop energy. After breaking all 20 particles in a set, the broken product is sieved at an aperture size, one tenth of the original particle size. Thus, the percent passing mass gives a direct reading of the t_{10} value for breakage at that energy level.

There are two alternative methods of preparing the particle sets for breakage testing: the particle selection method and the cut core method. The particle selection method is the most commonly used as it is generally less time consuming. The cut core method requires less material, so tends to be used as a fallback method, only when necessary to cope with restricted sample availability.

4.3.1 Particle Selection Method

For the particle selection method, the test is carried out on material in one of three alternative size fractions: -31.5+26.5, -22.4+19 or -16+13.2 mm. The largest size fraction is preferred but requires more material.

In the particle selection method, particles are chosen so that their individual masses lie within ±30% of the target mass and the mean mass for each set of 20 lies within ±10% of the target mass. A typical set of particles is shown in Figure 28.

Figure 28 – A Typical Set of Particles for Breakage (Particle Selection Method)

Before commencing breakage tests on the particles, the ore density is determined by first weighing a representative sample of particles in air and then in water.

4.3.2 Cut Core Method

The cut core method uses cut pieces of quartered (slivered) drill core. Whole core or half core can be used, but when received in this form it needs to be first quartered as a preliminary step in the procedure. Once quartered, any broken or tapered ends of the quartered lengths are cut, to square them off. Before the lengths of quartered core are cut to produce the pieces for testing, each one is weighed in air and then in water, to obtain a density measurement and a measure of its mass per unit length.

The size fraction targeted when the cut core method is used depends on the original core diameter. The target size fraction is selected to ensure that pieces of the correct volume will have “chunky” rather than “slabby” proportions.

Having measured the density of the core, the target volume can be translated into a target mass and with the average mass per unit length also known, an average cutting interval can be determined for the core.

Sufficient pieces of the quartered core are cut to generate 100 particles. These are then divided into the five sets of 20 and broken in the JK Drop-Weight tester at the five different energy levels. Within each set, the three possible orientations of the particles are equally represented (as far as possible, given that there are 20 particles). The orientations prescribed for testing are shown in Figure 29.

Figure 29 – Orientations of Pieces for Breakage (Cut Core Method)

The cut core method cannot be used for cores with diameters exceeding 70 mm, where the particle masses would be too large to achieve the highest prescribed energy level.

4.4 SMC Test® Results

The SMC Test® results for the six samples from University of Oulu Project are given in Table 18. This table includes the average rock density and the DWi (Drop-Weight index) that is the direct result of the test procedure. The values determined for the M_{ia}, M_{ih} and M_{ic} parameters developed by SMCT are also presented in this table. The M_{ia} parameter represents the coarse particle component (down to 750 µm), of the overall comminution energy and can be used together with the M_{ib} (fine particle component) to estimate the total energy requirements of a conventional comminution circuit. The use of these parameters is explained further in APPENDIX C. The derived estimates of parameters A, b and t_a that are required for JKSimMet comminution modelling are given in Table 19.

Also included in the derived results are the SAG Circuit Specific Energy (SCSE) values. The SCSE value is derived from simulations of a “standard” circuit comprising a SAG mill in closed circuit with a pebble crusher. This allows $A*b$ values to be described in a more meaningful form. SCSE is described in detail in APPENDIX A.

In the case of the six samples from University of Oulu Project, the A and b estimates are based on DWi versus A and b correlations derived from the Integrated JKDW & SMC Test.

Table 18 - SMC Test® Results

Sample Designation	*DWi* (kWh/m³)	*DWi* (%)	*Mi* Parameters (kWh/t)			SG
			Mia	*Mih*	*Mic*	
Mine B	8.81	77	20.4	16.0	8.3	3.20
Mine A	9.82	86	24.2	19.3	10.0	2.95
Mine D	4.39	22	12.9	8.8	4.5	2.90
Mine F	1.36	3	3.5	1.9	1.0	4.22
Mine C	9.74	85	23.8	18.9	9.8	2.98
Mine E	2.74	9	9.2	5.7	2.9	2.80

For more details on how the M_{ia}, M_{ih} and M_{ic} parameters are derived and used, see APPENDIX C or go to the SMC Testing website at http://www.smctesting.com/about and click on the link to download Steve Morrell's paper on this subject.

Table 19 – Parameters derived from the SMC Test® Results

Sample Designation	Calibration Sample	*A*	*b*	t_a	*SCSE (kWh/t)*
Mine B	Mine B	81.9	0.44	0.29	11.5
Mine A	Mine A	72.7	0.41	0.26	12.13
Mine D	Mine D	72.7	0.85	0.55	8.46
Mine F	Mine F	78.8	3.95	1.91	4.58
Mine C	Mine C	100.0	0.30	0.26	12.18
Mine E	Mine E	66.2	1.44	0.88	7.02

The influence of particle size on the specific comminution energy needed to achieve a particular t_{10} value can also be inferred from the SMC Test® results. The energy requirements for five particle sizes, each crushed to three different t_{10} values, are presented in Table 20.

Table 20 – Crusher Simulation Model Specific Energy Matrix

Sample Designation	Particle Size (mm)														
	14.5			20.6			28.9			41.1			57.8		
	t_{10} Values (%) for Given Specific Energies in kWh/t														
	10	20	30	10	20	30	10	20	30	10	20	30	10	20	30
Mine B	0.42	0.89	1.43	0.34	0.73	1.17	0.28	0.60	0.96	0.23	0.49	0.78	0.19	0.41	0.65
Mine A	0.49	1.03	1.65	0.41	0.87	1.38	0.34	0.73	1.17	0.29	0.61	0.97	0.24	0.52	0.83
Mine D	0.20	0.41	0.66	0.18	0.38	0.62	0.17	0.36	0.57	0.16	0.33	0.53	0.15	0.31	0.50
Mine F	0.04	0.09	0.14	0.04	0.08	0.13	0.03	0.07	0.12	0.03	0.07	0.11	0.03	0.06	0.10
Mine C	0.43	0.92	1.47	0.39	0.83	1.33	0.35	0.75	1.20	0.32	0.67	1.07	0.29	0.61	0.97
Mine E	0.13	0.28	0.48	0.12	0.27	0.45	0.11	0.25	0.42	0.10	0.23	0.39	0.10	0.21	0.36

The SMC Test® database now contains over 50,000 test results on samples representing more than 1300 different deposits worldwide.

Around 99% of the DWi values lie in the range 0.5 to 14.0 kWh/m^3, with soft ores being at the low end of this range and hard ores at the high end.

A cumulative graph of DWi values from the SMC Test® Database is shown in Figure 30 below. This graph can be used to compare the DWi of the material from University of Oulu Project, with the entire population of ores in the SMCT database. The figures on the y-axis of the graph represent the percentages of all ores tested that are softer than the x-axis (DWi) value selected.

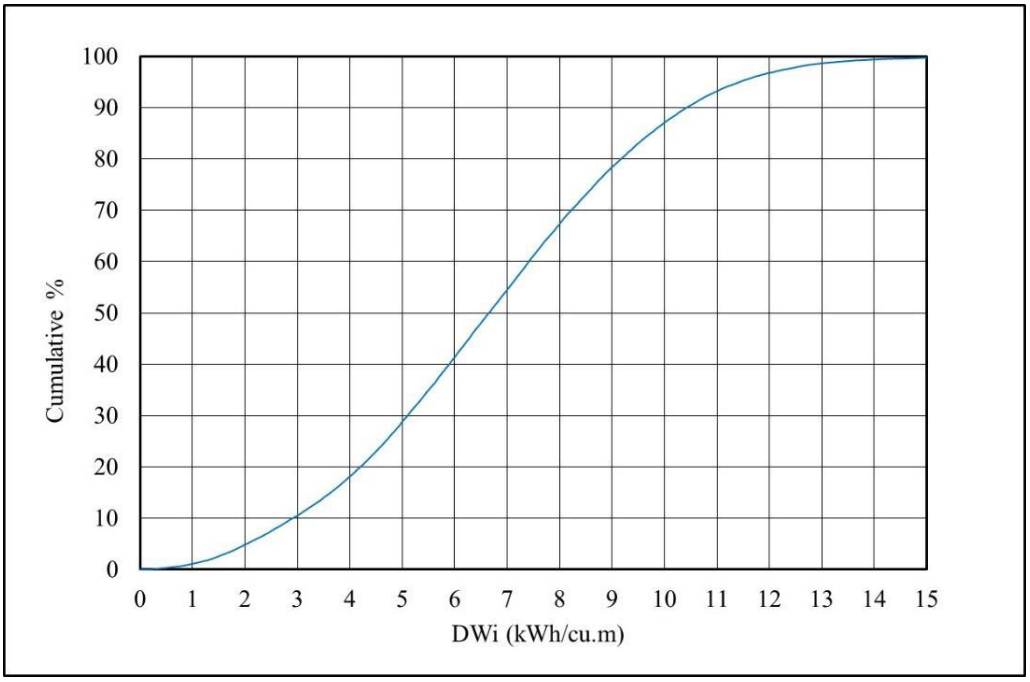

Figure 30 – Cumulative Distribution of DWi Values in SMCT Database

A further cumulative distribution graph is provided in Figure 31 to allow a comparison of the M_{ia}, M_{ih} and M_{ic} values obtained for the University of Oulu Project material, with the entire population of values for these parameters contained in the SMCT database.

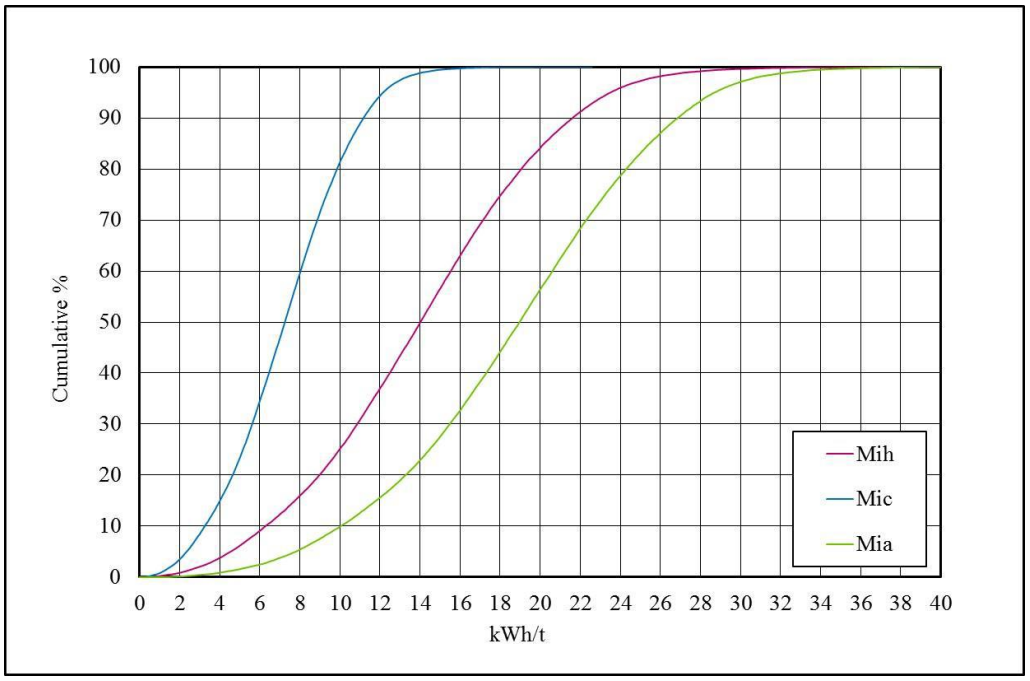

Figure 31 - Cumulative Distribution of M_{ia}, M_{ih} and M_{ic} Values in the SMCT Database

The value of $A*b$, which is also a measure of resistance to impact breakage, is calculated and presented in Table 21, which also gives a comparison to the population of samples in the JKTech database, with the percent of samples present in the JKTech database that are softer. Note that in contrast to the DWi, a high value of $A*b$ means that an ore is soft whilst a low value means that it is hard.

Table 21 – Derived Values for $A*b$, t_a and SCSE

Sample Designation	*A*b*		*t_a*		*SCSE (kWh/t)*	
	Value	**%**	**Value**	**%**	**Value**	**%**
Mine B	36.0	69.8	0.29	79.1	11.5	84.0
Mine A	29.8	85.1	0.26	84.3	12.13	89.9
Mine D	61.8	28.7	0.55	35.7	8.46	31.2
Mine F	311.3	1.0	1.91	3.6	4.58	0.2
Mine C	30.0	84.5	0.26	84.3	12.18	90.4
Mine E	95.3	12.5	0.88	16.4	7.02	12.1

In Figure 32 and Figure 33 below, histogram style frequency distributions for the $A*b$ values and for the SCSE values in the JKTech DW database are shown respectively.

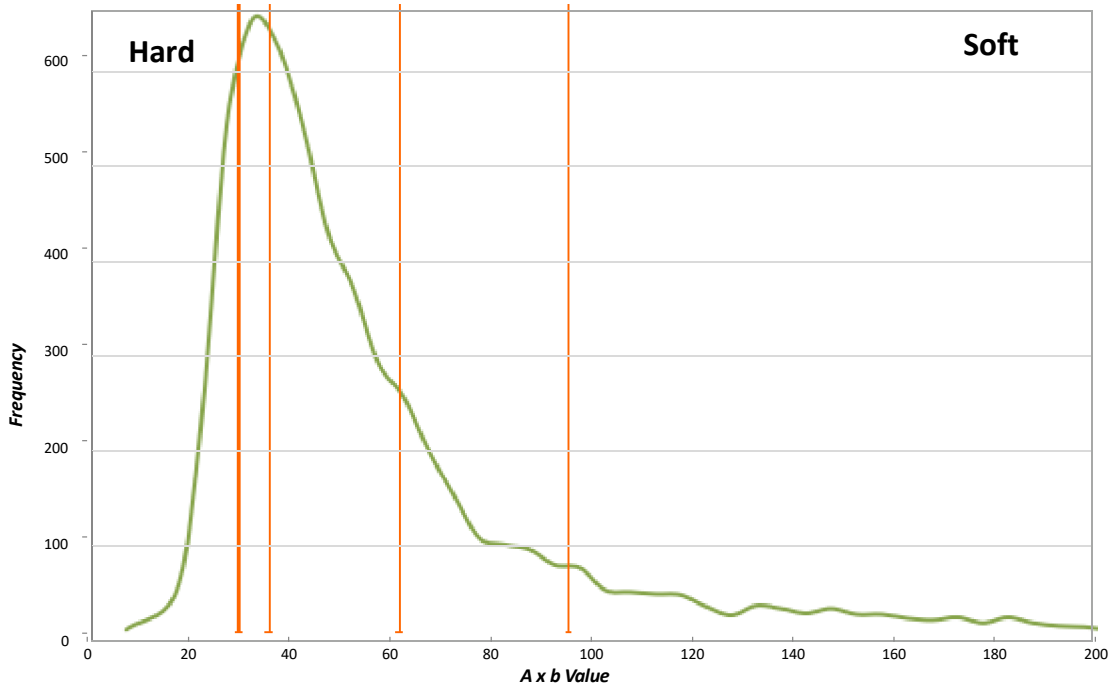

Figure 32 - Frequency Distribution of $A*b$ in the JKTech Database

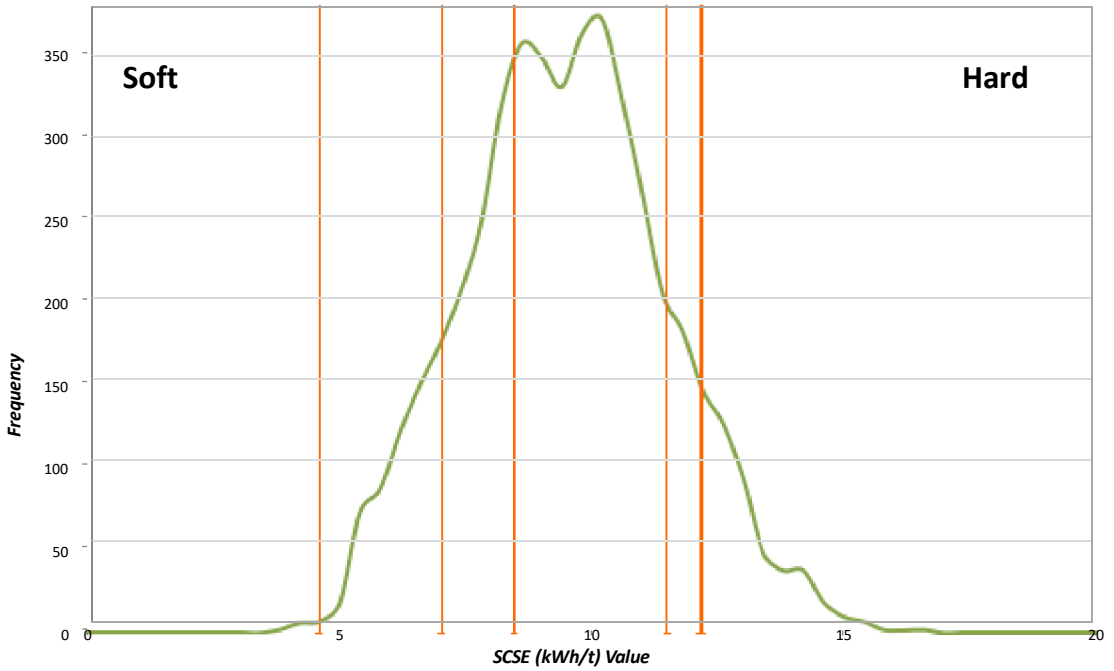

Figure 33 - Frequency Distribution of SCSE in the JKTech Database

5 REFERENCES

Andersen, J. and Napier-Munn, T.J., 1988, "Power Prediction for Cone Crushers", Third Mill Operators' Conference, Aus.I.M.M (Cobar, NSW), May 1988, pp 103 - 106

Bailey, C., *et al*, 2009. "What Can Go Wrong in Comminution Circuit Design?", Proceedings of the Tenth Mill Operators' Conference, (Adelaide, SA), pp. 143–149

Bond, F.C., 1961. "Crushing and Grinding Calculations Parts I and II", British *Chemical Engineering*, Vol 6, Nos 6 and 8

Leung, K. 1987. "An Energy-Based Ore Specific Model for Autogenous and Semi-Autogenous Grinding Mills." Ph.D. Thesis. University of Queensland (unpublished)

Leung, K., Morrison, R.D. and Whiten, W.J., 1987. "An Energy Based Ore Specific Model for Autogenous and Semi-autogenous Grinding", Copper *87*, Vina del Mar, Vol. 2, pp 71 - 86

Levin, J., 1989. Observation on the bond standard grindability test, and a proposal for a standard grindability test for fine materials. SAIMM 89 (1), 13-21.

Morrell, S. 1996. "Power Draw of Wet Tumbling Mills and Its Relationship to Charge Dynamics - Parts I and II", *Transaction Inst. Min. Metall.* (Sect C: Mineral Process Extr. Metall.), 105, 1996, pp C43-C62

Morrell, S., 2004[a]. *Predicting the Specific Energy of Autogenous and Semi-autogenous Mills from Small Diameter Drill Core Samples*. Minerals Engineering, Vol 17/3 pp 447-451

Morrell, S., 2004[b]. *An Alternative Energy-Size Relationship To That Proposed By Bond For The Design and Optimisation Of Grinding Circuits*. International Journal of Mineral Processing, 74, 133-141.

Morrell, S., 2006. *Rock Characterisation for High Pressure Grinding Rolls Circuit Design*, Proc International Autogenous and Semi Autogenous Grinding Technology,Vancouver, vol IV pp 267-278.

Morrell,S., 2008, *A method for predicting the specific energy requirement of comminution circuits and assessing their energy utilisation efficiency*, *Minerals Engineering*, Vol. 21, No. 3.

Shi, F. and Kojovic, T., 2007. Validation of a model for impact breakage incorporating particle size effect. Int. Journal of Mineral Processing, 82, 156-163.

Veillette, G., and Parker, B., 2005. Boddington Expansion Project Comminution Circuit Features and Testwork, Randol Gold Forum Proceedings.

6 DISCLAIMER

Warranty by JKTech

a. JKTech will use its best endeavours to ensure that all documentation, data, recommendations, information, advice and reports ("Material"), provided by JKTech to the client ("Recipient"), is accurate at the time of providing it.

Extent of Warranty by JKTech

b. JKTech does not make any representations as to any matter, fact or thing that is not expressly provided for in the Material.

c. JKTech does not give any warranty, nor accept any liability in connection with the Material, except to the extent, if any, required by law or specifically provided in writing by JKTech to the Recipient.

d. JKTech will not be liable to the Recipient for any claims relating to Material in any language other than in English.

e. If, apart from this Disclaimer, any warranty would be implied whether by law, custom or otherwise, that warranty is to the full extent permitted by law excluded.

f. The Recipient will promptly advise JKTech in writing of any losses, damages, compensation, liabilities, amounts, monetary and non-monetary costs and expenses ("Losses"), incurred or likely to be incurred by the Recipient or JKTech in connection with the Material, and any claims, actions, suits, demands or proceedings ("Liabilities") which the Recipient or JKTech may become liable in connection with the Material.

Indemnity and Release by the Recipient

g. The Recipient indemnifies, releases, discharges and saves harmless, JKTech against any and all Losses and Liabilities, suffered or incurred by JKTech, whether under the law of contract, tort, statutory duty or otherwise as a result of:
   i) the Recipient relying on the Material;
   ii) any liability for infringement of a third party's trade secrets, proprietary or confidential information, patents, registered designs, trademarks or names, copyright or other protected rights; and
   iii) any act or omission of JKTech, any employee, agent or permitted sub-contractor of JKTech in connection with the Material.

Limit of Liability

h. JKTech's liability to the Recipient in connection with the Material, whether under the law of contract, tort, statutory duty or otherwise, will be limited to the lesser of:
   i) the total cost of the job; or
   ii) JKTech providing amended Material rectifying the defect.

Exclusion of Consequential Loss

i. JKTech is not liable to the Recipient for any consequential, special or indirect loss (loss of revenue, loss of profits, business interruption, loss of opportunity and legal costs and disbursements), in connection with the Material whether under the law of contract, tort, statutory duty or otherwise.

Defects

j. The Recipient must notify JKTech within seven days of becoming aware of a defect in the Material. To the extent that the defect is caused by JKTech's negligence or breach of contract, JKTech may, at its discretion, rectify the defect.

Duration of Liability

k. After the expiration of one year from the date of first providing the Material to the client, JKTech will be discharged from all liability in connection with the Material. The Recipient (and persons claiming through or under the Recipient) will not be entitled to commence any action, claim or proceeding of any kind whatsoever after that date, against JKTech (or any employee of JKTech) in connection with the Material.

Contribution

l. JKTech's liability to the Recipient for any loss or damage, whether under the law of contract, tort, statutory duty or otherwise will be reduced to the extent that an act or omission of the Recipient, its employees or agents, or a third party to whom the Recipient has disclosed the Material, contributed to the loss or damage.

Severability

m. If any provision of this Disclaimer is illegal, void, invalid or unenforceable for any reason, all other provisions which are self-sustaining and capable of separate enforcement will, to the maximum extent permitted by law, be and continue to be valid and enforceable.

APPENDICES

APPENDIX A. SAG CIRCUIT SPECIFIC ENERGY (SCSE)

For a little over 20 years, the results of JK Drop Weight tests and SMC tests have been reported in part as A, b and t_a parameters. A and b are parameters which describe the response of the ore under test to increasing levels of input energy in single impact breakage. A typical t_{10} v Ecs curve resulting from a Drop Weight test is shown in App Figure 1.

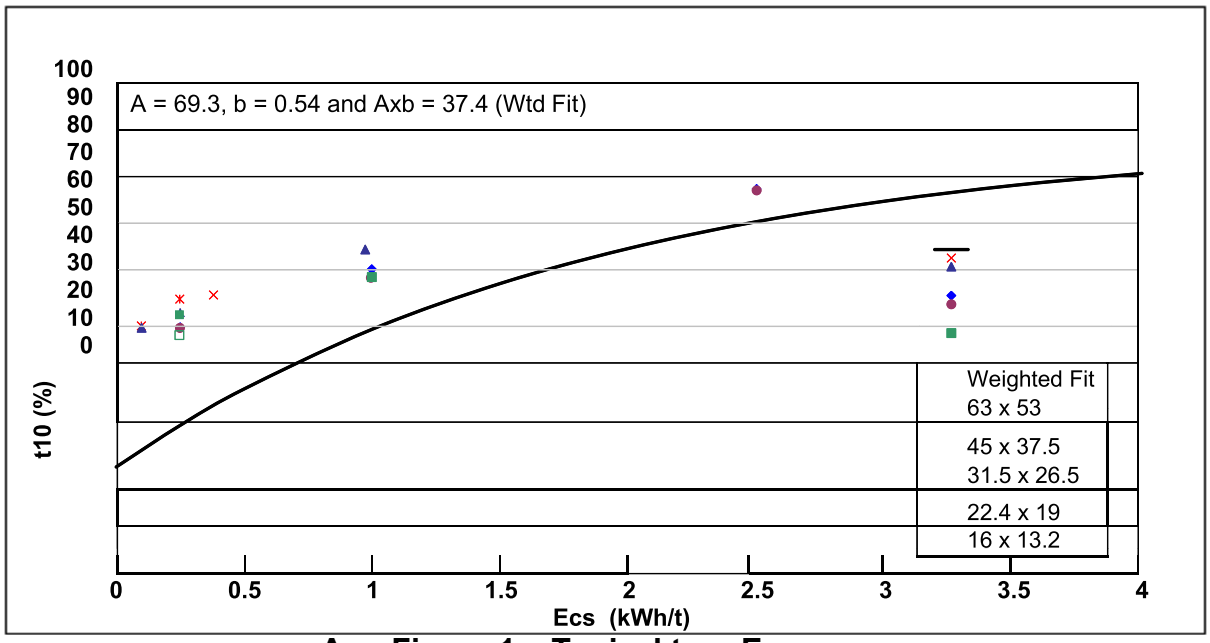

App Figure 1 – Typical t_{10} v Ecs curve

The curve shown in App Figure 1 is represented by an equation which is given in Equation 1.

$$t_{10} = A(1 - e^{-b.Ecs}) \qquad \text{Equation 1}$$

The parameters A and b are generated by least squares fitting Equation 1 to the JK Drop Weight test data. The parameter t_a is generated from a tumbling test.

Both A and b vary with ore type but having two parameters describing a single ore property makes comparison difficult. For that reason the product of A and b, referred to as A*b, which is related to the slope of the t_{10} – E_{cs} curve at the origin, has been universally accepted as the parameter which represents an ore's resistance to impact breakage.

The parameters A, b and t_a have no physical meaning in their own right. They are ore hardness parameters used by the AG/SAG mill model in JKSimMet which permits prediction of the product size distribution and the power draw of the AG/SAG mill for a given feed size distribution and feed rate. In a design situation, the dimensions of the mill are adjusted until the load in the mill reaches 25 % by volume when fed at the required feed rate. The model predicts the power draw under these conditions and from the power draw and throughput the specific energy is determined. The specific energy is mainly a function of the ore hardness (A and b values), the feed size and the dimensions of the mill (specifically the aspect ratio) as well as to a lesser extent the

operating conditions such as ball load, mill speed, grate/pebble port size and pebble crusher activity.

There are two drawbacks to the approach of using A*b as the single parameter to describe the impact resistance of a particular ore. The first is that A*b is inversely related to impact resistance, which adds unnecessary complication. The second is that A*b is related to impact resistance in a non-linear manner. As mentioned earlier this relationship and how it affects comminution machine performance can only be predicted via simulation modelling. Hence to give more meaning to the A and b values and to overcome these shortcomings, JKTech Pty Ltd and SMC Testing Pty Ltd have developed a “standard” simulation methodology to predict the specific energy required for a particular tested ore when treated in a “Standard” circuit comprising a SAG mill in closed circuit with a pebble crusher. The flowsheet is shown in App Figure 2 .

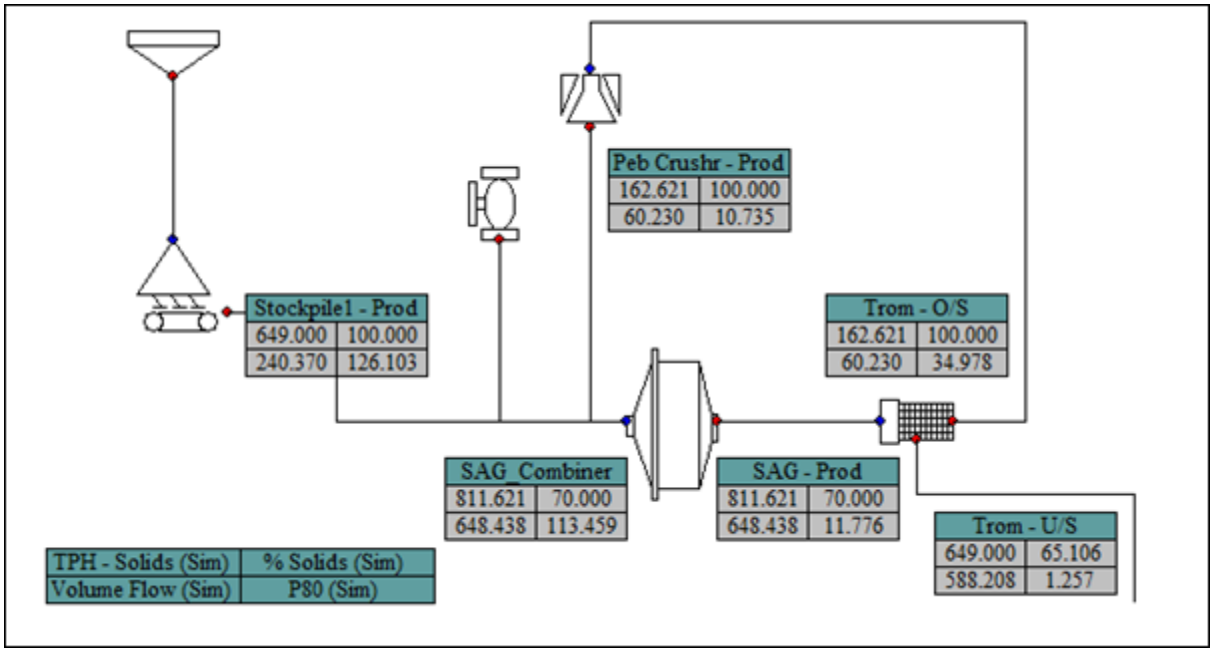

App Figure 2 – Flowsheet used for “Standard” AG/SAG circuit simulations

The specifications for the “standard” circuit are:

- SAG Mill
  - inside shell diameter to length ratio of 2:1 with 15 ° cone angles
  - ball charge of 15 %, 125 mm in diameter
  - total charge of 25 %
  - grate open area of 7 %
  - apertures in the grate are 100 % pebble ports with a nominal aperture of 56 mm
- Trommel
  - Cut Size of 12 mm
- Pebble Crusher
  - Closed Side Setting of 10 mm
- Feed Size Distribution
  - F_{80} from the t_a relationship given in Equation 2

The feed size distribution is taken from the JKTech library of typical feed size distributions and is adjusted to meet the ore specific 80 % passing size predicted using the Morrell and Morrison (1996) F_{80} – t_a relationship for primary crushers with a closed side setting of 150 mm given in Equation 2.

$$F_{80} = 71.3 - 28.4 * \ln(t_a) \qquad \text{Equation 2}$$

Simulations were conducted with A*b values ranging from 15 to 400, t_a values ranging from 0.145 to 3.866 and solids SG values ranging from 2.1 to 4.5. For each simulation, the feed rate was adjusted until the total load volume in the SAG mill was 25 %. The predicted mill power draw and crusher power draw were combined and divided by the feed rate to provide the specific energy consumption. The results are shown in App Figure 3.

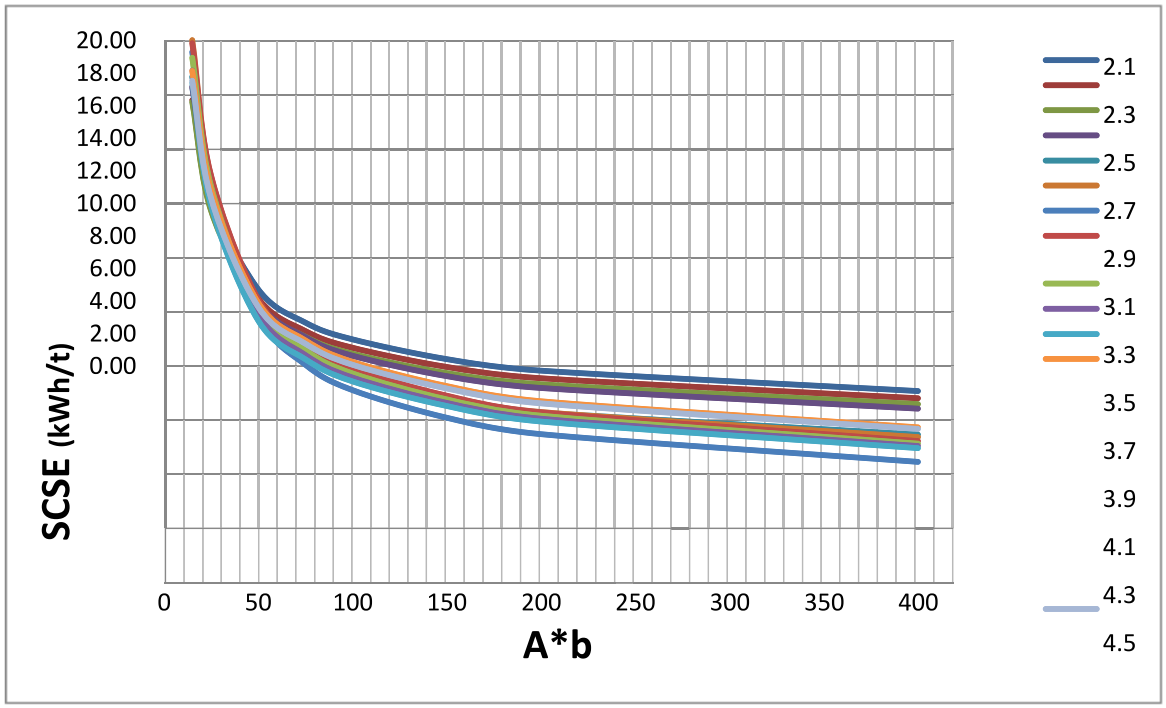

App Figure 3 – The relationship between A*b and specific energy at varying SG for the "Standard" circuit.

It is of note that the family of curves representing the relationship between Specific energy and A*b for the "standard" circuit is very similar to the specific energy – A*b relationship for operating mills published in Veillette and Parker, 2005 and reproduced here in App Figure 4.

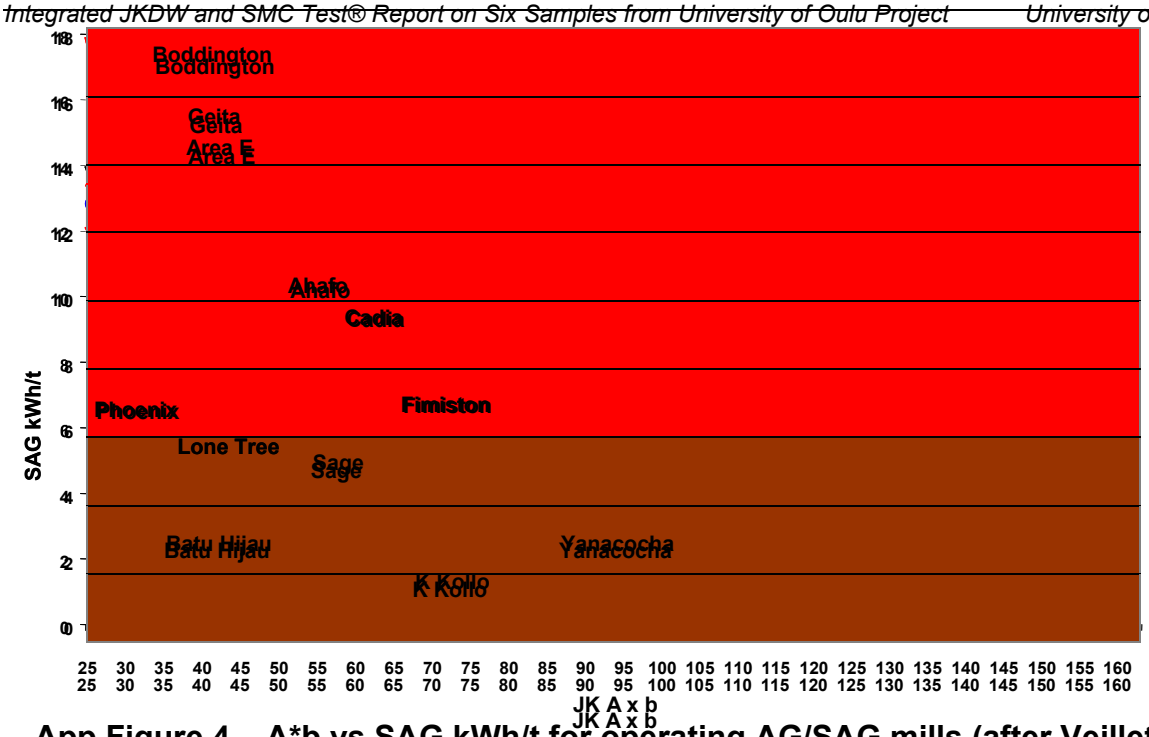

App Figure 4 – A*b vs SAG kWh/t for operating AG/SAG mills (after Veillette and Parker, 2005).

Of course, the SCSE quoted value will not necessarily match the specific energy required for an existing or a planned AG/SAG mill due to differences in the many operating and design variables such as feed size distribution, mill dimensions, ball load and size and grate, trommel and pebble crusher configuration. The SCSE is an effective tool to compare in a relative manner the expected behaviour of different ores in AG/SAG milling in exactly the same way as the Bond laboratory ball mill work index can be used to compare the relative grindability of different ores in ball milling (Bond, 1961 and Rowland and Kjos, 1980). However the originally reported A and b parameters which match the SCSE will be still be required in JKSimMet simulations of a proposed circuit to determine the AG/SAG mill specific energy required for that particular grinding task. Guidelines for the use of JKSimMet for such simulations were given in Bailey *et al*, 2009.

APPENDIX B. BACKGROUND TO THE DROP WEIGHT TEST

B 1 Introduction

This section provides a brief description of the JK Drop-Weight test procedure.

To characterise ore breakage at different energy levels, the JKTech method uses two complimentary techniques:

1. To characterise breakage at moderate to high energy levels (i.e. impact breakage), a JK Drop-Weight device is used.

2. To characterise breakage at low energy inputs (i.e. the abrasion component of breakage), a tumbling test is used.

B 2 Impact Breakage Testing

The JK Drop-Weight device comprises a steel drop-weight that can be raised by a winch to a known height. A pneumatic switch releases the drop-weight, which then falls under gravity and impacts on a rock particle that is positioned on a steel anvil. The device is enclosed in Perspex shielding and incorporates a variety of features to ensure operator safety. By varying the height from which the drop-weight is released and the mass of the drop-weight, a very wide range of energy inputs can be generated. A schematic drawing of the device is given in App Figure 5.

After release, the drop-weight descends under the influence of gravity and impacts the target particle.

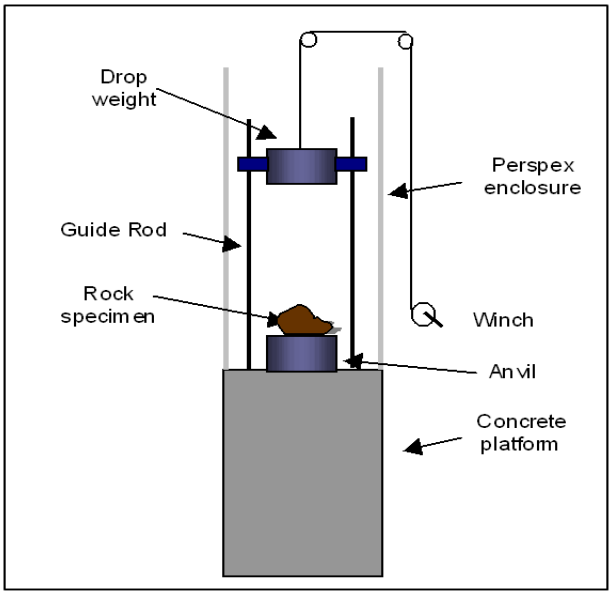

App Figure 5 - The JK Drop Weight Tester

The particle is broken and the drop-weight is brought to rest at a distance above the anvil approximately equal to the largest product particle. The difference in distance between the initial starting point and the final resting place of the drop-weight is used to calculate the energy that is expended in breaking the particle. Thus

$$E_i = Mg(h - x_M)$$ Equation 3

where:

E_i = energy used for breakage

M = drop-weight mass

g = gravitational constant

h = initial height of the drop-weight above the anvil

x_M = final height of the drop-weight above the anvil.

Providing the drop-weight does not rebound after impact, the application of Equation 3 is valid. Where rebound occurs an additional term is required to account for the energy re-transmitted to the drop-weight. Rebound has been seen to occur only at elevated input energies. This energy will be assessed during the test work program. It is likely, however, that its magnitude will be relatively small and can be ignored with only a minimal loss in accuracy.

The assumption is made that all the energy provided is utilised in the breakage of the particle. Thus

$$E_{cs} = E_{is} = E_i/m$$ Equation 4

where:

E_{is} = specific input energy

E_{cs} = specific comminution energy

m = mean particle mass

To test an ore type, the original 100 kg sample is sized into selected fourth-root-of-two size fractions. Ten (10) to thirty (30) particles are required in each size fraction for each energy level, depending on particle mass. Typically fifteen (15) size/energy combinations are selected. The input energy levels for a particular test are designed to suit ore hardness but a standard set of energies are used whenever possible.

The breakage products of all particles for each size/energy combination are collected and sized. The size distribution produced is normalised with respect to the original particle size. For a wide range of energy inputs, particle sizes and ore types, the relative size distributions remain similar in shape and can be fully characterised by a single point on the distribution. The JKTech convention is to use the percentage passing one-tenth of the original particle size. This is referred to as the "t_{10}" value.

In the manner described above, a set of t_{10} and Ecs values are produced for the 15 energy/size combinations.

B 3 Abrasion Breakage Testing

It is possible to characterise low energy (abrasion) breakage with a miniature drop-weight and repeated impacts. However, Leung (1987) demonstrated that a tumbling test of selected single size fractions could produce a similar result with less experimental effort.

The standard abrasion test tumbles 3 kg of -55+38 mm particles for 10 minutes at 70% critical speed in a 305 mm by 305 mm laboratory mill fitted with 4 x 6 mm lifter bars. The resulting product is then sized and the t_{10} value for the product is determined.

The mean particle size of the original size fraction 55 x 38 mm is 45.7 mm. The t_{10} size is 1/10 x 45.7 = 4.57 mm.

B 4 Using Standard DW Test Results in JKSimMet

B 4.1 SAG/autogenous Mill Model

In the SAG/autogenous mill, both breakage mechanisms discussed in Section 2 are assumed to occur. The parameters used in the model are given in Table 4.

B 4.1.1 High Energy or Impact Breakage

To represent the impact breakage mechanism in the model, the 15 pairs of t_{10}/Ecs data from the JK Drop-Weight test are subjected to non-linear least squares techniques to fit Equation 1, which describes the relationship between breakage and impact energy:

$$t_{10} = A(1 - e^{-b.Ecs}) \qquad \text{Equation 1}$$

In this equation, A and b are the fitted parameters. These parameters can then be used in the JKSimMet SAG/autogenous mill model which incorporates the same relationship.

B 4.1.2 Low Energy or Abrasion Breakage

As discussed in B 3, the abrasion test results in a t_{10} figure. The abrasion parameter used in the model, ta, is defined as

$$t_a = t_{10}/10 \qquad \text{Equation 5}$$

For example, if t_{10} = % passing 4.57 mm = 4.0%, then $t_a = 4.0 / 10 = 0.40$.

B 4.1.3 Combined Breakage

These two sets of parameters representing the two breakage modes are used in combination by the model to generate an ore specific appearance function. The scaling factor of 10 is applied in the calculation of t_a so that the relative proportions of high and low energy breakage represented in the combined appearance function are correct.

The assumption is made that all brittle rock types break with the same general pattern and this pattern is built into the model. This assumption does not mean that the amount of energy required to achieve a particular t_{10} is the same for all brittle rocks. It simply means that if a single particle is broken to a particular t_{10} value, then the complete size distribution of the broken fragments is known.

This assumption is not perfect but is quite adequate for the purposes of the SAG/autogenous model.

To use the results of testing, the ore type parameters A and b (from JK Drop-Weight testing) and t_a (from abrasion testing), are entered into the SAG/autogenous mill model in JKSimMet, together with machine dependent parameters of mill size, grate size, ball load, etc. The simulation predicts product size and mill load using appropriate breakage rates. The simulator can then also be used to predict mill performance with variations in screen and classifier configurations or even with recycle crushing.

Details of the SAG/autogenous mill model are given in Leung (1987) and Leung, Morrison, and Whiten (1987). The power prediction for SAG/autogenous mills is based on calculations which are described in Morrell (1996).

B 4.2 Crusher Model

For the crusher model, only the high energy or impact breakage test results are used. These are presented in a somewhat different manner from the SAG/autogenous mill model.

The assumption that all brittle rocks break with the same breakage pattern is not made and the pattern for the ore under test is used. The parameters used by the crusher model are tabulated in the results section of this report. The appearance function defines the shape of the breakage distribution curve at various degrees of "broken-ness", as defined by t_{10}. The specific comminution energy table defines the amount of energy required to achieve varying levels of "broken-ness". The form of the specific comminution energy table reflects the fact that the energy required to achieve a certain degree of breakage is sometimes found to be dependent on the initial particle size.

Details of the crusher model including power prediction are described in Andersen and Napier-Munn (1988).

B 4.3 Limitations

Experience to date demonstrates that the JK Drop-Weight test is appropriate for brittle ores over a wide range of hardness. However, it is not useful for ores which undergo plastic deformation rather than brittle fracture, such as those of high clay content.

The testing procedure is limited by the maximum particle size tested. If the ore is fractured or weaker at larger particle sizes, then JKSimMet simulations will be conservative.

For autogenous mills it is essential to have competent material in the range 150 mm to 100 mm in the feed to form the media. If autogenous milling is seriously contemplated, testing of media competency at larger particle sizes should be conducted. This can be achieved by JK Drop-Weight testing, media competency testing or full pilot plant testing.

APPENDIX C. BACKGROUND AND USE OF THE SMC TEST®

C 1 Introduction

The SMC Test® was developed to provide a range of useful comminution parameters through highly controlled breakage of rock samples. Drill core, even quartered small diameter core is suitable. Only relatively small quantities of sample are required and can be re-used to conduct Bond ball work index tests.

The results from conducting the SMC Test® are used to determine the so-called drop-weight index (DW_i), which is a measure of the strength of the rock, as well as the comminution indices M_{ia}, M_{ih} and M_{ic} . The SMC Test® also estimates the JK rock breakage parameters A, b and t_a as well as the JK crusher model's $t10$-Ecs matrix, all of which are generated as part of the standard report output from the test.

In conjunction with the Bond ball mill work index the DW_i and the M_i suite of parameters can be used to accurately predict the overall specific energy requirements of circuits containing:

- AG and SAG mills.
- Ball mills
- Rod mills
- Crushers
- High Pressure Grinding Rolls (HPGR)

The JK rock breakage parameters can be used to simulate crushing and grinding circuits using JKTech's simulator – JKSimMet.

C 2 Simulation Modelling and Impact Comminution Theory

When a rock fragment is broken, the degree of breakage can be characterised by the "t_{10}" parameter. The t_{10} value is the percentage of the original rock mass that passes a screen aperture one tenth of the original rock fragment size. This parameter allows the degree of breakage to be compared across different starting sizes.

The specific comminution energy (Ecs) has the units kWh/t and is the energy applied during impact breakage. As the impact energy is varied, so does the t_{10} value vary in response. Higher impact energies produce higher values of t_{10}, which of course means products with finer size distributions.
The equation describing the relationship between the t_{10} and Ecs is given below.

$$t_{10} = A(1 - e^{-b.Ecs}) \qquad \text{Equation 1}$$

As can be seen from this equation, there are two rock breakage parameters A and b that relate the t_{10} (size distribution index) to the applied specific energy (Ecs). These parameters are ore specific and are normally determined from a full JK Drop-Weight test.

A typical plot of t_{10} vs Ecs from a JK Drop-Weight test is shown in App Figure 6. The relationship is characterised by the two-parameter equation above, where t_{10} is the dependent variable.

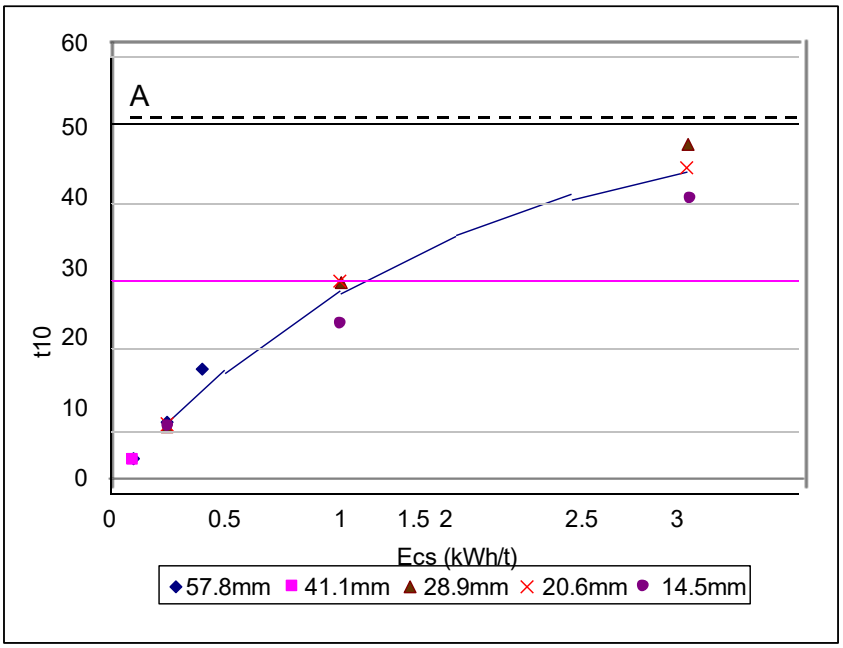

App Figure 6 - Typical t_{10} v Ecs Plot

The t_{10} can be thought of as a "fineness index" with larger values of t_{10} indicating a finer product size distribution. The value of parameter A is the limiting value of t_{10}. This limit indicates that at higher energies, little additional size reduction occurs as the Ecs is increased beyond a certain value. $A*b$ is the slope of the curve at 'zero' input energy and is generally regarded as an indication of the strength of the rock, lower values indicating a higher strength.

The SMC Test® is used to estimate the JK rock breakage parameters A and b by utilizing the fact that there is usually a pronounced (and ore specific) trend to decreasing rock strength with increasing particle size. This trend is illustrated in App Figure 7 which shows a plot of $A*b$ versus particle size for a number of different rock types.

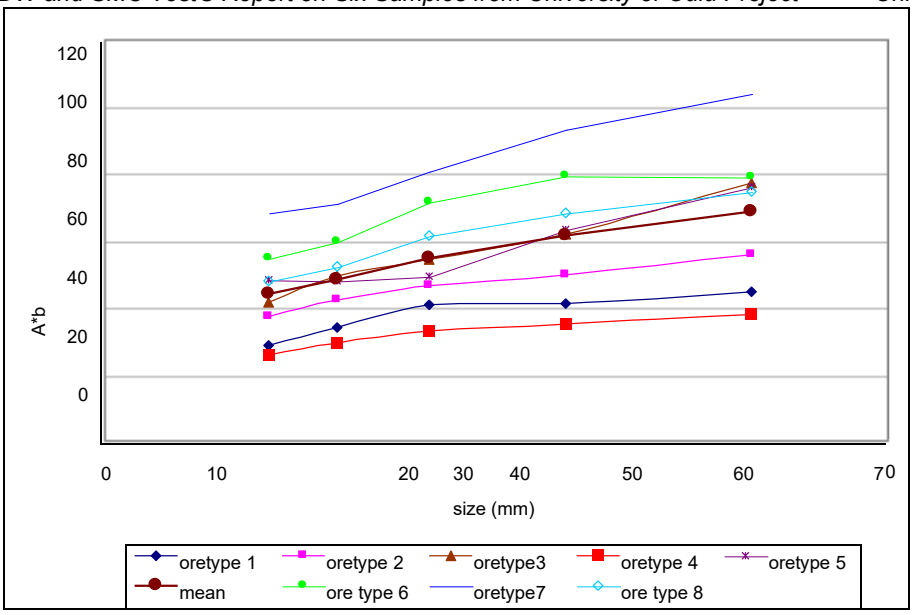

App Figure 7 - Size Dependence of A*b for a Range of Ore Types

In the case of a conventional JK Drop-Weight test these values are effectively averaged and a mean value of A and b is reported. The SMC Test® uses a single size and makes use of relationships such as that shown in App Figure 7 to predict the A and b of the particle size that has the same value as the mean for a full JK Drop-Weight test.

An example of this is illustrated in App Figure 8, where the observed values of the product $A*b$ are plotted against those predicted using the DWi. Each of the data points in App Figure 8 is a result from a different ore type within an orebody.

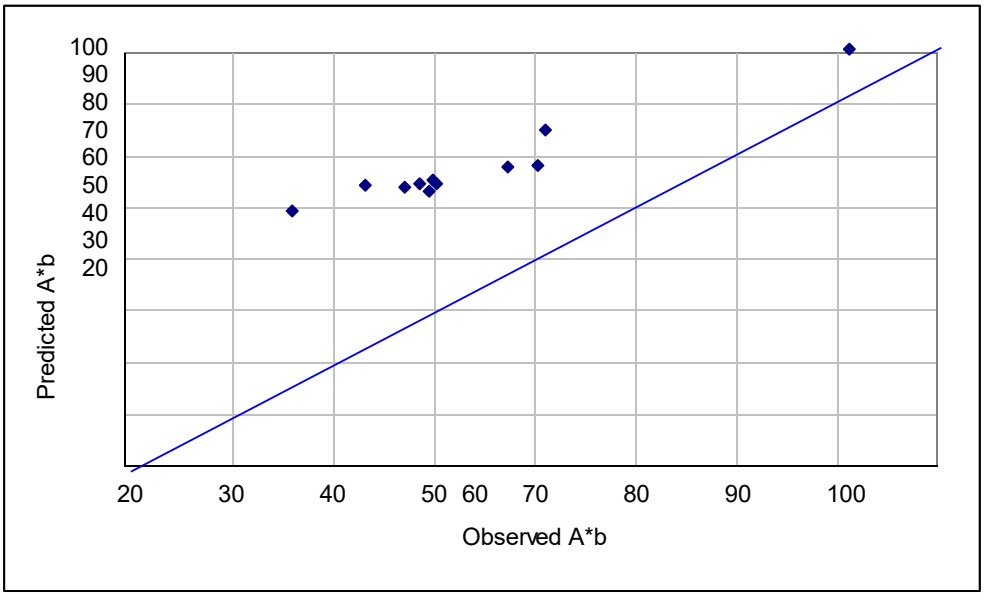

App Figure 8 - Predicted v Observed A*b

The A and b parameters are used with Equation 1 and relationships such as illustrated in App Figure 7 to generate a matrix of Ecs values for a specific range of t_{10} values and

particle sizes. This matrix is used in crusher modelling to predict the power requirement of the crusher given a feed and a product size specification (Napier-Munn et al (1996)).

The A and b parameters are also used in AG/SAG mill models, such as those in JKSimMet, for predicting how the rock will break inside the mill. From this description the models can predict what the throughput, power draw and product size distribution will be (Napier-Munn et al (1996)). Modelling also enables a detailed flowsheet to be built up of the comminution circuit response to changes in ore type. It also allows optimisation strategies to be developed to overcome any deleterious changes in circuit performance predicted from differences in ore type. These strategies can include both changes to how mills are operated (eg ball load, speed etc) and changes to feed size distribution through modification of blasting practices and primary crusher operation (mine-to-mill).

C 3 Power-Based Equations

C 3.1 General

The DW_i, M_{ia}, M_{ih} and M_{ic} parameters are used in so-called power-based equations which predict the specific energy of the associated comminution machines. The approach divides comminution equipment into three categories:

- Tumbling mills, eg AG, SAG, rod and ball mills
- Conventional reciprocating crushers, eg jaw, gyratory and cone
- HPGRs

Tumbling mills are described using 2 indices: M_{ia} and M_{ib}
Crushers have one index: M_{ic}
HPGRs have one index: M_{ih}

For tumbling mills the 2 indices relate to "coarse" and "fine" ore properties plus an efficiency factor which represents the influence of a pebble crusher in AG/SAG mill circuits. "Coarse" in this case is defined as spanning the size range from a P80 of 750 microns up to the P80 of the product of the last stage of crushing or HPGR size reduction prior to grinding. "Fine" covers the size range from a P80 of 750 microns down to P80 sizes typically reached by conventional ball milling, ie about 45 microns. The choice of 750 microns as the division between "coarse" and "fine" particle sizes was determined during the development of the technique and was found to give the best overall results across the range of plants in SMCT's data base. Implicit in the approach is that distributions are parallel and linear in log-log space.

The work index covering grinding in tumbling mills of coarse sizes is labelled M_{ia}. The work index covering grinding of fine particles is labelled Mib (Morrell, 2008). M_{ia} values are provided as a standard output from a SMC Test® (Morrell, 2004a) whilst M_{ib} values can be determined using the data generated by a conventional Bond ball mill work index test (M_{ib} is NOT the Bond ball work index). M_{ic} and M_{ih} values are also provided as a standard output from a SMC Test® (Morrell, 2009).

The general size reduction equation is as follows (Morrell, 2004b):

$$W_i = M_i . 4(x_2^{f(x2)} - x_1^{f(x1)})$$ Equation 6

where

M_i = Work index related to the breakage property of an ore (kWh/tonne); for grinding from the product of the final stage of crushing to a P80 of 750 microns (coarse particles) the index is labelled Mia and for size reduction from 750 microns to the final product P80 normally reached by conventional ball mills (fine particles) it is labelled M_{ib}. For conventional crushing M_{ic} is used and for HPGRs Mih is used.

Wi = Specific comminution (kWh/tonne)

x_2 = 80% passing size for the product (microns)

x_1 = 80% passing size for the feed (microns)

$f(x_j)$ = -(0.295 + x_j/1000000) (Morrell, 2006) Equation 7

For tumbling mills the specific comminution energy (Wi) relates to the power at the pinion or for gearless drives - the motor output. For HPGRs it is the energy inputted to the rolls, whilst for conventional crushers Wi relates to the specific energy as determined using the motor input power less the no-load power.

C 3.2 Specific Energy Determination for Comminution Circuits

The total specific energy (W_T) to reduce primary crusher product to final product size is given by:

$$W_T = W_a + W_b + W_c + W_h + W_s$$ Equation 8

where

W_a = specific energy to grind coarser particles in tumbling mills

W_b = specific energy to grind finer particles in tumbling mills

W_c = specific energy for conventional crushing

W_h = specific energy for HPGRs

W_s = specific energy correction for size distribution

Clearly only the W values associated with the relevant equipment in the circuit being studied are included in Equation 8.

C 3.2.1 Tumbling mills

For coarse particle grinding in tumbling mills Equation 6 is written as:

$$W_a = K_1 M_{ia} . 4(x_2^{f(x2)} - x_1^{f(x1)})$$ Equation 9

where

K_1 = 1.0 for all circuits that do not contain a recycle pebble crusher and 0.95 where circuits do have a pebble crusher

x_1 = P_{80} in microns of the product of the last stage of crushing before grinding

x_2 = 750 microns

M_{ia} = Coarse ore work index and is provided directly by SMC Test®

For fine particle grinding Equation 6 is written as:

$$W_b = M_{ib}.4(x_3^{f(x3)} - x_2^{f(x2)})$$ Equation 10

where

x_2 = 750 microns

x_3 = P_{80} of final grind in microns

M_{ib} = Provided by data from the standard Bond ball work index test using the following equation (Morrell, 2006):

$$M_{ib} = {}^{18.18}/_{P_1^{0.295}(Gbp)(p_{80}^{f(p80)} - f_{80}^{f(f80)})}$$ Equation 11

where

Mib = fine ore work index (kWh/tonne)

P_1 = closing screen size in microns

Gbp = net grams of screen undersize per mill revolution

p_{80} = 80% passing size of the product in microns

f_{80} = 80% passing size of the feed in microns

Note that the Bond ball work index test should be carried out with a closing screen size which gives a final product P80 similar to that intended for the full scale circuit.

C 3.2.2 Conventional Crushers and HPGR

Equation 6 for conventional crushers is written as:

$$W_c = S_c K_2 M_{ic}.4(x_2^{f(x2)} - x_1^{f(x1)})$$ Equation 12

where

S_c = coarse ore hardness parameter which is used in primary and secondary crushing situations. It is defined by Equation 13 with K_s set to 55.

K_2 = 1.0 for all crushers operating in closed circuit with a classifying screen. If the crusher is in open circuit, eg pebble crusher in a AG/SAG circuit, K_2 takes the value of 1.19.

x_1 = P_{80} in microns of the circuit feed

x_2 = P_{80} in microns of the circuit product

M_{ic} = Crushing ore work index and is provided directly by SMC Test®

The coarse ore hardness parameter (S) makes allowance for the decrease in ore hardness that becomes significant in relatively coarse crushing applications such as primary and secondary cone/gyratory circuits. In tertiary and pebble crushing circuits it is normally not necessary and takes the value of unity. In full scale HPGR circuits where feed sizes tend to be higher than used in laboratory and pilot scale machines the parameter has also been found to improve predictive accuracy. The parameter is defined by Equation 13.

$$S = K_s(x_1.x_2)^{-0.2}$$ Equation 13

where

K_s = machine-specific constant that takes the value of 55 for conventional crushers and 35 in the case of HPGRs

x_1 = P_{80} in microns of the circuit feed

x_2 = P_{80} in microns of the circuit product

Equation 6 for HPGR's crushers is written as:

$$W_h = S_h K_3 M_{ih}.4(x_2^{f(x2)} - x_1^{f(x1)}) \quad \text{Equation 14}$$

where

S_h = coarse ore harness parameter as defined by Equation 13 and with K_s set to 35

K_3 = 1.0 for all HPGRs operating in closed circuit with a classifying screen. If the HPGR is in open circuit, K3 takes the value of 1.19.

x_1 = P_{80} in microns of the circuit feed

x_2 = P_{80} in microns of the circuit product

M_{ih} = HPGR ore work index and is provided directly by SMC Test®

C 3.2.3 Specific Energy Correction for Size Distribution (Ws)

Implicit in the approach described in this appendix is that the feed and product size distributions are parallel and linear in log-log space. Where they are not, allowances (corrections) need to be made. By and large, such corrections are most likely to be necessary (or are large enough to be warranted) when evaluating circuits in which closed circuit secondary/tertiary crushing is followed by ball milling. This is because such crushing circuits tend to produce a product size distribution which is relatively steep when compared to the ball mill circuit cyclone overflow. This is illustrated in App Figure 9, which shows measured distributions from an open and closed crusher circuit as well as a ball mill cyclone overflow. The closed circuit crusher distribution can be seen to be relatively steep compared with the open circuit crusher distribution and ball mill cyclone overflow. Also the open circuit distribution more closely follows the gradient of the cyclone overflow. If a ball mill circuit were to be fed two distributions, each with same P80 but with the open and closed circuit gradients in App Figure 9, the closed circuit distribution would require more energy to grind to the final P80. How much more energy is required is difficult to determine. However, for the purposes of this approach it has been assumed that the additional specific energy for ball milling is the same as the difference in specific energy between open and closed crushing to reach the nominated ball mill feed size. This assumes that a crusher would provide this energy. However, in this situation the ball mill has to supply this energy and it has a different (higher) work index than the crusher (ie the ball mill is less energy efficient than a crusher and has to input more energy to do the same amount of size reduction). Hence from Equation 12, to crush to the ball mill circuit feed size (x_2) in open circuit requires specific energy equivalent to:

$$W_c = 1.19 * M_{ic}.4(x_2^{f(x2)} - x_1^{f(x1)}) \quad \text{Equation 15}$$

For closed circuit crushing the specific energy is:

$$W_c = 1 * M_{ic}.4(x_2^{f(x2)} - x_1^{f(x1)}) \quad \text{Equation 16}$$

The difference between the two (Equation 15 and Equation 16) has to be provided by the milling circuit with an allowance for the fact that the ball mill, with its lower energy

efficiency, has to provide it and not the crusher. This is what is referred to in Equation 8 as W_s and for the above example is therefore represented by:

$$W_s = 0.19 * M_{ia}.4(x_2^{f(x2)} - x_1^{f(x1)}) \quad \text{Equation 17}$$

Note that in Equation 17 M_{ic} has been replaced with M_{ia}, the coarse particle tumbling mill grinding work index.

In AG/SAG based circuits the need for W_s appears to be unnecessary as App Figure 10 illustrates. Primary crusher feeds often have the shape shown in App Figure 10and this has a very similar gradient to typical ball mill cyclone overflows. A similar situation appears to apply with HPGR product size distributions, as illustrated in App Figure 11. Interestingly SMCT's data show that for HPGRs, closed circuit operation appears to require a lower specific energy to reach the same P80 as in open circuit, even though the distributions for open and closed circuit look to have almost identical gradients. Closer examination of the distributions in fact shows that in closed circuit the final product tends to have slightly less very fine material, which may account for the different energy requirements between the two modes of operation. It is also possible that recycled material in closed circuit is inherently weaker than new feed, as it has already passed through the HPGR previously and may have sustained micro-cracking. A reduction in the Bond ball mill work index as measured by testing HPGR products compared it to the Bond ball mill work index of HPGR feed has been noticed in many cases in the laboratory (see next section) and hence there is no reason to expect the same phenomenon would not affect the recycled HPGR screen oversize.

It follows from the above arguments that in HPGR circuits, which are typically fed with material from closed circuit secondary crushers, a similar feed size distribution correction should also be applied. However, as the secondary crushing circuit uses such a relatively small amount of energy compared to the rest of the circuit (as it crushes to a relatively coarse size) the magnitude of size distribution correction is very small indeed – much smaller than the error associated with the technique - and hence may be omitted in calculations.

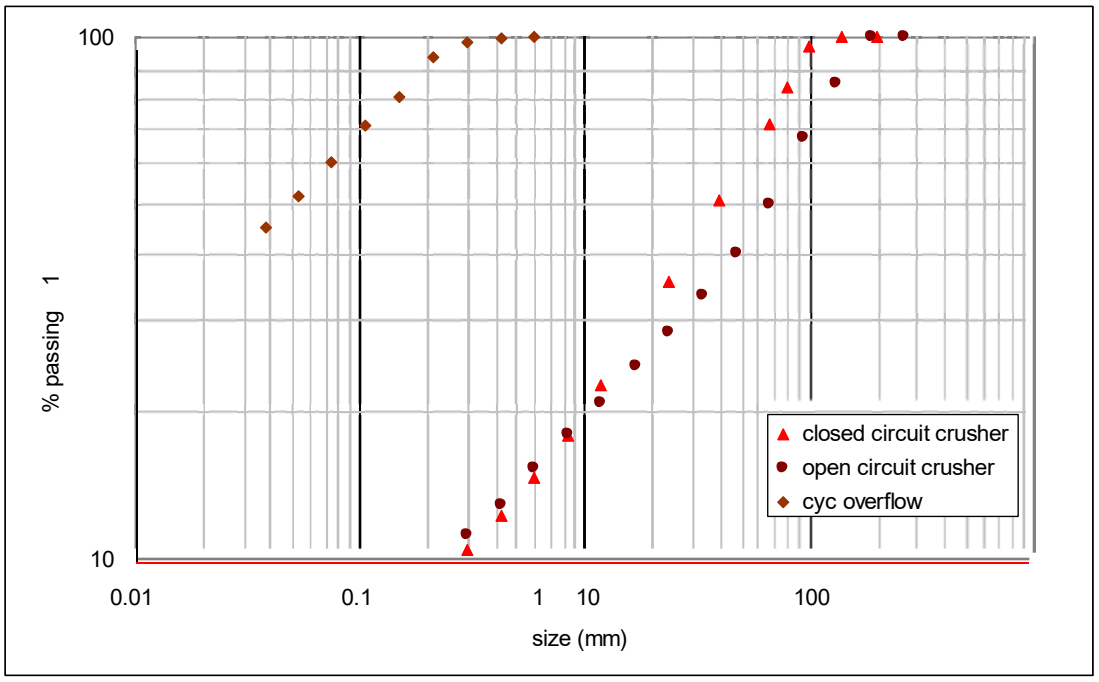

App Figure 9 – Examples of Open and Closed Circuit Crushing Distributions Compared with a Typical Ball Mill Cyclone Overflow Distribution

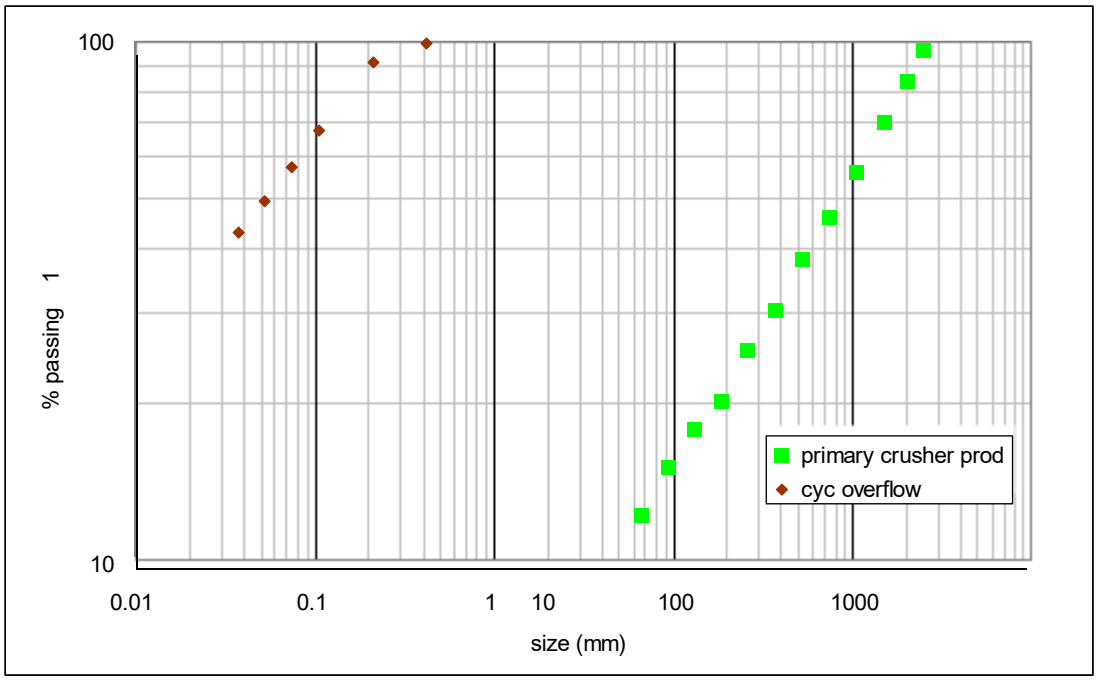

App Figure 10 – Example of a Typical Primary Crusher (Open and Circuit) Product Distribution Compared with a Typical Ball Mill Cyclone Overflow Distribution

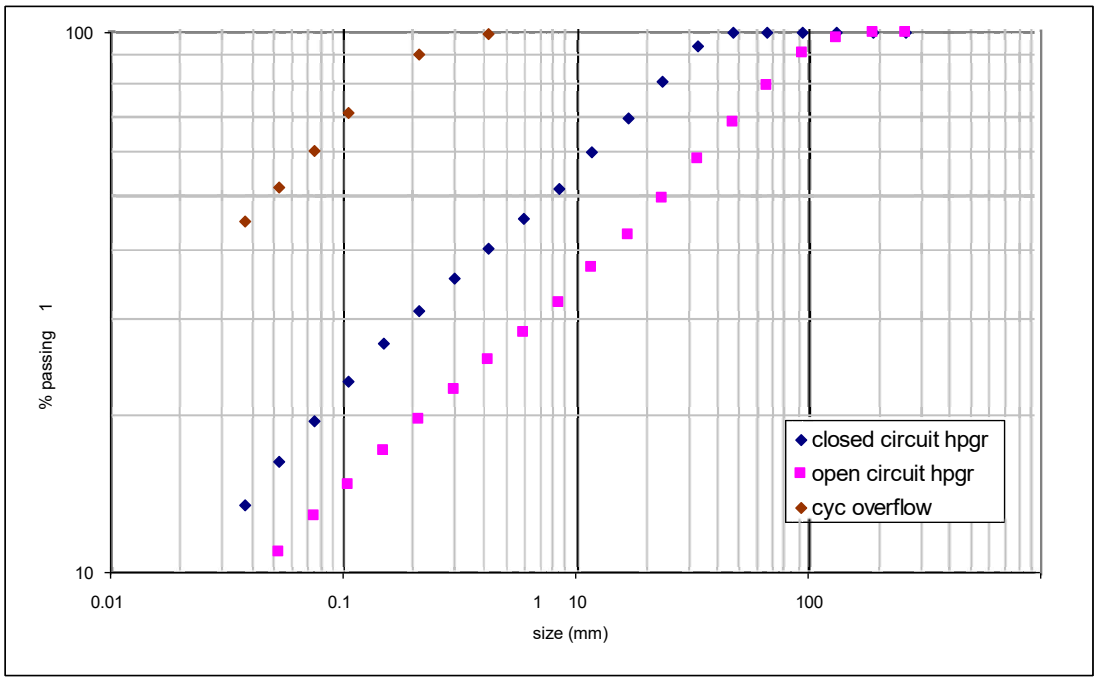

App Figure 11 – Examples of Open and Closed Circuit HPGR Distributions Compared with a Typical Ball Mill Cyclone Overflow Distribution

C 3.2.4 Weakening of HPGR Products

As mentioned in the previous section, laboratory experiments have been reported by various researchers in which the Bond ball work index of HPGR products is less than that of the feed. The amount of this reduction appears to vary with both material type and the pressing force used. Observed reductions in the Bond ball work index have typically been in the range 0-10%. In the approach described in this appendix no allowance has been made for such weakening. However, if HPGR products are available which can be used to conduct Bond ball work index tests on then M_{ib} values obtained from such tests can be used in Equation 10. Alternatively the M_{ib} values from Bond ball mill work index tests on HPGR feed material can be reduced by an amount that the user thinks is appropriate. Until more data become available from full scale HPGR/ball mill circuits it is suggested that, in the absence of Bond ball mill work index data on HPGR products, the M_{ib} results from HPGR feed material are reduced by no more than 5% to allow for the effects of micro-cracking.

C 3.3 Validation

C 3.3.1 Tumbling Mill Circuits

The approach described in the previous section was applied to over 120 industrial data sets. The results are shown in App Figure 12. In all cases, the specific energy relates to the tumbling mills contributing to size reduction from the product of the final stage of crushing to the final grind. Data are presented in terms of equivalent specific energy at the pinion. In determining what these values were on each of the plants in the data base it was assumed that power at the pinion was 93.5% of the measured gross (motor input) power, this figure being typical of what is normally accepted as being reasonable

to represent losses across the motor and gearbox. For gearless drives (so-called wrap-around motors) a figure of 97% was used.

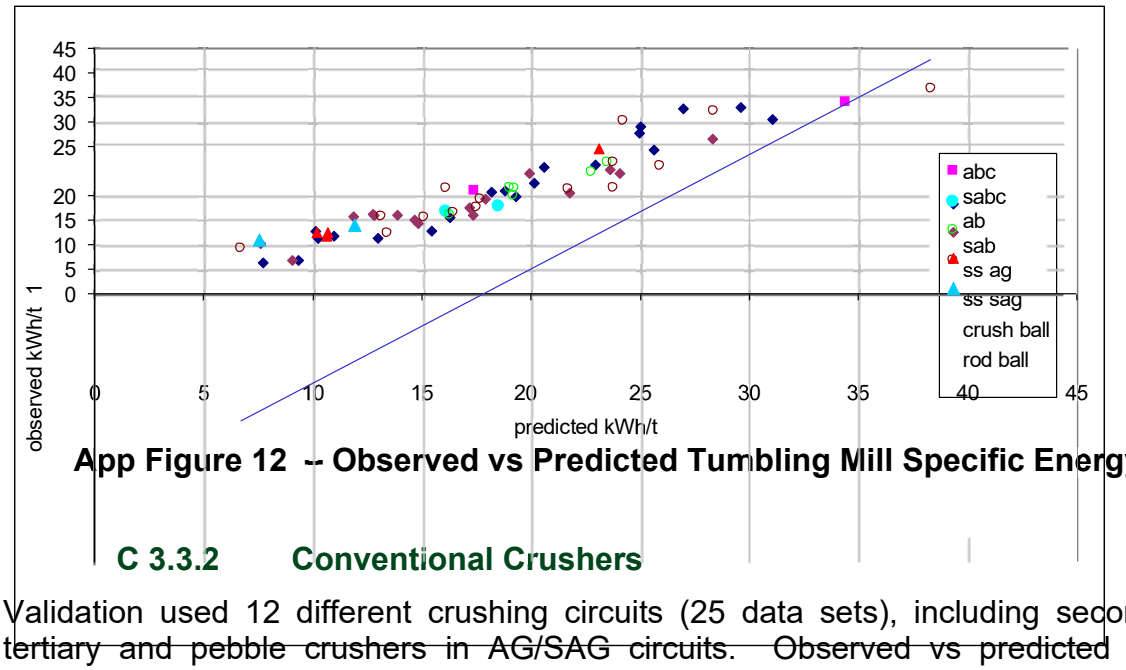

App Figure 12 -- Observed vs Predicted Tumbling Mill Specific Energy

C 3.3.2 Conventional Crushers

Validation used 12 different crushing circuits (25 data sets), including secondary, tertiary and pebble crushers in AG/SAG circuits. Observed vs predicted specific energies are given in App Figure 13. The observed specific energies were calculated from the crusher throughput and the net power draw of the crusher as defined by:

Net Power = Motor Input Power – No Load Power Equation 18

No-load power tends to be relatively high in conventional crushers and hence net power is significantly lower than the motor input power. From examination of the 25 crusher data sets the motor input power was found to be on average 20% higher than the net power.

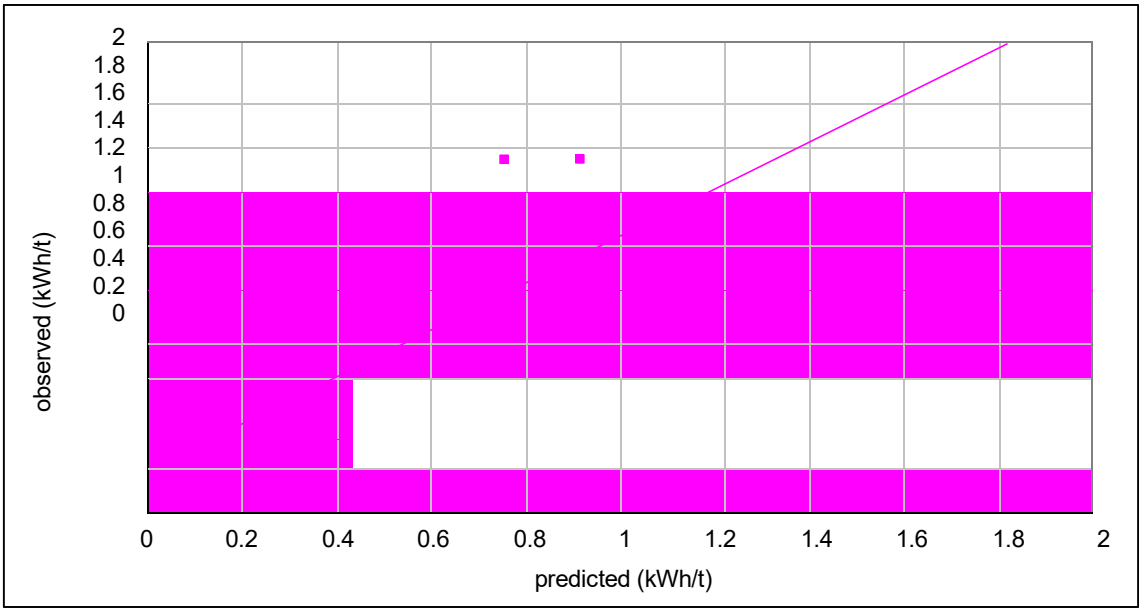

App Figure 13 – Observed vs Predicted Conventional Crusher Specific Energy

C 3.3.3 HPGRs

Validation for HPGRs used data from 19 different circuits (36 data sets) including laboratory, pilot and industrial scale equipment. Observed vs predicted specific energies are given in App Figure 14. The data relate to HPGRs operating with specific grinding forces typically in the range 2.5-3.5 N/mm^2. The observed specific energies relate to power delivered by the roll drive shafts. Motor input power for full scale machines is expected to be 8-10% higher.

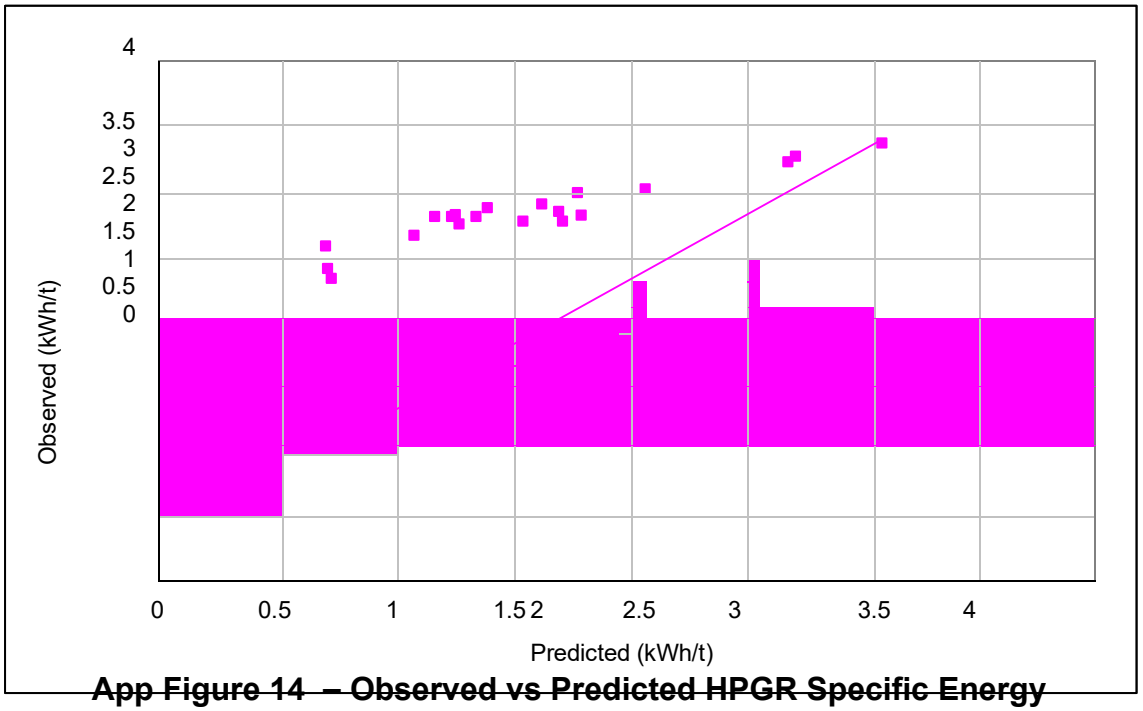

App Figure 14 – Observed vs Predicted HPGR Specific Energy

C 4 WORKED EXAMPLES

A SMC Test® and Bond ball work index test were carried out on a representative ore sample. The following results were obtained:
SMC Test®:
M_{ia} = 19.4 kWh/t
M_{ic} = 7.2 kWh/t
M_{ih} = 13.9 kWh/t
Bond test carried out with a 150 micron closing screen:
M_{ib} = 18.8 kWh/t
Three circuits are to be evaluated:

- SABC
- HPGR/ball mill
- Conventional crushing/ball mill

The overall specific grinding energy to reduce a primary crusher product with a P_{80} of 100 mm to a final product P_{80} of 106 µm needs to be estimated.

C 4.1 SABC Circuit

Coarse particle tumbling mill specific energy:

$$W_a = 0.95 * 19.4 * 4 * \left(750^{-(0.295+750/1000000)} - 100000^{-(0.295+100000/1000000)}\right)$$

= 9.6 kWh/t
Fine particle tumbling mill specific energy:

$$W_b = 18.8 * 4 * \left(106^{-(0.295+106/1000000)} - 750^{-(0.295+750/1000000)}\right)$$

= 8.4 kWh/t
Pebble crusher specific energy:

In this circuit, it is assumed that the pebble crusher feed P_{80} is 52.5mm. As a rule of thumb this value can be estimated by assuming that it is 0.75 of the nominal pebble port aperture (in this case the pebble port aperture is 70mm). The pebble crusher is set to give a product P_{80} of 12mm. The pebble crusher feed rate is expected to be 25% of new feed tph.

$$W_c = 1.19 * 7.2 * 4 * \left(12000^{-(0.295+12000/1000000)} - 52500^{-(0.295+52500/1000000)}\right)$$

= 1.12 kWh/t when expressed in terms of the crusher feed rate
= 1.12 * 0.25 kWh/t when expressed in terms of the SABC circuit new feed rate
= 0.3 kWh/t of SAG mill circuit new feed

Total net comminution specific energy:

W_T = 9.6 + 8.4 + 0.3 kWh/t
= 18.3 kWh/t

C 4.2 HPGR/Ball Milling Circuit

In this circuit primary crusher product is reduced to a HPGR circuit feed P_{80} of 35 mm by closed circuit secondary crushing. The HPGR is also in closed circuit and reduces the 35 mm feed to a circuit product P_{80} of 4 mm. This is then fed to a closed circuit ball mill which takes the grind down to a P_{80} of 106 µm.
Secondary crushing specific energy:

$$W_c = 1*55*\left(35000\ *100000\ \right)^{-0.2}*7.2*4*\left(35000\ ^{-(0.295+35000/1000000)}-100000\ ^{-(0.295+100000/1000000)}\right)$$ =

0.4 kWh/t

HPGR specific energy:

$$W_h = 1*35*(4000\ *35000\ )^{-.2}*13.9*4*\left(4000\ ^{-(0.295+4000/1000000)}-35000\ ^{-(0.295+35000/1000000}\right)$$

= 2.4 kWh/t

Coarse particle tumbling mill specific energy:

$$W_a = 1*19.4*4*\left(750\ ^{-(0.295+750/1000000)}-4000\ ^{-(0.295+4000/1000000}\right)$$

= 4.5 kWh/t

Fine particle tumbling mill specific energy:

$$W_b = 18.8*4*\left(106\ ^{-(0.295+106/1000000)}-750\ ^{-(0.295+750/1000000}\right)$$

= 8.4 kWh/t

Total net comminution specific energy:

W_T = 4.5 + 8.4 + 0.4 + 2.4 kWh/t
= 15.7 kWh/t

C 4.3 Conventional Crushing/Ball Milling Circuit

In this circuit primary crusher product is reduced in size to P_{80} of 6.5 mm via a secondary/tertiary crushing circuit (closed). This is then fed to a closed circuit ball mill which grinds to a P80 of 106 µm.
Secondary/tertiary crushing specific energy:

$$W_c = 1*7.2*4*\left(6500\ ^{-(0.295+6500/1000000)}-100000\ ^{-(0.295+100000/1000000}\right)$$ =

1.7 kWh/t

Coarse particle tumbling mill specific energy :

$$W_a = 1*19.4*4*\left(750^{-(0.295+750/1000000)} - 6500^{-(0.295+6500/1000000}\right)$$

= 5.5 kWh/t

Fine particle tumbling mill specific energy:

$$W_b = 18.8*4*\left(106^{-(0.295+106/1000000)} - 750^{-(0.295+750/1000000}\right)$$

= 8.4 kWh/t

Size distribution correction;

$$W_s = 0.19*19.4*4*\left(6500^{-(0.295+6500/1000000)} - 100000^{-(0.295+100000/1000000}\right)$$

= 0.9 kWh/t

Total net comminution specific energy:

W_T = 5.5 + 8.4 + 1.7 + 0.9kWh/t

= 16.5 kWh/t